

University of Windsor

Scholarship at UWindor

Electronic Theses and Dissertations

Theses, Dissertations, and Major Papers

1-1-1986

Research into polymeric insulating materials for high voltage outdoor insulators.

Ravindranath Srinivasan Gorur
University of Windsor

Follow this and additional works at: <https://scholar.uwindsor.ca/etd>

Recommended Citation

Gorur, Ravindranath Srinivasan, "Research into polymeric insulating materials for high voltage outdoor insulators." (1986). *Electronic Theses and Dissertations*. 6138.
<https://scholar.uwindsor.ca/etd/6138>

This online database contains the full-text of PhD dissertations and Masters' theses of University of Windsor students from 1954 forward. These documents are made available for personal study and research purposes only, in accordance with the Canadian Copyright Act and the Creative Commons license—CC BY-NC-ND (Attribution, Non-Commercial, No Derivative Works). Under this license, works must always be attributed to the copyright holder (original author), cannot be used for any commercial purposes, and may not be altered. Any other use would require the permission of the copyright holder. Students may inquire about withdrawing their dissertation and/or thesis from this database. For additional inquiries, please contact the repository administrator via email (scholarship@uwindsor.ca) or by telephone at 519-253-3000ext. 3208.

NOTE TO USERS

This reproduction is the best copy available.

UMI[®]

RESEARCH INTO POLYMERIC INSULATING MATERIALS FOR HIGH
VOLTAGE OUTDOOR INSULATORS

by

RAVINDRANATH SRINIVASAN GORUR

A Dissertation
Submitted to the
Faculty of Graduate Studies and Research
through the Department of
Electrical Engineering in Partial Fulfillment
of the requirements for the Degree
of Doctor of Philosophy at
the University of Windsor

Windsor, Ontario, Canada
1986

UMI Number: DC53235

INFORMATION TO USERS

The quality of this reproduction is dependent upon the quality of the copy submitted. Broken or indistinct print, colored or poor quality illustrations and photographs, print bleed-through, substandard margins, and improper alignment can adversely affect reproduction.

In the unlikely event that the author did not send a complete manuscript and there are missing pages, these will be noted. Also, if unauthorized copyright material had to be removed, a note will indicate the deletion.

UMI[®]

UMI Microform DC53235
Copyright 2009 by ProQuest LLC
All rights reserved. This microform edition is protected against
unauthorized copying under Title 17, United States Code.

ProQuest LLC
789 East Eisenhower Parkway
P.O. Box 1346
Ann Arbor, MI 48106-1346

© Ravindranath Srinivasan Gorur 1986
All Rights Reserved

Dedicated
to
THE LORD
and
MY PARENTS

ABSTRACT

The electrical performance of polymeric insulating materials was studied in a fog chamber with ac and dc voltage stress. The materials examined were elastomers of high temperature vulcanized (HTV) silicone rubber and ethylene propylene diene monomer (EPDM) rubber and epoxy resins, all containing either alumina trihydrate (ATH) filler or silica filler, or both.

Material performance was found to be strongly affected by the experimental conditions. In fog produced with low (250 $\mu\text{S}/\text{cm}$) conductivity water, silicone rubber performed better than EPDM samples, whereas in fog produced with high (≥ 1000 $\mu\text{S}/\text{cm}$) conductivity water, the order of performance was reversed. The epoxy samples exhibited an inferior performance when compared to the elastomers. Better agreement with service experience was obtained by evaluating the materials in low rather than in high conductivity fog.

The mechanisms by which fillers impart tracking and erosion resistance to the insulating materials was also dependent on the experimental conditions. These were investigated through measurements of released gases and surface temperature during dry band arcing and weight loss and Thermo Gravimetric Analysis (TGA) of the materials. Studies of filler

dispersion by Energy Dispersive X-ray Analysis (EDAX) showed that material degradation in high conductivity fog could be initiated in areas with highly non-uniform filler dispersion.

Material surface study by Electron Spectroscopy for Chemical Analysis (ESCA) demonstrated that the migration of mobile low molecular weight chains to the surface was responsible for the hydrophobicity exhibited by silicone rubber material despite the accumulation of surface contamination.

The tracking and erosion resistance of materials was very similar with ac and +dc voltage stress but was significantly reduced with -dc for vertically oriented rods (polarity refers to the top electrode). For horizontally oriented rods, there was no discernable difference in the performance with ac, +dc and -dc.

A theoretical study to model the effect of dry band discharges on materials is presented. Good agreement of the predicted behavior of materials with the experimental findings was established.

Insulators made from the above materials were studied to determine the correlation with tests using cylindrical rods of material. Cylindrical rods yielded similar results as insulators and in less time. The shape of the sheds which provide a protective leakage path had a significant effect on the insulator performance.

ACKNOWLEDGEMENTS

I would like to express my deep appreciation and gratitude to my supervisors, Dr. E. A. Cherney and Dr. R. Hackam, for giving me the opportunity to work in an extremely interesting and practical field of research. Their encouragement, assistance and suggestions in every aspect of the work is gratefully acknowledged. I sincerely thank Ontario Hydro for supporting Dr. E. A. Cherney's participation in this research.

I would like to thank Dr. K. G. Rutherford of the Chemistry Department, for his help in various aspects of the work dealing with polymer chemistry.

I would like to thank Mr. T. Orbeck, Dow Corning Corporation, for his valuable suggestions which made this work all the more interesting.

I would like to thank Dr. T. W. McDonald of the Mechanical Engineering Department, for his valuable ideas in the development of the theoretical model.

The fruitful discussions with Dr. G. R. G. Raju, Dr. A. Watson and Dr. Yamauchi (Engineering Materials Department) are gratefully acknowledged.

I wish to thank Mr. D. McAvoy for his efficient implementation of the software in a very easy to use manner.

I wish to thank the Natural Sciences and Engineering Council of Canada for providing the funds for this project. I am also grateful to the IEEE Dielectric and Electrical Insulation Society for the 1984 Fellowship award.

I wish to thank National Rubber, Toronto, Ontario; Reliable Electric Company, Chicago, Illinois; Dow Corning Corporation, Midland, Michigan; SWS Corporation, Adrian, Michigan; and Ontario Hydro, Toronto, for providing the samples for this research.

I wish to thank Mr. D. Liebsh, Central Research, and members of his staff, Mr. L. Beaudry, Mr. E. Gwyther, Mr. G. Hamelin, Mr. R. Clarke and Mr. S. Budinsky for all their assistance during this work. I would also like to thank Mr. A. Johns, Mr. J. M. Novosad and Mr. A. Thibert of the Electrical Engineering Department, Mr. J. Robinson of the Engineering Materials Department, Mr. R. New, Mr. M. Fuerth and Mr. A. Ditchburn of the Chemistry Department for all their technical assistance.

TABLE OF CONTENTS.

ABSTRACT	ii
ACKNOWLEDGEMENTS	iv
Chapter I: INTRODUCTION	1
1.1 Factors Contributing to Increased Usage of Polymeric Insulators	3
1.2 Utility Concerns Regarding The Use Of Polymeric Insulators	7
1.3 Review of Previous Work	9
1.3.1 Role of Filler	9
1.3.2 Test Methods to Evaluate Material Performance Under Accelerated Aging	12
1.3.3 Environmental Factors Influencing Material Performance	13
1.3.4 Effect of Voltage Type on Material Performance . .	14
1.3.5 Theoretical Studies to Predict Polymeric Material Performance Under Dry Band Arcing	14
1.4 Research Objectives	15
Chapter II: EXPERIMENTAL SET-UP	17
2.1 Fog Chamber	17
2.2 Test Supply	19
2.3 Data Acquisition System	20
2.4 Electrical Protection	22
2.5 Electrodes	22
Chapter III: AC PERFORMANCE OF POLYMERIC INSULATING MATERIALS	24
3.1 Introduction	24
3.2 Details of Material Samples	25
3.3 Experimental Conditions	27
3.4 Material Performance in High (1600 $\mu\text{S}/\text{cm}$) Conductivity Fog	28
3.4.1 Modes of Failure	28
3.4.2 Time to Failure	28
3.5 Parameters Monitored to Obtain Information on Surface Aging	30

3.5.1	Introduction	30
3.5.2	Cumulative Charge as an Index of Surface Aging	31
3.5.3	Peak Current Pulses as an Index of Surface Aging	34
3.5.4	Flashover Voltage as an Index of Surface Aging	35
3.5.5	Weight Loss as an Index of Surface Aging	40
3.6	Weight Loss as a Function of Electric Stress	43
3.7	Cumulative Charge as a Function of Electric Stress	46
3.8	Correlation With Standard Accelerated Aging Tests	47
3.9	Material Performance as a Function of Water Conductivity	49
3.9.1	Need For Such A Study	49
3.9.2	Samples	51
3.9.3	Experimental Conditions	52
3.9.4	Time to Failure.	52
3.9.4.1	Low (250 μ S/cm) Conductivity Fog	53
3.9.4.2	High (1000 μ S/cm) Conductivity Fog	54
3.9.5	Leakage Current and Cumulative Charge	55
3.9.5.1	Low Conductivity Fog.	55
3.9.5.2	High (1000 μ S/cm) Conductivity Fog.	58
3.9.6	Weight Loss as a Function of Water Conductivity	60
3.10	Correlation of the Results of Low Conductivity Fog Test with Service Experience	61
3.11	Effect on Certain Simulated Environmental Degrading Factors on the Tracking and Erosion Resistance of Materials	63
3.11.1	Resistance to Moisture Ingress.	63
3.11.2	Resistance to Alkali Attack	64
3.11.3	Resistance to Hydrocarbon Solvent Attack	67
3.12	Summary	69

Chapter IV: A COMPARATIVE STUDY OF THE AC AND DC PERFORMANCE OF POLYMERIC MATERIALS AND INSULATORS 70

4.1	Introduction	70
4.2	Experimental	71
4.3	Time to Failure	72
4.3.1	Low Conductivity Fog	73
4.3.2	High Conductivity Fog	73
4.4	Leakage Current and Cumulative Charge	74
4.4.1	Low Conductivity Fog	74
4.4.2	High Conductivity Fog	76
4.5	Effect of Scale Deposit on Material Performance	77
4.6	Material Degradation as a Function of Supply Polarity	79
4.7	Weight Loss due to Dry Band Arcing	81
4.8	Effect of Sample Orientation on Material Performance	83
4.9	Performance of Polymeric Insulators	84
4.9.1	Details of Insulators Evaluated	84
4.9.2	Insulator Performance	88

4.10 Summary	94
Chapter V: EXPERIMENTAL TECHNIQUES USED TO INVESTIGATE MATERIAL PERFORMANCE UNDER ACCELERATED AGING	96
5.1 Introduction	96
5.2 Mechanisms by which Fillers Impart Tracking and Erosion to Polymeric Materials	97
5.2.1 Measurement of Released Gases During Dry Band Arcing	97
5.2.2 Measurements of Surface Temperature During Dry Band Arcing	98
5.2.3 Thermo Gravimetric Analysis (TGA) of Polymeric Materials	100
5.2.4 Dominant Filler Mechanisms in Low and High Conductivity Fog	103
5.3 Surface Studies by Energy Dispersive X-ray Analysis (EDAX)	106
5.3.1 Principle of EDAX	106
5.3.2 Distribution of Filler in Samples	108
5.3.3 Distribution of Filler in Failed Samples	111
5.4 Material Surface Study	113
5.4.1 Introduction	113
5.4.2 Principle of ESCA	115
5.4.3 Results Using ESCA	118
5.5 Summary	121
Chapter VI: THEORETICAL MODEL TO PREDICT THE PERFORMANCE OF POLYMERIC MATERIALS DURING DRY BAND ARCING	122
6.1 Introduction	122
6.2 Effect of ATH or Silica Fillers on the Thermal Conductivity and Diffusivity of Materials	123
6.3 Heat Flux Q due to Dry Band Arcing	126
6.4 Surface Heat Transfer Coefficient	128
6.5 Duration of Dry Band Arcing	130
6.6 Surface Temperature During Dry Band Arcing	132
6.7 Correlation of Model Predictions With Experimental Findings	133
Chapter VII: CONCLUSIONS	137
Chapter VIII: RECOMMENDATIONS FOR FURTHER WORK	142

Appendix A: Data Acquisition System	146
A.1 Algorithm for Numerical Integration	147
A.2 Program Design	148
A.2.1 HELLO	149
A.2.2 SAMPLE	149
A.2.3 SAMPLE.CODE	150
 Appendix B: Timing Circuit	 153
 BIBLIOGRAPHY	 155
 PUBLICATIONS FOR THESIS	 160
 VITA AUCTORIS	 162

LIST OF FIGURES.

1.1	Typical Construction of a Polymeric Insulator. Reproduced From [3].	2
2.1	General View of the Experimental Set-Up.	18
2.2	Schematic Diagram of the Fog Chamber.	19
2.3	Schematic Diagram of the Data Acquisition System.	21
3.1	Time to Failure as a Function of Average Electric Stress.	29
3.2	Cumulative Charge with Time for Silicone Rubber Samples.	32
3.3	Cumulative Charge with Time for EPR samples.	33
3.4	Cumulative Charge with Time for Epoxy Samples.	33
3.5	Flashover Voltage with Time for Silicone Rubber Samples. 1 pu=12.2kV _{rms}	36
3.6	Flashover Voltage with Time for EPR samples. 1 pu=12.2kV _{rms}	37
3.7	Flashover Voltage with Time for Epoxy Samples. 1 pu=9kV _{rms}	37

3.8	Weight Loss with Time for Silicone Rubber Samples.	41
3.9	Weight Loss with Time for EPR Samples.	42
3.10	Weight Loss with Time for Epoxy Samples.	42
3.11	Final Weight Loss as a Function of Average Electric Stress.	43
3.12	Silicone Rubber Samples Before and After Salt-Fog Test. UN: Sample Before Test.	44
3.13	EPR Samples Before and After Salt-Fog Test. UN: Sample Before Test.	45
3.14	Epoxy Samples Before and After Salt-Fog Test. UN: Sample Before Test.	45
3.15	Cumulative Charge with Time as a Function of Average Electric Stress.	47
3.16	Cumulative Charge with Time in Low Conductivity Fog.	56
3.17	EPDM Samples Before and After Low and High Conductivity Test.	57
3.18	Count of Peak Current Pulses above 15mA.	58
3.19	Cumulative Charge with Time in High Conductivity Fog.	59
3.20	Final Weight Loss as a Function of Water Conductivity.	61
4.1	Cumulative Charge with Time in Low Conductivity Fog.	75
4.2	Cumulative Charge with Time in High Conductivity Fog.	77
4.3	Typical Erosion in ATH filled EPDM Samples in High Conductivity Fog with (1) +dc and (2) -dc.	80
4.4	Weight Loss with Time in High Conductivity Fog.	82
4.5	Insulator Profiles Evaluated.	87
4.6	Erosion Leading to Tracking Failure of Insulator D in High Conductivity Fog with -dc .	92

4.7	Erosion Failure of Insulator E in High Conductivity Fog with -dc.	93
4.8	Tracking in Insulator F in Low Conductivity Fog with -dc.	94
5.1	TGA Plots of EPDM Samples.	101
5.2	Typical TGA plots of Silicone Rubber Samples of Table 3.4.	102
5.3	Typical TGA plot of Silicone Rubber Samples of Table 3.1.	103
5.4	Distribution of Filler Particles in Silicone Rubber Samples SE and SA.	109
5.5	Distribution of Filler Particles in Epoxy Sample XA.	110
5.6	Distribution of Filler Particles in Silicone Rubber Sample SD.	111
5.7	Distribution of Filler Particles in EPDM Sample EB.	112
5.8	Typical ESCA Spectrum of Silicone Rubber Material.	117
6.1	Effective Thermal Conductivity and Diffusivity of ATH and Silica Filled Rubber Samples. . .	125
6.2	Time of Arcing as a Function of Water Film Thickness.	131
6.3	Hot Spot Temperature as a Function of Time and Leakage Current for Rubber Samples with 120 pph of Inorganic Filler.	133
A.1	Flow Chart of Program SAMPLE.	150
A.2	Flow Chart of Program SAMPLE.CODE.	152
B.1	Schematic of the Timing Circuit.	154

LIST OF TABLES.

3.1	Identification of Materials Studied.	26
3.2	Peak Current Pulses Prior To Failure.	35
3.3	Results From Fog Chamber and Tracking Wheel Test.	49
3.4	Time to Failure in Low and High Conductivity Fog.	53
3.5	Time to Failure for Samples Subjected to 6N NaOH for 30 Days.	66
3.6	Physical Changes and Time to Failure for Samples Held in Naphtha.	68
4.1	Material Details and Performance in ac, +dc and -dc.	72
4.2	Effect of Orientation on Material Performance in High Conductivity Fog with -dc.	83
4.3	Insulator Details and Performance with ac, +dc and -dc.	89
4.4	Cumulative Charge For Insulators with ac, +dc and -dc.	90
4.5	Time to Failure of Insulators at Various Electric Stress in Low Conductivity Fog with -dc.	91
5.1	Surface Analysis of Silicone Rubber and EPDM Samples.	119
5.2	Effect of Corona and Recovery on Surface Composition of Silicone Rubber.	120
6.1	Physical Constants of Materials Evaluated.	124
6.2	Distribution of the Conduction Period of Dry Band Discharges.	128
6.3	Time to Failure and Leakage Current as a Function of Electric Stress in Low Conductivity Fog.	134

Chapter I

INTRODUCTION

Outdoor insulators made from inorganic materials such as porcelain and glass have been used on overhead power lines since the turn of the century. These materials, despite being brittle [1], have performed remarkably well in the majority of cases. The main reason for their successful electrical performance can be attributed to their capacity to withstand the heat of dry band discharges for prolonged periods of time without being degraded [2], which occurs on energized insulators when the surface is covered by a moist layer of contamination. After a long record of useful service, insulators made from porcelain or glass are being challenged by insulators made from relatively new polymeric materials.

The typical construction of a polymeric insulator is shown in Fig. 1.1 [3]. It consists of:

1. A central fiber glass rod which provides mechanical strength to the unit. The glass fibers are usually 'E' type and bonded by epoxy or polyester resin [4]. As voltage and moisture leads to tracking of the rod in a relatively short time, it is protected by a weathershed which also imparts the necessary wet flashover strength to the insulator.

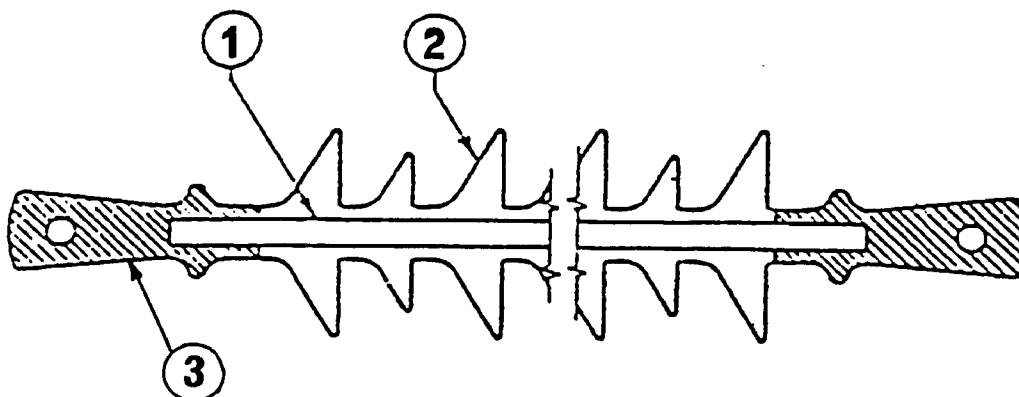


Figure 1.1: Typical Construction of a Polymeric Insulator. Reproduced From [3].

2. An encapsulating weathershed which provides the required electrical insulating properties. Among the wide range of polymeric materials available [4], service experience has shown that the materials suitable for weathersheds are high temperature vulcanized (HTV) silicone rubber, ethylene propylene rubber (EPR) and epoxy resins. The ethylene propylene diene monomer (EPDM) form of rubber is the most suitable type under the generic class of EPR [4].
3. The metal end terminations which are generally galvanized iron or high strength aluminum alloy. The attachment of the end fitting to the fiber glass core is by a wedge system, by crimping technique or by a tapered cone using an epoxy resin as a grout [4].

Owing to the nature of materials used and the method of construction, polymeric insulators are also referred to as organic, non-ceramic, synthetic, composite and plastic insulators.

1.1 Factors Contributing to Increased Usage of Polymeric Insulators

The use of polymeric insulators which began since about 1967 [5] has been gaining popularity for the following reasons:

1. The brittle nature of porcelain and glass has caused such insulators to shatter when struck by bullets from vandals. Polymeric insulators, which do not destruct in a similar manner, are therefore used as an alternative in vandal prone areas. Although these new materials have certain known weaknesses regarding their ability to withstand dry band discharges and long term durability, they still prove to be profitable as they are not required to be replaced as frequently as porcelain or glass [6].
2. In recent years transmission and distribution lines using horizontal line post insulators have become very popular. This is due to the advantages of elimination of cross arms and reduction in tower height offered by line posts, which helps in reducing construction costs. Power lines using line posts, due to their compact construction, are more aesthetically pleasing than lines using pin or suspension type insulators. Porcelain line posts, due to their poor impact strength, have been damaged from mechanical shock loading from sources such as impact of vehicle to the base of a pole, ice dropping from conductors and insu-

lator breakage due to vandalism [7]. The transfer of mechanical shock from one pole to another can result in insulator breakage over a few spans and dropping of the conductor. The use of polymeric line posts, which possess a much superior impact strength, has considerably reduced such failures and hence improved the line reliability [7]. Currently in the United States, about 30% of line post insulators applied are polymeric.

3. Porcelain and glass are high surface energy materials [8], that is, they allow a continuous water film to be formed easily on the surface. As this is necessary for leakage current to flow, in contaminated areas it may attain sufficient magnitude to cause external flashover. There are many sources of contamination in the outdoor environment such as sea salt, road salt, cement dust, fly ash, bird droppings, fertilizer and many types of industrial emissions. Contamination related flashover has been one of the biggest factors contributing to power outages [9]. They can be minimized either by washing the insulators or by coating them with a hydrophobic material such as grease, which prevents the formation of a continuous surface water film. Coating insulators with grease is not a long term solution [10] and washing is expensive if it needs to be done frequently. On the other hand, poly-

meric materials are inherently low surface energy materials [8] and the tendency for water to form a continuous film is considerably reduced. Silicone rubber material has shown that it prevents water filming for prolonged periods, despite the accumulation of surface contamination [11]. Therefore, the use of silicone rubber insulators in contaminated areas has proved to be more advantageous [6,11]. The longer leakage distance and smaller shed diameter also improves the contamination performance of polymeric insulators by increasing the resistance to leakage current [6].

4. dc transmission lines have certain advantages over ac lines [12] and their number has been steadily increasing. The problem of insulator contamination is accentuated in dc application due to the more effective accumulation by electrostatic forces [10]. Due to a lower contamination related flashover voltage, insulators used on dc lines are characterized by a longer leakage distance when compared to ac lines for the same voltage [10]. Because of the longer leakage distance for the same connection length, a higher strength to weight ratio and better ability to prevent continuous water films possessed by certain polymeric materials, their use can result in a more compact line construction than is possible with porcelain or glass.

5. Polymeric insulators are much lighter in weight. Therefore, their use results in reduced storage, handling and construction costs [4].
6. The low cost of base materials required to make porcelain is offset by the expensive kilns and long manufacturing times which are necessary [1]. The manufacture of porcelain is, in many cases, an art. High expansive cement has led to many failures of porcelain suspension insulators [13]. Although the initial cost of polymeric insulators was much higher than porcelain, increased competition has led to reduced cost. Presently, this cost is comparable or cheaper than porcelain for distribution [14].

The comparable cost coupled with the above advantages has led to the increased use of polymeric insulators. For example, in Canada alone there are about 150,000 insulators used annually on distribution lines and in the United States their number is about 10 times greater. There is a feeling [14] that porcelain and glass suspension insulators have seen their last days at least on distribution lines. Thus, polymeric insulators can be thought of as a second generation of insulators for overhead power lines.

1.2 Utility Concerns Regarding The Use Of Polymeric Insulators

1. The prime concern is in the life of these insulators. Polymeric materials are characterized by a relatively poor thermal stability (less than 500 °C) [15] and therefore can be degraded by the heat of dry band discharges. Material degradation could be in the form of tracking or erosion. Tracking [16] refers to the formation of a continuous conducting carbonaceous products on the surface formed as a result of polymer degradation, thereby making the material useless for electrical applications. Tracking is minimized by the use of inorganic fillers. Filled materials erode [4] and in time, the fiber glass rod can be exposed to the environment at which point the useful life of the insulator can be considered ended. Polymeric materials also "age" in an outdoor environment. Aging refers to the gradual loss of useful material properties with time. Aging in an outdoor environment is due to the susceptibility of the material to be attacked by ultra-violet radiation from sunlight, moisture, acids, alkalis, industrial emissions and extreme variations in temperature [4,17]. At this stage it is not known whether materials that show good insulating properties when new, will retain them after 40 years of service. Thus the long term durability of the weathershed

materials constitutes a major concern. Although the existing laboratory accelerated aging tests [16] are effective in ranking materials, the long term performance of these materials cannot be predicted from these tests.

2. The design of polymeric insulators has not yet been standardized as they are for porcelain. The designs have varied since their evolution and will continue to do for several more years. Too many changes in design has been a major utility concern [18].
3. The long term mechanical strength of polymeric insulators has been another major concern. Unlike porcelain and glass insulators, where mechanical strength is a function of material only, with polymeric insulators, the mechanical strength is both material and time dependent [7]. Therefore, the mechanical strength when new may not be the same after a few years in service. The long term mechanical strength in tension (for suspension and dead end insulators), compression (for post insulators), torsion (for dead end insulators), and cantilever (for line posts) is not fully known. Unlike porcelain insulators where power arc does not affect the mechanical strength, polymeric insulators could suffer a reduction in their mechanical strength [19]. Thus, the reduction in the long term mechanical strength could be accentuated.

4. As experience with polymeric insulators is relatively limited, there are no standards developed to aid utilities in their application. Lack of standards has been another major concern [18].

The goal of this research is to obtain a better understanding of the performance of polymeric materials in contaminated environments. The materials under study are the most widely used materials for outdoor insulation, namely, HTV silicone rubber and EPDM rubber and epoxy resins.

1.3 Review of Previous Work

1.3.1 Role of Filler

Fillers are used in polymeric materials to improve the tracking and erosion resistance. The improvement is largely dependent on the mechanisms by which the fillers operate during dry band arcing. For materials containing hydrated filler like ATH, it has been suggested that the heat of dry band arcing liberates the water of hydration as steam. The steaming action (sputtering) physically removes the carbonaceous products formed as a result of polymer degradation, thereby preventing tracking. This is referred to as the physical cleaning action [20].

A chemical mechanism has also been suggested wherein at high temperature ($>600^{\circ}\text{C}$) the water of hydration of the filler combines with free carbon from the polymer to form gaseous products such as CO or CO_2 , which escapes from the surface. Thus free carbon on the surface is prevented [20].

Volume effects of the filler in which with increasing filler concentration, fewer organic molecules are exposed to the heat of dry band arcing, is another mechanism responsible for imparting tracking or erosion resistance. The higher thermal conductivity of the filler is believed to help in better heat dissipation and prevent hot spots from forming [21].

As the physical and chemical mechanisms are operative only with hydrated fillers, it can be expected that ATH filler imparts higher resistance to tracking and erosion to materials than does silica filler. This is indeed the case as demonstrated by laboratory tests [20]. But in the field there have also been successful applications of insulators with silica filler [5]. Silica is less expensive to use than ATH. In addition, the drawbacks associated with the use of fillers such as, reduction in volume and surface resistivity, increase in dielectric loss angle and permittivity and water absorption, are considerably lower [21] when silica is used as a filler. Therefore, it is important to uncover the dominant mechanisms by which fillers impart tracking and erosion resistance to materials as it will then enable the selection of the correct filler type to be used.

The dependence of tracking and erosion on filler concentration has not been fully established. It is of practical interest to determine if there is a filler threshold level beyond which little improvement in material performance is

obtained, because of difficulties encountered in manufacturing when high filler levels are used. It has been shown [21] for epoxy material, that a filler level of 40 to 50% is the threshold level. As there is very little information available for silicone rubber and EPR, it is desirable to determine whether the filler threshold level, in terms of its effectiveness varies with material.

It is expected that increased electric stress leads to higher temperature during dry band arcing. Material tracking and erosion are therefore dependent on electric stress and this has been recognized [22]. However, as material performance is also dependent on filler type and concentration, the threshold level must therefore be dependent on the magnitude of electric stress. It is desirable to establish the dependence of filler threshold level to the magnitude of electric stress, thereby permitting the correct specification of filler level for the intended application.

Molded polymeric materials containing inorganic filler can be expected to have some dispersion in filler uniformity. The view that filler dispersion plays an important role in the initiation of tracking and erosion has been held for some time, but up to now this has not been shown experimentally. There have been instances where insulators have shown preferential tracking or erosion along mold joins [23]. It is important to discover whether dispersion is responsible for the initiation of tracking and erosion in order to improve on insulation designs.

1.3.2 Test Methods to Evaluate Material Performance Under Accelerated Aging

To assess the contamination performance of polymeric materials, artificial test methods are used. Test philosophies have been based on the mechanisms of contamination deposit and wetting conditions. Numerous test methods such as the ASTM tests [16], the Tracking Wheel test [16], the IEC salt-fog and clean-fog tests [24] have been developed. A common feature of these tests is that materials are required to have substantial fillers (above 50% by weight) in order to pass these tests [16]. Therefore, the outcome is more dependent on filler type and concentration than on the polymer type. But, it has been experienced both from outdoor tests [23] and service conditions [11] that successful performance is more dependent on the type of polymer than on filler type or its concentration. For example, silicone rubber insulators have performed better than any other type [23] in contaminated areas and the filler concentration in these has been generally very low. Although the mechanisms involved are not fully understood, the successful performance of silicone rubber insulators has been attributed to the capacity of the material to maintain a hydrophobic surface for prolonged periods, despite the accumulation of surface contamination [11]. On the other hand, there have been instances [23] of tracking failure of EPDM and epoxy insulators with substantial filler which have shown excellent

track resistance in laboratory tests [3]. Thus, there is a contradiction between the results from laboratory tests and service experience. It is important to understand the reasons for the contradiction as it will then facilitate the development of suitable test procedures for meaningful evaluation of polymeric materials.

The parameters monitored in the earlier laboratory tests in order to obtain an indication of surface aging have been time to failure, peak leakage current, weight loss due to dry band arcing and the integral of leakage current or cumulative charge [25]. Due to lack of systematic work there has been no consensus on the parameter which gives the best indication of surface aging and subsequent material failure. From the point of view of standardizing test methods, it is desirable to evaluate the merits of these parameters and suggest the most relevant parameter which gives the best indication of material aging.

1.3.3 Environmental Factors Influencing Material Performance

For successful application of polymeric insulators, it is important to know the effect of certain environmental elements mentioned in section 1.2, on the tracking and erosion resistance of the weathershed materials. It has been shown that [17] UV and extreme temperature changes do not have any detrimental effects on the tracking and erosion resistance. It has also been shown [26] that the tracking and erosion

resistance of silicone rubber material with silica filler is reduced due to moisture ingress. Little information is available on the effect of moisture ingress on silica filled EPDM material. In addition, the effect of acids, alkalis and hydrocarbon solvents, which may exist in industrial and coastal areas, on the tracking and erosion resistance of materials is not fully known. Therefore, for successful application of polymeric insulators such information needs to be obtained.

1.3.4 Effect of Voltage Type on Material Performance

Material performance has been reported mostly for ac. Material tracking or erosion can be expected to be more severe with dc than with ac, due to the greater accumulation of contamination due to electrostatic forces [10]. As there is very little reported [27] on the performance of materials with dc, a detailed study is necessary for the successful application of polymeric insulators on dc lines.

1.3.5 Theoretical Studies to Predict Polymeric Material Performance Under Dry Band Arcing

Dry band discharges which occasionally lead to flashover of porcelain or glass insulators do not normally cause material degradation. But polymeric materials, due to their relatively low thermal stability, could degrade from dry band discharges before flashover. Theoretical models which predict the effect of dry band discharges on polymeric materials, of

which there are few [28,29], are of greater relevance in the application of polymeric insulators, than models which predict flashover of contaminated insulators, of which there are many [9]. In the few models developed so far, the widely used materials containing inorganic fillers have not been considered. The effect of accumulation of contamination, which is inevitable in outdoor environments, on material performance has also not been considered. Although it has been suggested that prolonged dry band arcing in a particular spot is responsible for initiating degradation, there are no models to validate this. Therefore, it is desirable to develop a model that takes the above factors into consideration, which can be used to predict the performance of materials under dry band arcing.

1.4 Research Objectives

1. To uncover the dominant mechanisms by which fillers impart tracking and erosion resistance to materials.
2. To determine the type and threshold level of filler for the three types of materials.
3. To determine whether filler dispersion is responsible for initiating tracking or erosion.
4. To determine the capabilities of different parameters to characterize surface aging and suggest the most suitable parameter to be monitored in accelerated aging tests.

5. To determine the factors which are responsible for the contradiction between the results from laboratory tests and service experience.
6. To uncover the mechanisms responsible for prolonged hydrophobicity in silicone rubber material.
7. To determine the effect of voltage type (ac or dc) on the tracking and erosion resistance of materials.
8. To determine the effect of the commonly found chemical pollutants on the tracking and erosion resistance.
9. To develop a theoretical model capable of predicting material performance under dry band arcing.

Chapter II

EXPERIMENTAL SET-UP

2.1 Fog Chamber

The fog chamber used in this study is shown in Fig. 2.1 and its schematic is shown in Fig. 2.2. It is a cubicle of side 2.54m made up of 3mm thick plexiglass sheets. The floor of the chamber is raised above the ground level by 45 cm and is sloped towards the center of the chamber to facilitate easy draining of water. The fog is created by nozzles which are dimensioned according to IEC specification 507 [24]. The chamber has four such nozzles placed equidistant on a pair of stainless steel tubes having an internal diameter of 8 mm and which forms a ring of 2.54 m in diameter. In this system the water is recycled from a reservoir and is handled by two corrosion resistant pumps. The pump which drives water into the chamber is 1/20 hp and the pump which drives water into the reservoir is 1/200 hp. The reservoir has a capacity of 250ℓ and the water in it is constantly stirred by a 1/2 hp motor. Water of the required conductivity is prepared by adding NaCl to tap water.

Water conductivity is measured by a conductivity meter (Horizon Model 1484) which is capable of measuring from 0 to 20,000 $\mu\text{S}/\text{cm}$. The water in the reservoir is changed at such

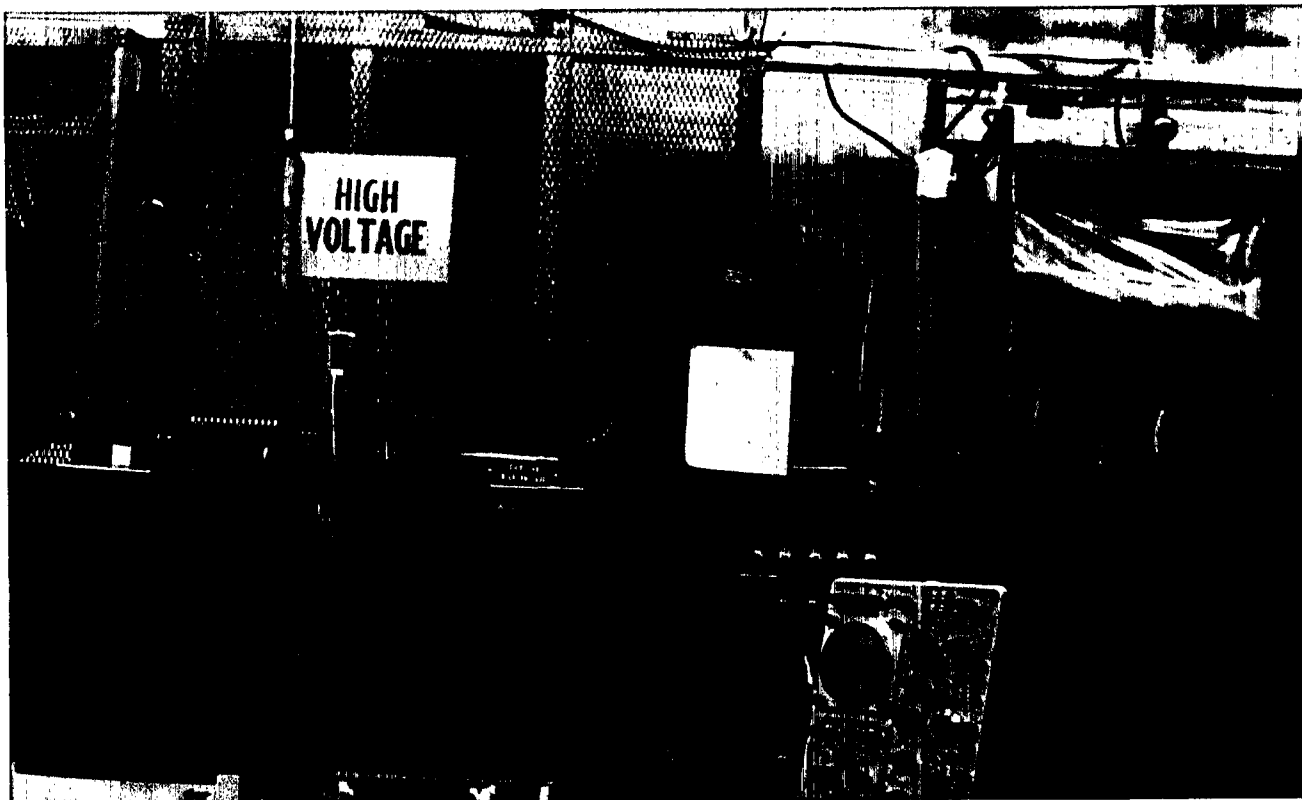


Figure 2.1: General View of the Experimental Set-Up.

times when the conductivity due to recycling increases by about 10% of the initial value. A stainless steel mesh located at the drain of the chamber prevents degradation deposits originating from the samples during dry band arcing, from entering the reservoir through the return pump.

A flowmeter (CALQFLO) in series with the input water line controls the water flow rate. In this system, the flow rate can be varied from 0 to 2.4 l/minute. The air pressure can be varied from 0.1 to 0.6 MPa by an air regulator.

There is provision for testing ten samples at the same time. The power supply to the samples is through a 25 kV

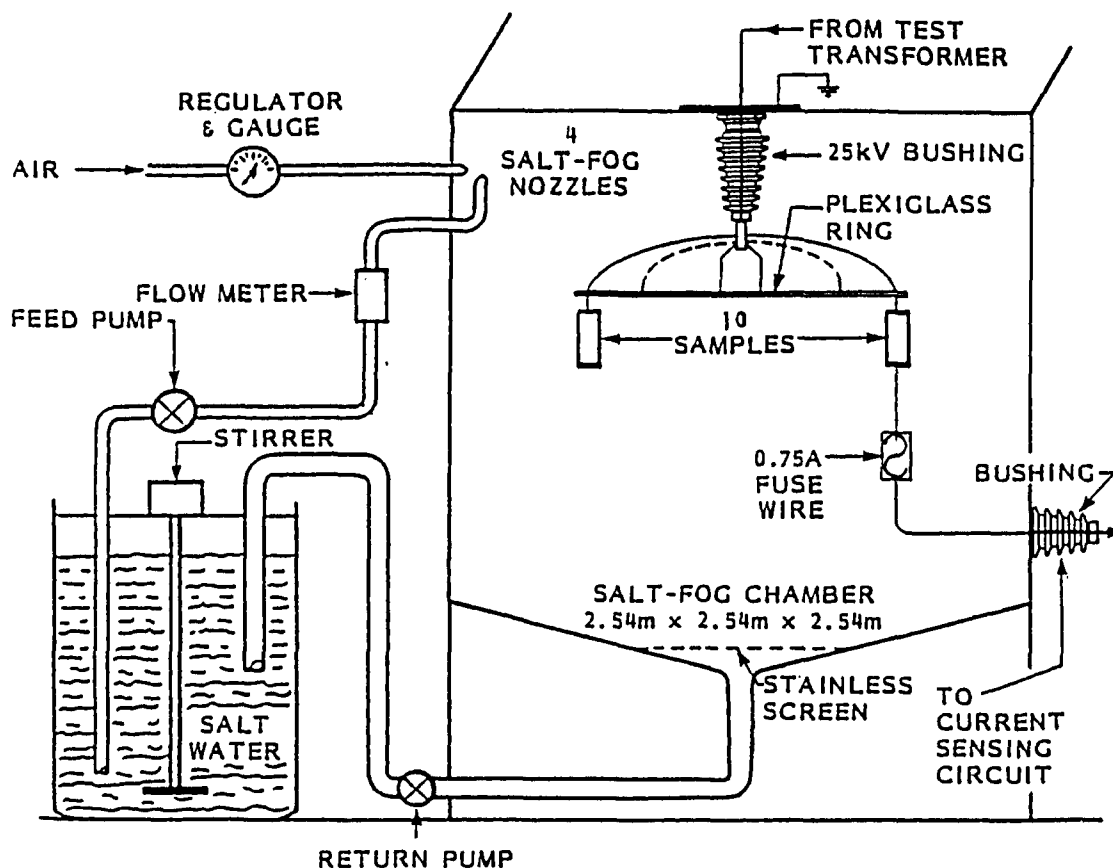


Figure 2.2: Schematic Diagram of the Fog Chamber.

porcelain bushing located at the top of the chamber. The bushing is regularly coated with silicone grease to prevent flashover.

2.2 Test Supply

The ac test supply is a 14.4 kV/220 V, 37.5 kVA distribution transformer. The output is controlled by a 10 kVA, 0 to 220 V variac.

The dc supply is obtained by half wave rectification of the 14.4 kV ac output. A 14.5 μ F/20 kV smoothing capacitor ensures that the ripple is less than 2%.

With ac or dc, the maximum voltage drop at the highest electric stress and water conductivity used was found to be less than 5%. This satisfies the supply stiffness requirement [30] necessary to conduct contamination studies.

2.3 Data Acquisition System

The data acquisition system used in this study is based on a paper by Jolly [25] and its schematic is shown in Fig. 2.3. It consists of an 8 bit, 16 channel analog-to-digital (A/D) converter (Mountain Computer Inc.) which continuously monitors the leakage current from all the samples under test. A microcomputer (64k Apple) processes the instantaneous currents to yield peak and average values on both the positive and negative half cycles. The integration of the current to obtain the cumulative charge is also carried out. In addition, the data acquisition system is programmed to give the number of leakage current pulses between preset limits of current values.

The sampling period of the A/D converter can be set over a wide interval of time (1 min to 6 hours). A typical period is 1 hour at the end of which the data accumulated is stored in a floppy disk and also printed out.

A numerical integration (trapezoidal rule) has been used to evaluate the cumulative charge ($\int i dt$). As this requires a number of points on the current waveform, the sampling frequency depends on the accuracy required: the higher the

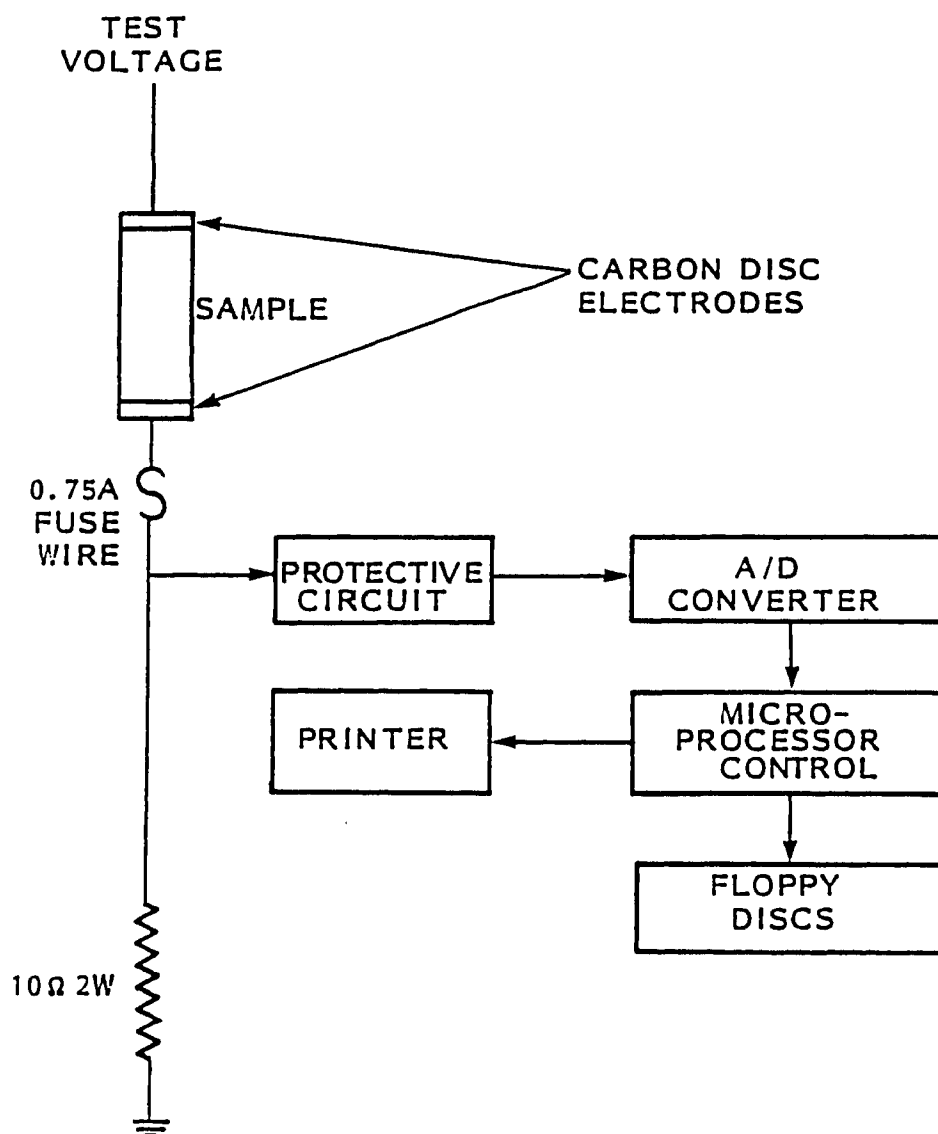


Figure 2.3: Schematic Diagram of the Data Acquisition System.

sampling frequency, lower is the error in numerical integration. In this system, the sampling frequency is variable from 4038 Hz when only one sample is tested to 520 Hz when ten samples are tested. At the lowest sampling frequency, the error involved for a sampling period of one hour is about 5%. The error was determined by comparison with a pure sine wave.

As the resolution of the 8-bit A/D converter used is 39 mV, it is necessary that the voltage signal fed to it be much higher than this value. The current sensing resistor is chosen such that for the lowest leakage current expected, the voltage drop across it is about 500 mV.

2.4 Electrical Protection

The data acquisition system is protected against damaging overvoltages which develop in the event of a flashover of any one of the samples. A combination of a 75 V low pressure fast (10 ns) spark gap and 4.7 V back-to-back Zener diode is used at the input of the A/D converter. Connected in series with each sample is a 0.75mA fuse wire enclosed in a glass tube which melts in the event of a flashover, ensuring that the power supply to the other samples is not interrupted. The controller variac is protected by a 50 A fuse and a 50 A circuit breaker.

2.5 Electrodes

It was suggested [25] that the material of the electrodes in this type of study could affect the outcome of the tests. Metal electrodes corrode, thereby modifying the local electric stress, and leave corrosion by products on the surface of the samples. Carbon electrodes were therefore recommended for these experiments. The electrodes used were 5mm thick carbon discs, 25mm in diameter with a 6.4mm hole drilled in

the center. Brass screws were used for mounting the electrodes on to the samples.

Chapter III

AC PERFORMANCE OF POLYMERIC INSULATING MATERIALS

3.1 Introduction

The performance of polymeric insulating materials in outdoor environments is dependent both on the type of weathered material and insulator design [26]. In order to compare the performance of various materials it is important that the insulator designs be identical. The use of cylindrical rods of different materials is not only less expensive and easy to make but also facilitates direct comparison of material performance as identical geometries are being compared.

Better understanding of material performance can be obtained if the materials are evaluated over a range of experimental conditions. In a fog chamber test, the parameters which can be varied in order to vary the test severity are the electric stress and water conductivity. This chapter describes the results of material evaluation with ac at different values of electric stress and water conductivity. Various methods to provide an indication of surface aging such as, measurement of the peak and average (of each half cycle) of the leakage current, the cumulative charge, periodic measurement of weight loss and flashover voltage have been investigated. The influence of inorganic filler, type

and concentration and the magnitude of electric stress on the tracking and erosion properties of materials are described. The effect of certain simulated environmental degrading factors on material performance are also described.

All the results reported are the average from at least two samples of the same composition for which the variation in the reported quantity was within $\pm 5\%$.

3.2 Details of Material Samples

The materials evaluated are listed in Table 3.1. In this study, the terms EPDM and EPR have been used to represent the same material. The silicone rubber and EPR samples were molded rods 25mm in diameter. Rod samples of epoxy were obtained by machining distribution insulators. The concentration of inorganic filler added to impart tracking and erosion resistance is denoted in pph which is the number of parts of filler added to one hundred parts of polymer formulation by weight. For protection against ultra-violet (UV) rays, the ATH and alumina filled EPR samples had about 0.5pph of ZnO or TiO and the silica filled EPR samples had about 0.5 pph of carbon black.

Table 3.1: Identification of Materials Studied.

The silicone rubber samples were supplied by SWS Corporation, Adrian, Michigan; The EPR samples were supplied by National Rubber, Toronto, Ontario. The epoxy samples XA and XB were machined from 25 kV class insulators of AB Chance Co. and C. K. Composites Inc. respectively.

MATERIAL TYPE	IDENTIFICATION	FILLER	
		TYPE	LEVEL (pph)
EPR	EO	NONE	0
	EA	$Al_2O_3 \cdot 3H_2O$	30
	EB	ALUMINA	60
	EC	TRIHYDRATE (ATH)	80
	ED		105
	EE		130
	EF		250
	EDA	Al_2O_3 (ALUMINA)	105
	EAS	SiO_2	30
	ECS	(SILICA)	80
	EES		130
	EFS		250
EPOXY	XA	$Al_2O_3 \cdot 3H_2O$	220
	XB		350
HTV SILICONE RUBBER	SA		30
	SB		60
	SC	$Al_2O_3 \cdot 3H_2O$	80
	SD		105
	SE		130

pph: PARTS PER HUNDRED OF POLYMER

3.3 Experimental Conditions

The experimental fog nozzle conditions of water flow rate of 1.6l/min and air pressure of 0.6MPa were chosen based on earlier work [30]. The samples were evaluated at an average electric stress (applied voltage/leakage distance) of 28V/mm and 40V/mm (values refer to rms) as outdoor insulators are normally operated in this range. If it can be shown that the tracking and erosion resistance is not significantly affected by a higher electric stress, then for insulators using such materials the leakage distance can be reduced. In order to investigate this, the materials were also evaluated at an electric stress of 60V/mm. The average electric stress was varied by keeping the supply voltage constant and varying the sample length. The sample lengths were 150, 105 and 70mm for an electric stress of 28, 40 and 60V/mm respectively. The samples were evaluated at water conductivities of 250, 1000 and 1600 $\mu\text{S/cm}$. These values were also chosen based on earlier work [30]. Based on preliminary experiments, it was found that a test duration of 500 hours was sufficient to bring out the relative performance of the various materials.

In order to avoid possible positional bias in the chamber, the location of the samples was interchanged after every 20 hours. This ensured that each sample was subjected to similar wetting conditions during the test.

3.4 Material Performance in High (1600 $\mu\text{S}/\text{cm}$) Conductivity Fog

3.4.1 Modes of Failure

Due to the vertical orientation of the samples and the relative position of the fog nozzles, tracking and erosion developed near the bottom electrode. Tracking and erosion progressed respectively upwards along the length and through the thickness of the samples. The silicone rubber samples which failed did so by erosion leading to mechanical separation or to flashover. Epoxy and EPR samples which failed did so by tracking.

3.4.2 Time to Failure

Fig. 3.1 shows the results of comparative tests done to examine the influence of material, filler type and concentration, and electric stress on the time to failure. The silica filled EPR samples were only evaluated at 40V/mm. The following points can be noted from the figure:

1. The magnitude of electric stress had a significant effect on the performance of the materials. The time to failure decreased with increasing electric stress. EPR samples EA and EB which did not fail at 28V/mm stress did so at higher stress. Similarly the silicone rubber samples SC and SD failed above 28V/mm stress.
2. For ATH levels up to 105 pph, EPR samples performed better than the silicone rubber samples. However,

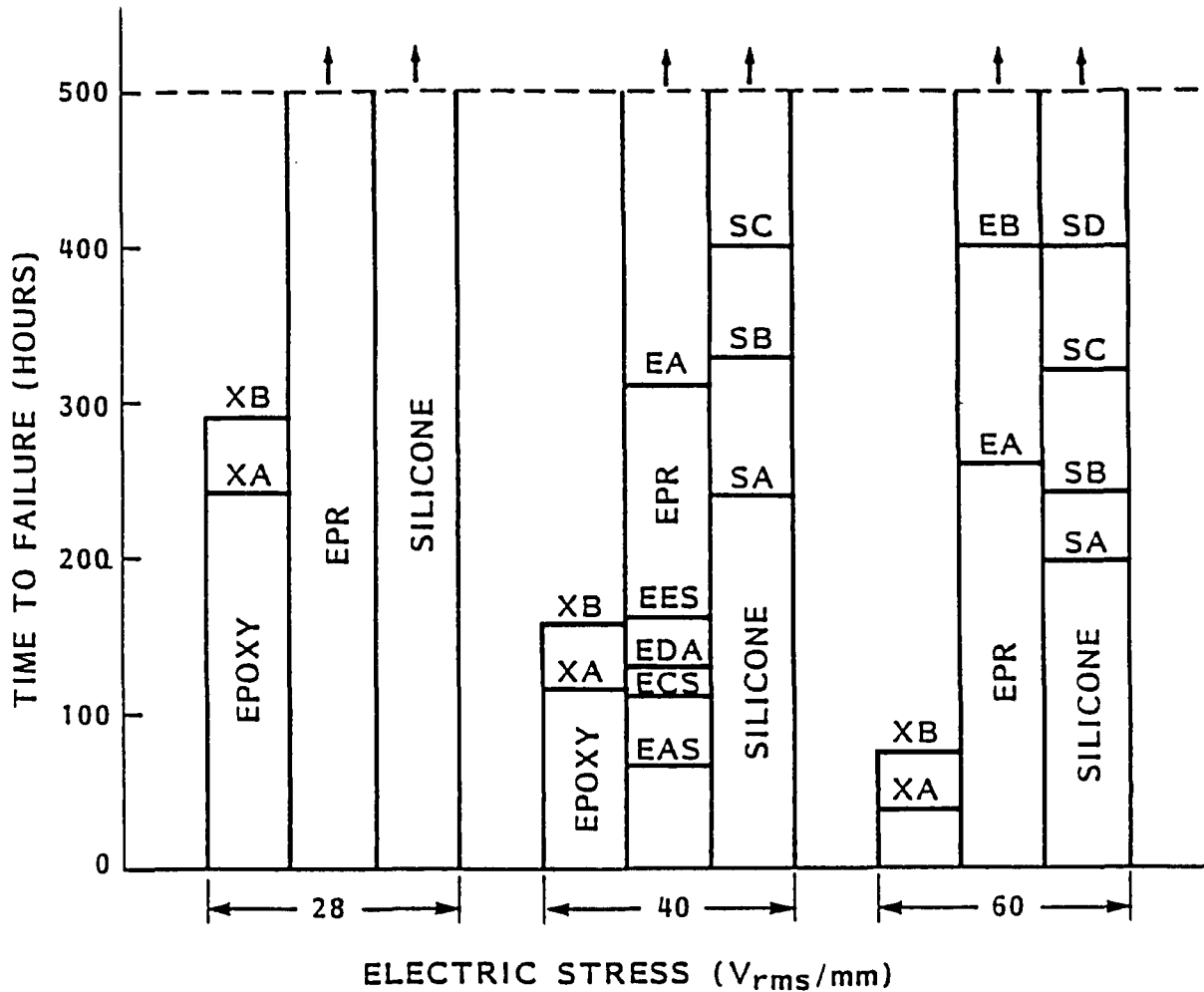


Figure 3.1: Time to Failure as a Function of Average Electric Stress in 1600 $\mu\text{S/cm}$ Fog.

above this level the order of performance was reversed.

3. The epoxy samples performed poorly in comparison to silicone rubber and EPR samples. This was the case despite the epoxy samples having higher levels of ATH filler.
4. Both EPR and silicone rubber samples showed a filler threshold level beyond which very little improvement in material performance was observed at constant elec-

tric stress. The ATH threshold level of 80 pph at 28V/mm stress increased to 105 and 130 pph for 40 and 60V/mm stress respectively.

5. Clearly, ATH filler imparts superior tracking and erosion resistance to EPR material than does silica or alumina filler.

3.5 Parameters Monitored to Obtain Information on Surface Aging

3.5.1 Introduction

It is expected that any changes in the surface of the material would be reflected by the leakage current and therefore this would give a good indication of material aging and subsequent failure. It was shown in preliminary experiments by Jolly [25] that the integral of the leakage current or the cumulative charge was linearly related to the weight loss due to dry band arcing. There were indications from outdoor tests [8] on ceramic and polymeric insulators that the number of peak current pulses above a preset threshold was dependent on the type of material which increased with time of exposure. As insulator flashover in contaminated environments is related to leakage current, if leakage current increases with time a corresponding decrease in the flashover voltage is to be expected.

The cumulative charge, number and amplitude of peak current pulses above a preset threshold, weight loss due to dry

band arcing and flashover voltage were monitored with the purpose of evaluating the effectiveness of each parameter to indicate surface aging and subsequent failure. The information about cumulative charge and the number and amplitude of current pulses above a preset threshold was obtained from the data acquisition system after every hour of the test. The samples were evaluated at an average electric stress of 40V/mm.

3.5.2 Cumulative Charge as an Index of Surface Aging

Leakage current is governed by the ability of materials to promote a continuous electrolytic film on the surface. Initially, due to the presence of a mold release agent, both silicone rubber and EPR samples showed very good water repellent properties and the average leakage current did not exceed 6mA. On the epoxy samples, because of their machined surface, a higher average leakage current (about 25mA) developed from the start of the test. However, higher leakage current (about 20mA) developed on the EPR and silicone rubber samples after 1 to 3 hours of exposure. On all materials the higher values of leakage current persisted for the duration of the test period.

The variation of cumulative charge with time for silicone rubber, EPR and epoxy samples is shown in Figs. 3.2, 3.3 and 3.4 respectively. It is evident from an examination of these figures that the cumulative charge does not really bring out the improved performance of these materials with increased

filler concentration. The variation of the cumulative charge with time is essentially linear both for the samples which passed and failed the test. This means that the average leakage current has a constant value throughout the test and does not increase near failure.

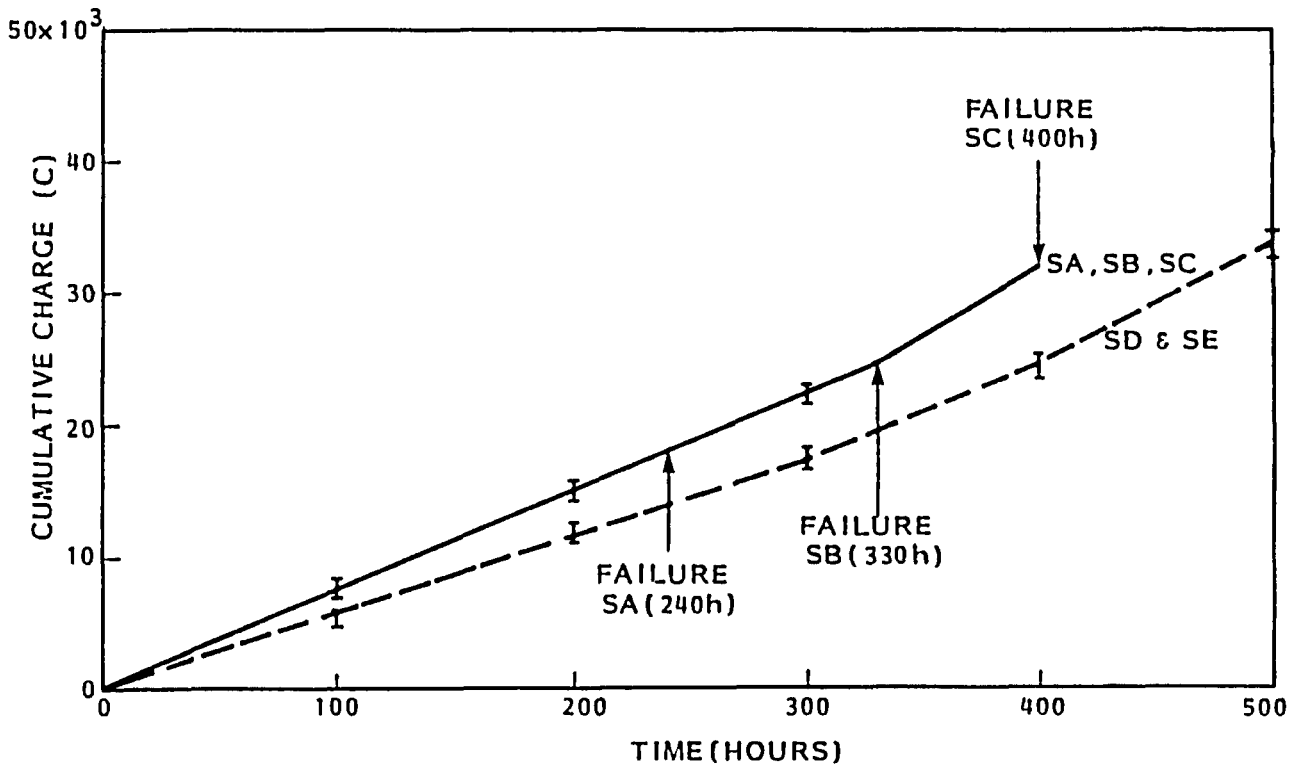


Figure 3.2: Cumulative Charge with Time for Silicone Rubber Samples.

Oscillographic monitoring of the samples during dry band arcing showed that on materials which did not track or erode a lower magnitude of current (typically a peak of 75 mA) was found to persist for a longer duration (typically 3 to 6 ms in each half cycle of the 60 Hz wave). In samples which began to track a higher magnitude of current (typically a peak of 150mA) was found to persist for a shorter duration

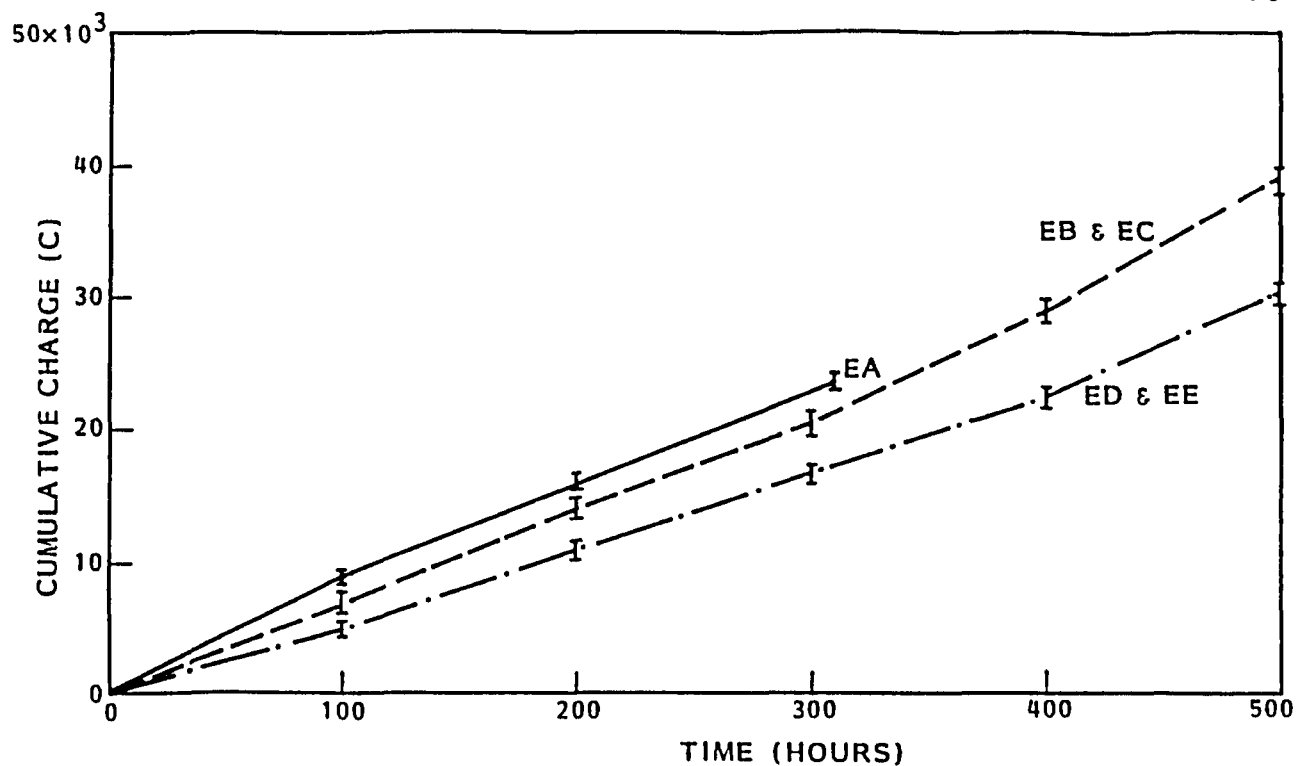


Figure 3.3: Cumulative Charge with Time for EPR samples.

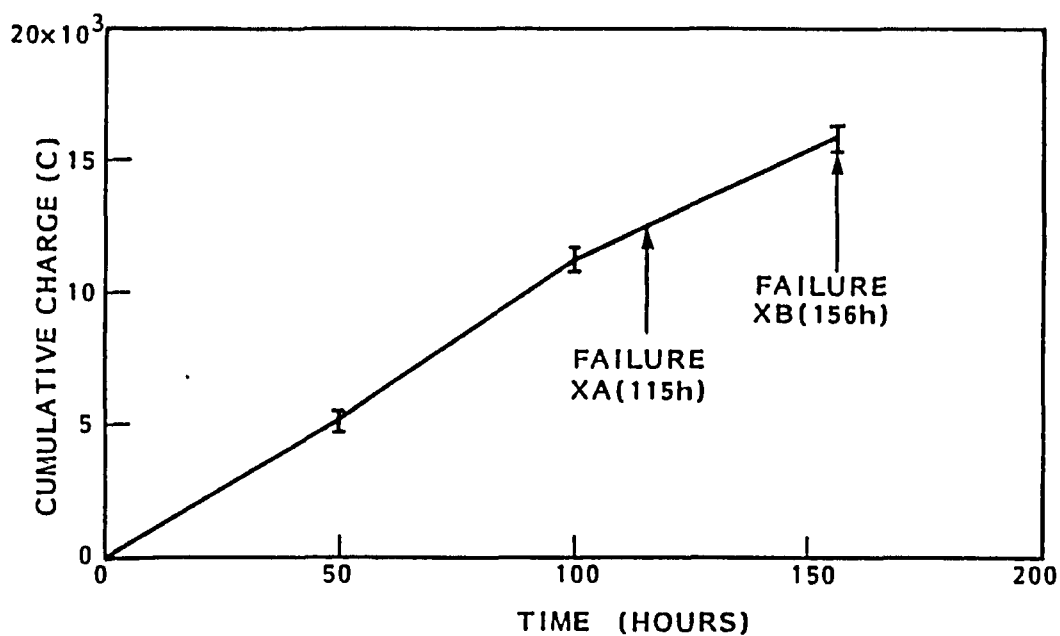


Figure 3.4: Cumulative Charge with Time for Epoxy Samples.

(1 to 3 ms in each half cycle of the 60 Hz wave). It was

also found that the tracked or eroded portion did not wet readily with water. This suggests that as the material begins to degrade, a higher inception voltage is necessary to establish dry band activity. The higher leakage current which follows gives rise to rapid dry band formation. Therefore, the average current essentially remains the same in both cases.

After the completion of the test, it was found that samples ED and EE had surfaces which were not markedly different in terms of roughness from the virgin samples. On the other hand, samples EA, EB and EC had surfaces which appeared weathered. As the surface roughness increases wetting, the leakage current and cumulative charge could be expected to be slightly higher for samples EA, EB and EC than for samples ED and EE as indeed found in the present study (Fig. 3.3).

3.5.3 Peak Current Pulses as an Index of Surface Aging

For materials which passed the test, the peak current did not exceed 100mA. On materials which failed by tracking or erosion leading to flashover, the peak current pulses above 150mA were registered about 4 to 5 hours prior to failure. The number of current pulses above 150mA also increased towards failure and is shown in Table 3.2. Therefore, this parameter gives an indication of surface aging.

Table 3.2: Peak Current Pulses Prior To Failure.

SAMPLE	FAILURE MECHANISM	HOURS PRIOR TO FAILURE	PEAK CURRENT (mA)	NUMBER OF PULSES >150 mA
SB	ELECTRICAL FAILURE	3	<150	0
		2	250	22
		1	>500	676
EA	TRACKING FAILURE	5	<150	0
		4	260	12
		3	300	1164
		2	>500	9368
		1	>500	38348
XA	TRACKING FAILURE	4	<150	0
		3	250	1588
		2	250	8840
		1	325	9604
XB	TRACKING FAILURE	4	<150	0
		3	260	1350
		2	290	9200
		1	325	11248

3.5.4 Flashover Voltage as an Index of Surface Aging

The variation in the flashover voltage with time of test for the three types of materials studied is shown in Figs. 3.5, 3.6 and 3.7. The flashover voltage was measured at the start and after every 100 hours of test. The experimental conditions of water flow rate and conductivity and air pressure were unchanged. To avoid possible variations due to sample positions in the chamber, the flashover voltage for all samples was determined at the same location in the chamber. The values reported are the average of at least five measure-

ments for which the variation in the flashover voltage was less than $\pm 3\%$.

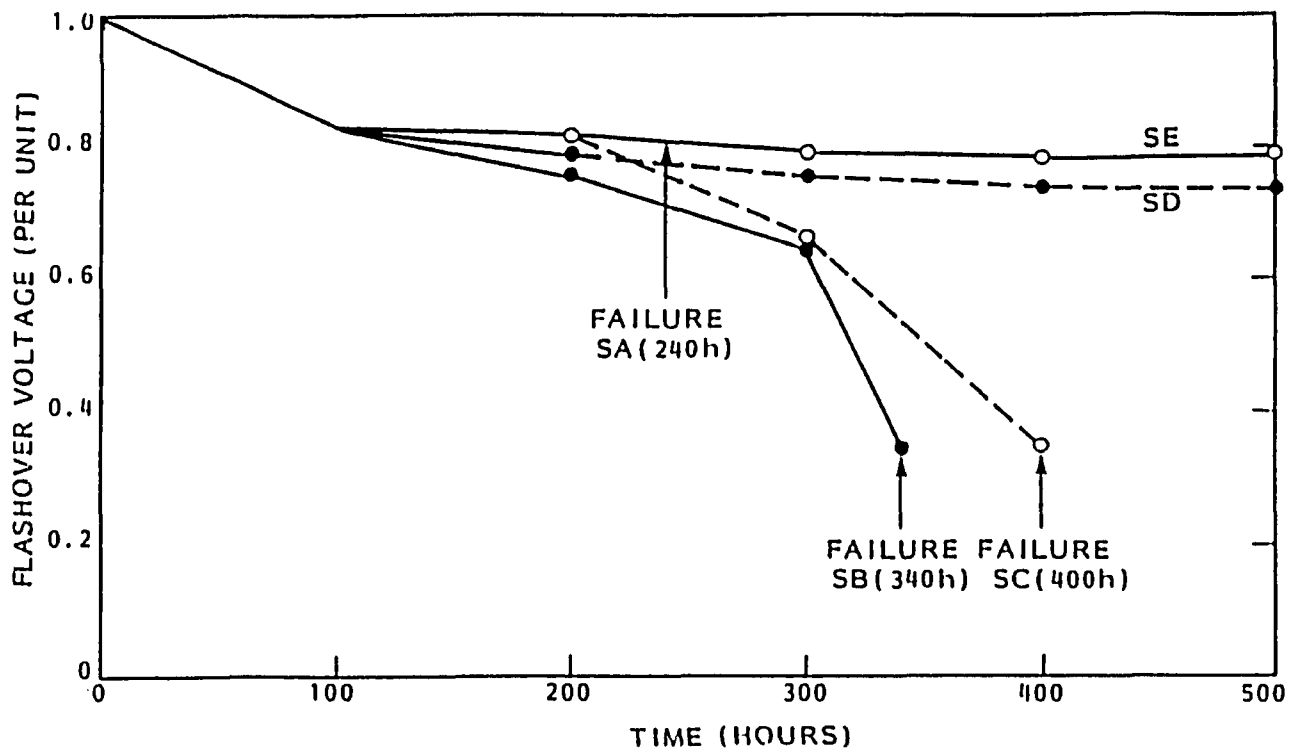


Figure 3.5: Flashover Voltage with Time for Silicone Rubber Samples. $1 \text{ pu} = 12.2 \text{ kV}_{\text{rms}}$.

The flashover voltage is dependent on the surface condition of the sample, the conductivity of the water, the separation between the two electrodes and the electrode geometry. At the start of the test, the silicone rubber and EPR samples which did not allow water filming had the same flashover voltage irrespective of the filler concentration (Figs. 3.5 and 3.6). However, the epoxy samples which permitted water filming exhibited a lower initial flashover voltage.

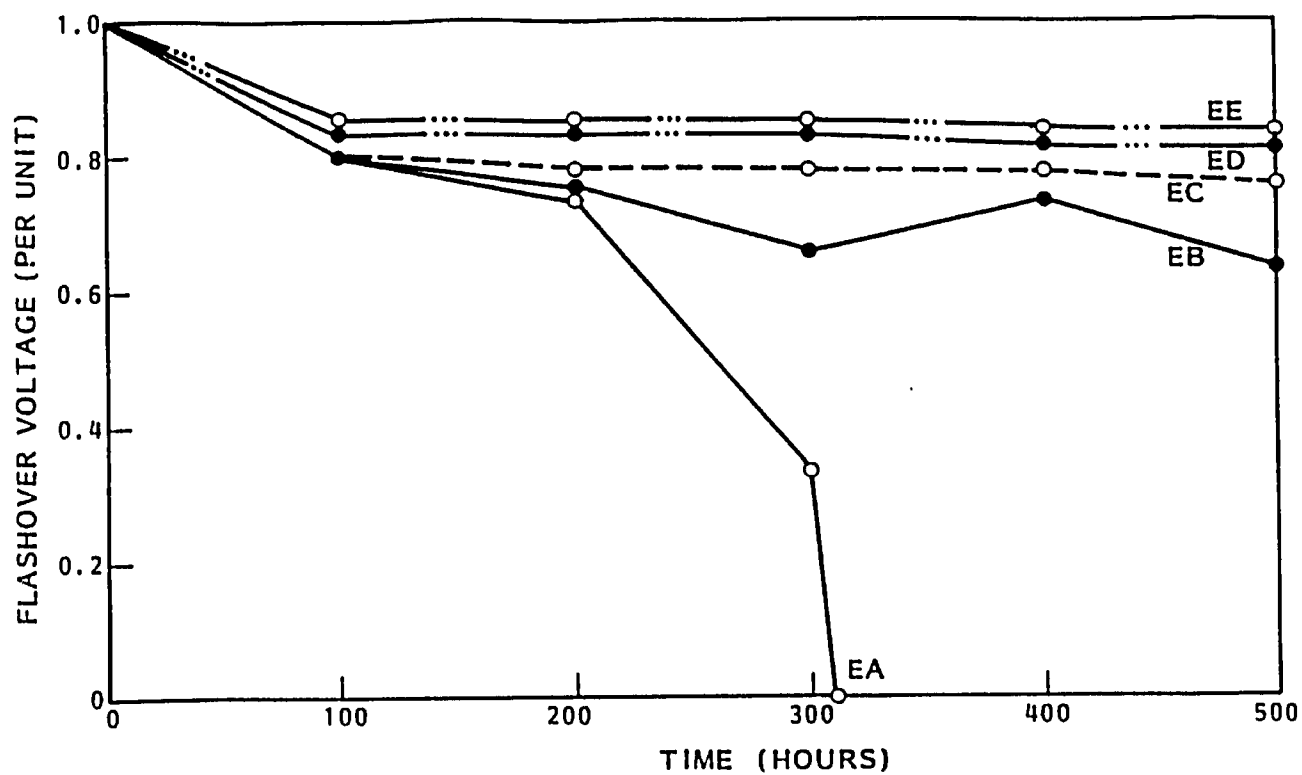


Figure 3.6: Flashover Voltage with Time for EPR samples. $1 \text{ pu} = 12.2 \text{ kV}_{\text{rms}}$.

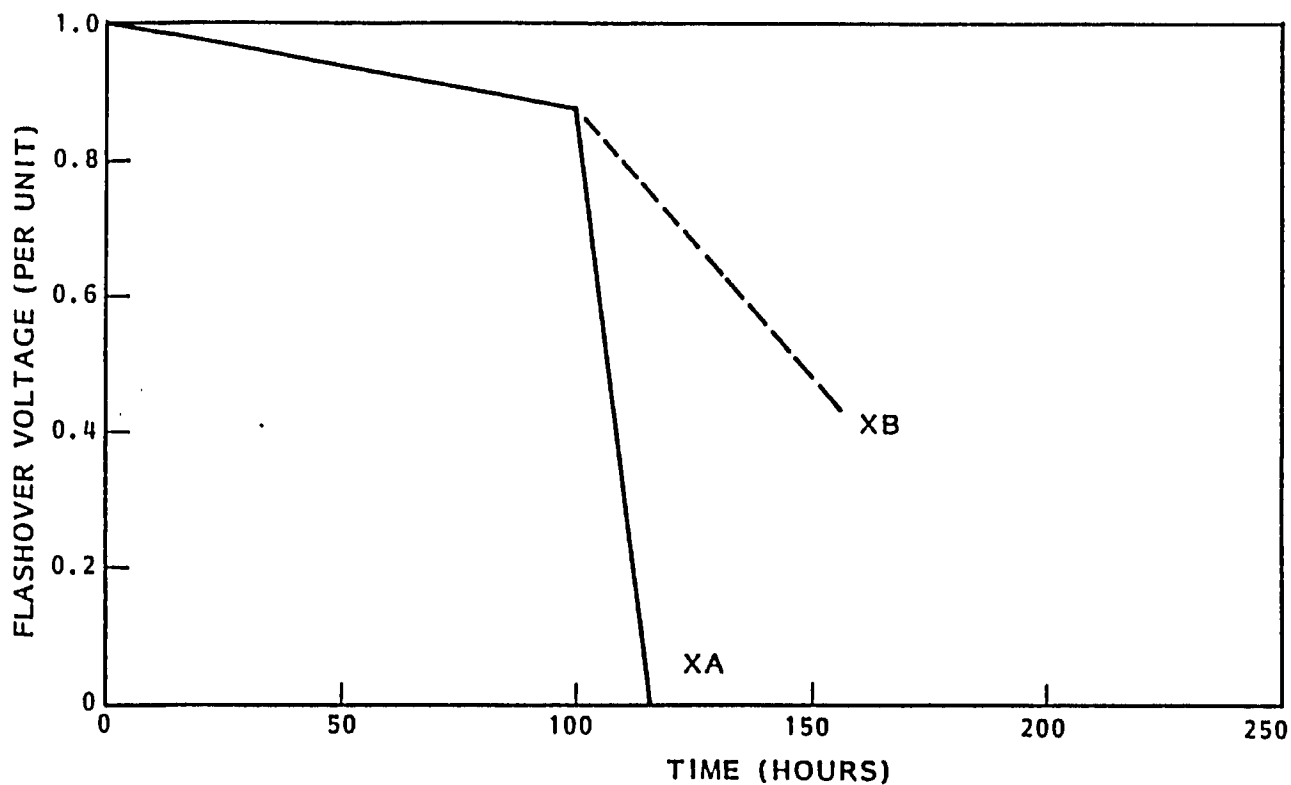


Figure 3.7: Flashover Voltage with Time for Epoxy Samples. $1 \text{ pu} = 9 \text{ kV}_{\text{rms}}$.

All the silicone rubber and EPR samples were found to wet out completely within 10 hours of exposure in the fog chamber to voltage stress. The reduction in the flashover voltage shown in Figs. 3.5 and 3.6 at 100 hours, is attributed to the change in the surface conditions of the samples which permitted water filming.

The reduction in the flashover voltage of the silicone rubber and EPR samples which passed the 500 hour salt fog test successfully was negligible between 100 and 500 hours (Figs. 3.5 and 3.6). A marked decrease in the flashover voltage was recorded for the silicone rubber samples SB and SC (Fig. 3.5). These samples failed due to the erosion extending along the entire length of the sample. The sample EA which tracked also showed a marked reduction in the flashover voltage just prior to tracking failure as can be seen from Fig. 3.6.

After 300 hours of test, track marks were produced on the surface of sample EB after three flashover measurements. These track marks caused a decrease in the flashover voltage at 300 hours as can be seen from Fig. 3.6. With further exposure, the carbon tracks were removed, probably by the physical action of the filler (discussed in chapter 5). This resulted in an increase in the flashover voltage when measured after 400 hours (Fig. 3.6).

The epoxy samples also showed a decrease in the flashover voltage as can be seen from Fig. 3.7. Initially, the samples

wetted out completely but the surface of the material was not water absorbent. The contact angle was measured and found to be about 90° . However, when these samples were inspected after 100 hours of exposure in the fog chamber, it was found that the surface absorbed water readily. The reduction of the flashover voltage measured at 100 hours shown in Fig. 3.7 is probably due to the thick water film on the surface.

An examination of Figs. 3.5, 3.6 and 3.7 reveals that the flashover voltage discriminates between materials that pass or fail the 500 hour aging test, but does not bring out the superior performance of the materials with increasing filler concentration. Materials which begin to track, where the weight loss would not be significant, show a sharp decrease in the flashover voltage.

The measurement of flashover voltage has the disadvantage that material degradation in the form of tracking or erosion could be initiated by the flashover and such samples on subsequent exposure to a relatively lower electric stress and fog could fail sooner. As this parameter did not give any valuable information about surface aging and subsequent failure it was not monitored in the rest of the experiments.

3.5.5 Weight Loss as an Index of Surface Aging

The measurements of the weight loss were done after every 20 hours of exposure in the fog chamber on a balance having a sensitivity of 0.1mg. The variation of the weight loss with time of test for the three types of materials tested is shown in Figs. 3.8, 3.9 and 3.10. For the silicone rubber samples which failed, the final weight loss was about 30%. Up to about 10 hours before failure, the weight loss was less than 1%. Rapid weight loss occurred within the last few hours of the test. The silicone rubber samples which passed the test showed less than 3% weight loss. It can be observed from Fig. 3.8 that the weight loss is lower in the samples having higher filler concentration.

The EPR samples which passed 500 hours of exposure showed a gradual weight loss with time (Fig. 3.9). The weight loss increased with decreasing filler concentrations. For these samples, the slight decrease in the flashover voltage appeared to be consistent with the increase in weight loss. The weight loss for the samples which failed by tracking (EA) was significantly more than for the samples which passed the test.

The epoxy samples showed very little (less than 1%) weight loss until hours prior to failure (Fig. 3.10). As for the silicone rubber samples which failed, failure of the epoxy samples was rapid.

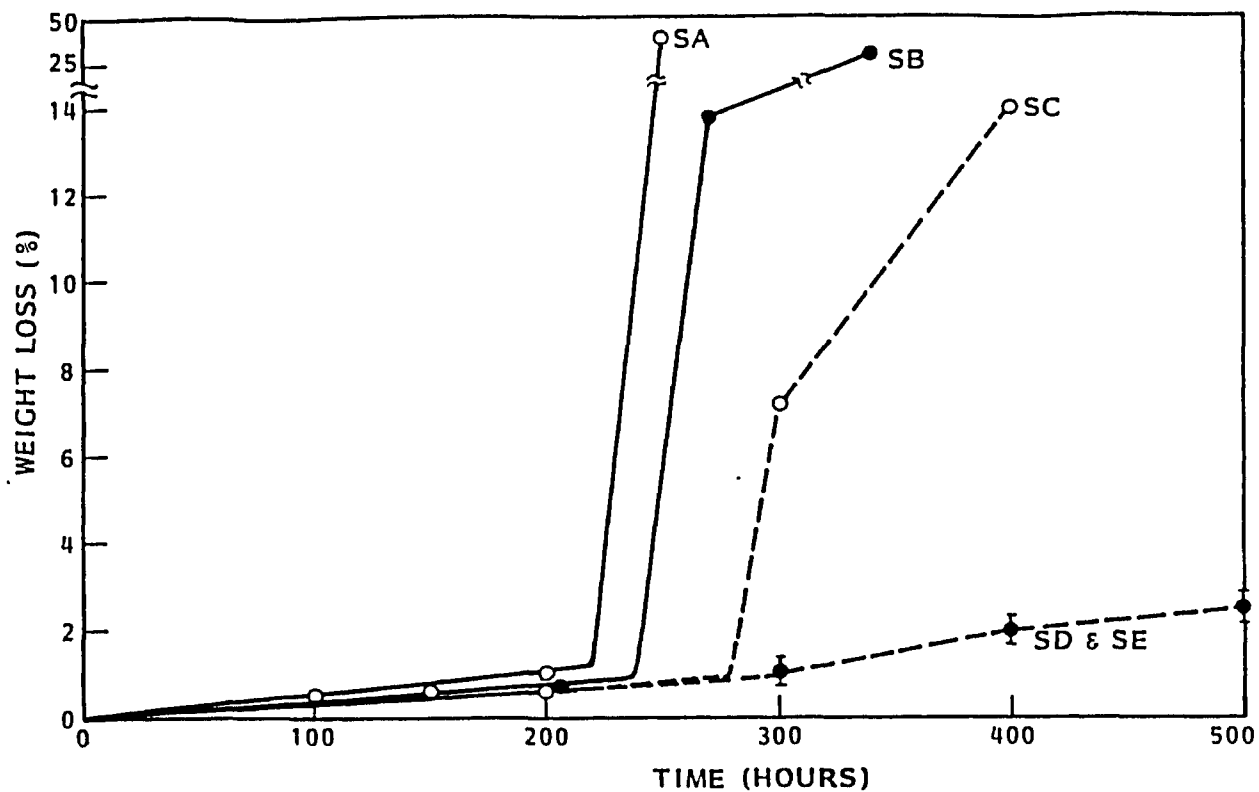


Figure 3.8: Weight Loss with Time for Silicone Rubber Samples.

A comparison of the weight loss and the flashover voltage for the three types of materials, shows that these two parameters are insufficient to describe the surface aging. In particular, these two parameters cannot predict the rapid failure observed in these samples.

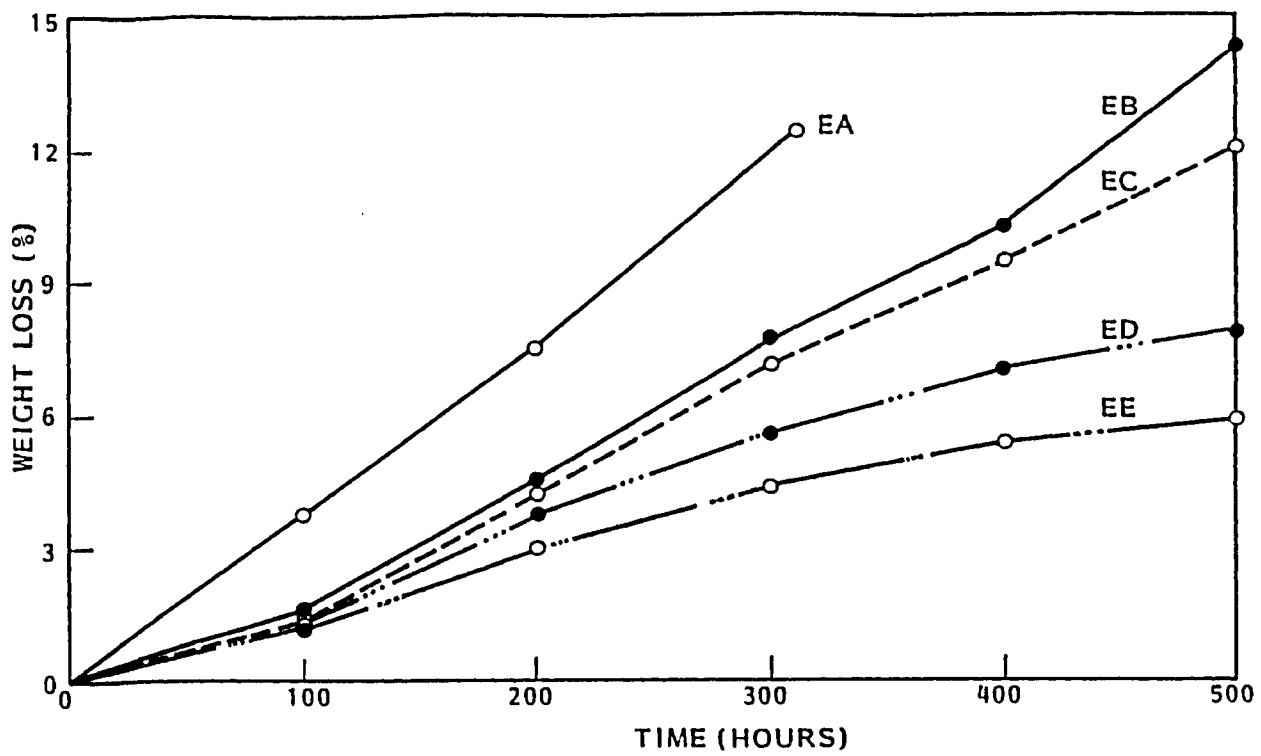


Figure 3.9: Weight Loss with Time for EPR Samples.

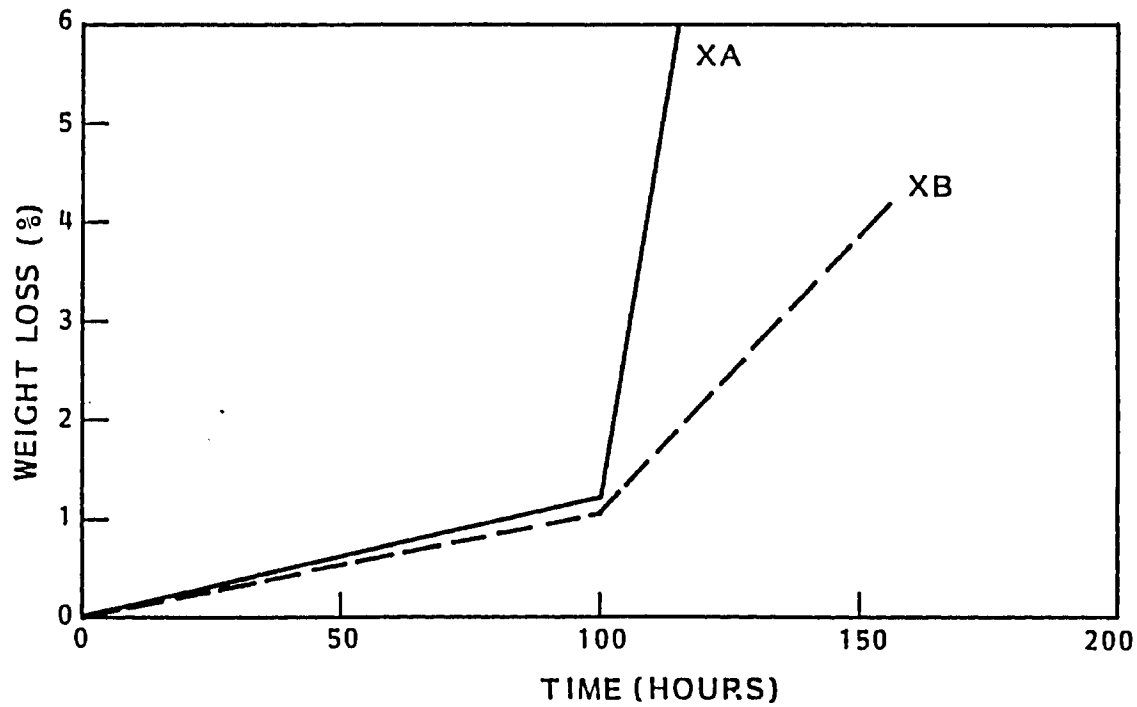


Figure 3.10: Weight Loss with Time for Epoxy Samples.

3.6 Weight Loss as a Function of Electric Stress

Fig. 3.11 shows the weight loss due to dry band arcing for the samples that passed the 500 hour test. The following points are evident:

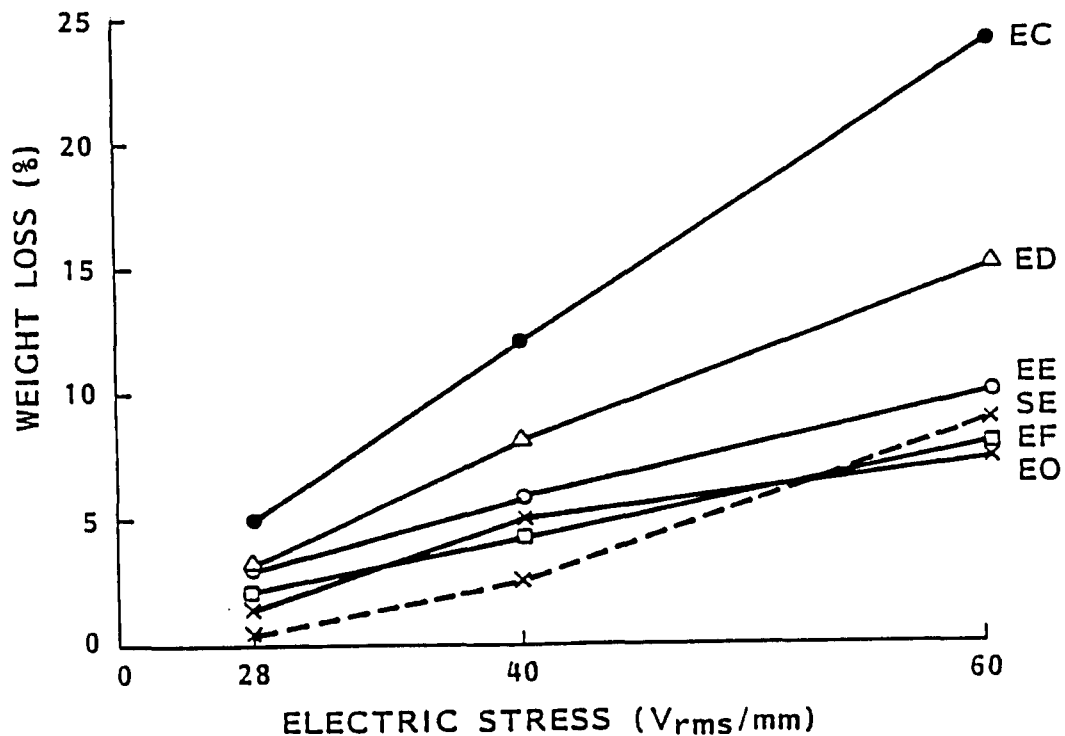


Figure 3.11: Final Weight Loss as a Function of Average Electric Stress.

1. The magnitude of the electric stress has a significant effect on the weight loss on EPR samples, increasing with increasing stress.
2. The concentration of filler has a marked effect on the weight loss on EPR samples, decreasing with increasing filler level.

Figs. 3.12, 3.13 and 3.14 show the material samples before and after the salt-fog test. The EPR samples which passed the test showed erosion which was more pronounced towards the bottom (ground) electrode as shown in samples EB and EC (Fig. 3.13). In the sample EA which tracked, the tracking failure was preceded by gradual increase in weight loss (10 to 25%, depending on the electric stress). In contrast, the silicone rubber samples which failed had very little weight loss (about 3%) when measured 1 to 10 hours prior to failure and thereafter degraded rapidly. SA, SB and SC in Fig. 3.12 show typical erosion failures of silicone rubber samples.



Figure 3.12: Silicone Rubber Samples Before and After Salt-Fog Test. UN: Sample Before Test.

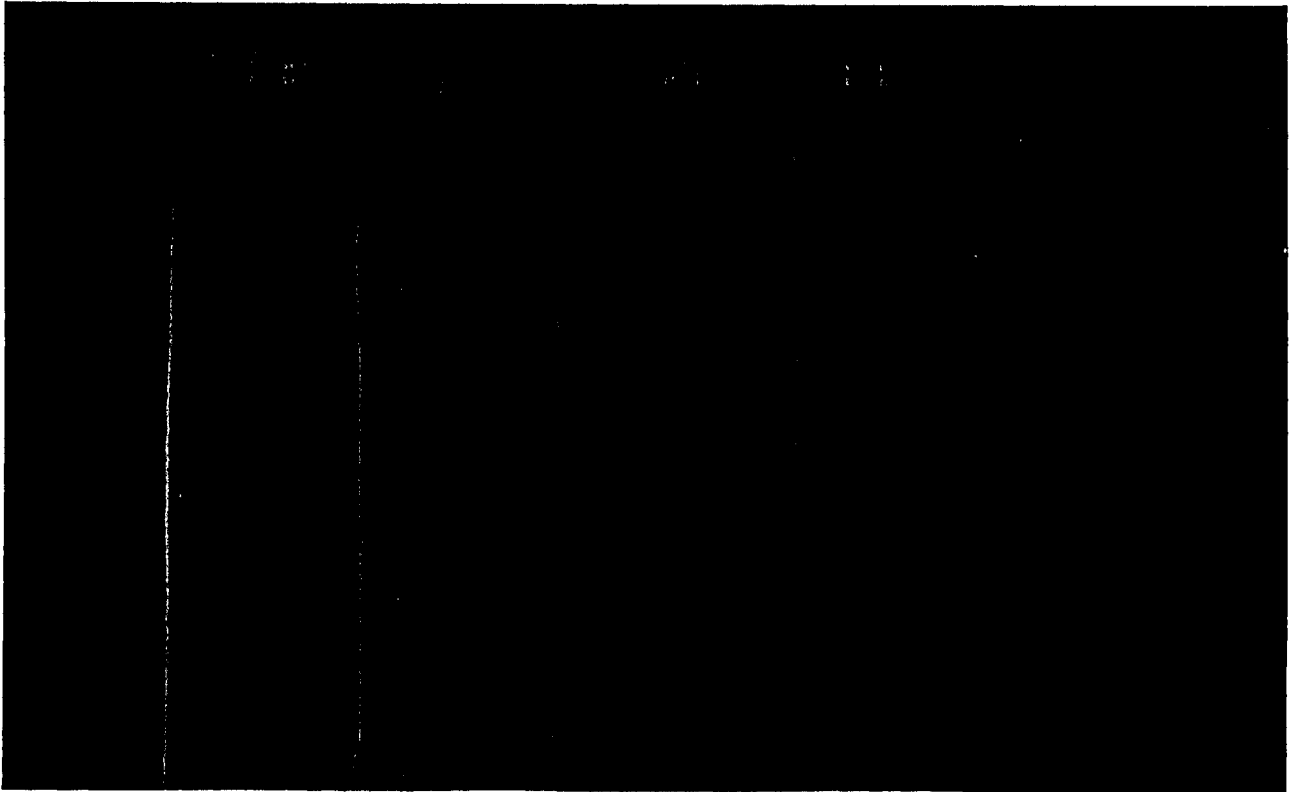


Figure 3.13: EPR Samples Before and After Salt-Fog Test.
UN: Sample Before Test.

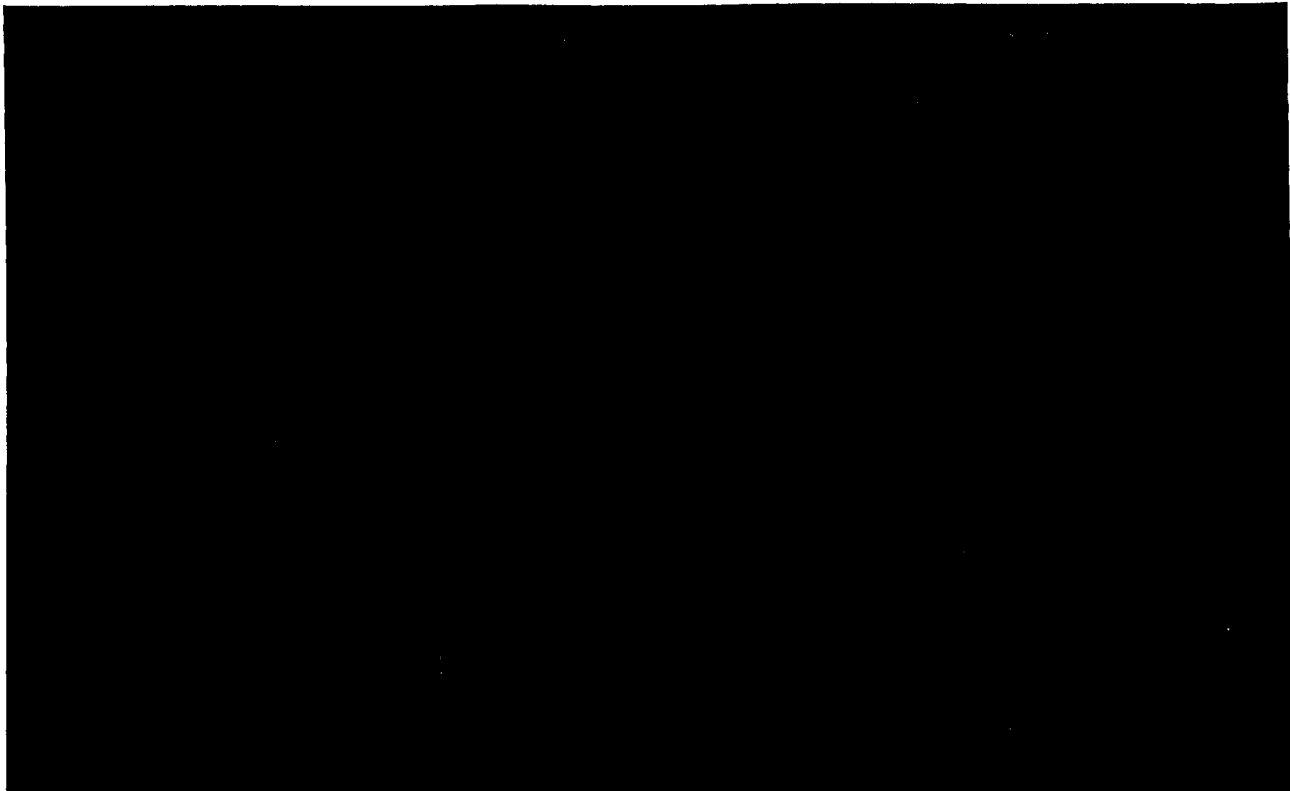


Figure 3.14: Epoxy Samples Before and After Salt-Fog Test.
UN: Sample Before Test.

3.7 Cumulative Charge as a Function of Electric Stress

The variation of cumulative charge with time of test is shown in Fig. 3.15. For clarity, plots for epoxy samples are not shown but were linear and about 20 to 30% higher than those shown for filled EPR and silicone rubber. The surface of the epoxy samples was found to become hygroscopic in less than 10 hours of exposure to salt-fog, thereby promoting a thicker electrolytic film on the surface. This accounts for the higher cumulative charge. It is evident that the cumulative charge, which is proportional to the energy dissipated during dry band arcing, is dependent on the magnitude of electric stress.

Plots 4, 5 and 6 in Fig. 3.15 are for the EPR sample EO containing no ATH filler. It is evident that the cumulative charge and therefore the leakage current is considerably lower than for samples of either EPR or silicone rubber that contain ATH filler. When these samples were removed after 500 hours of test, they showed no evidence of tracking. In addition, the weight loss due to dry band arcing was comparable to EPR sample EF containing 250 pph of ATH filler as shown in Fig. 3.11.

Fig. 3.11 shows that the weight loss in samples is reduced with increasing concentration of filler. Fig. 3.15

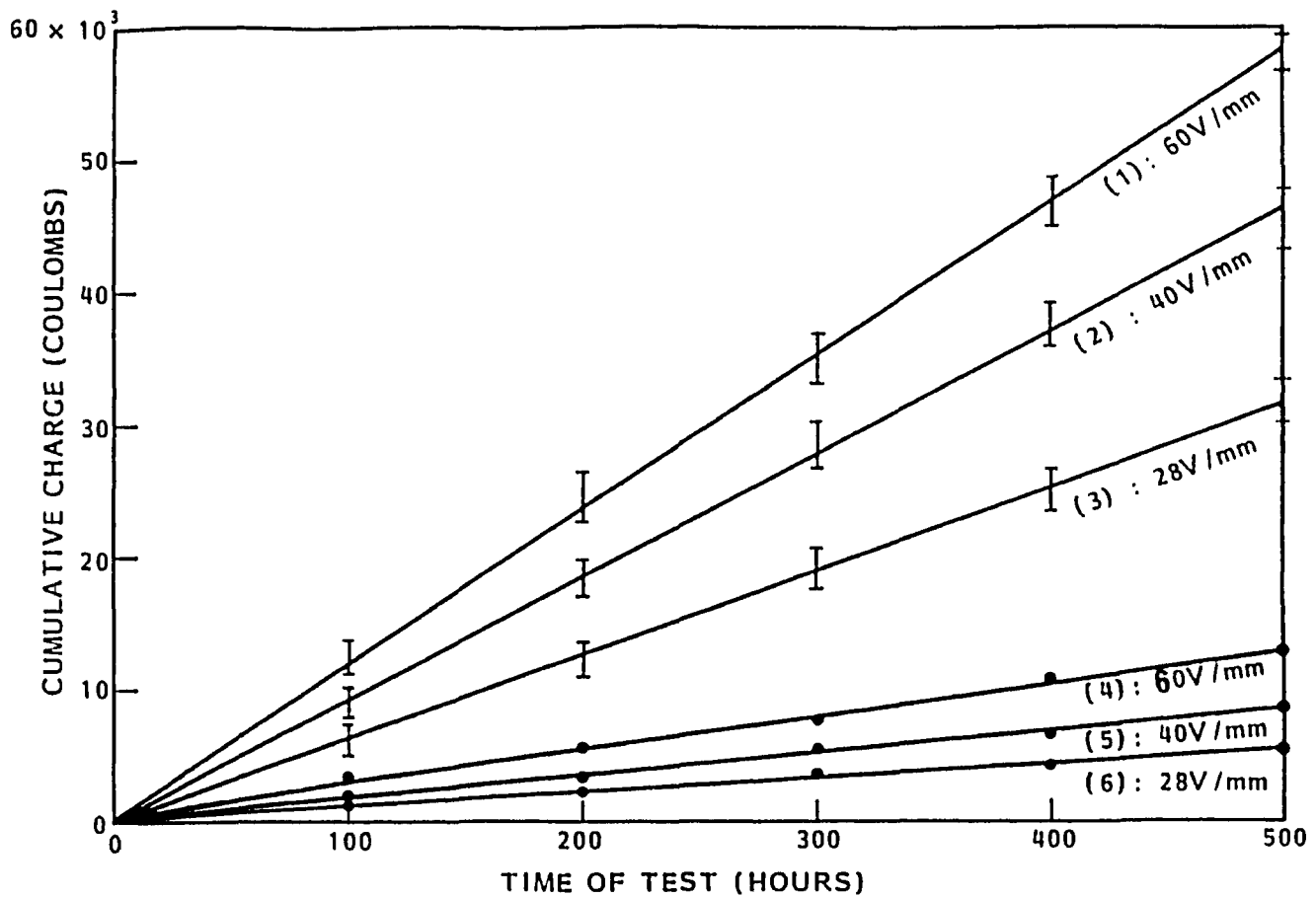


Figure 3.15: Cumulative Charge with Time as a Function of Average Electric Stress.

shows that the cumulative charge is constant. Therefore, the cumulative charge cannot be related to the weight loss as suggested by Jolly [25].

3.8 Correlation With Standard Accelerated Aging Tests

It is generally thought that polymeric materials when filled with substantial (>40% by weight) ATH filler simply erode and do not track. This is based on the results of ASTM tests [16,21]. The results of the fog chamber tests at 1600 $\mu\text{S}/\text{cm}$ tend to support this conclusion. To demonstrate this fur-

ther, the silicone rubber and EPR samples in Table 3.1 were also evaluated by the Tracking Wheel test [32] at Ontario Hydro. This test, in one form or another has been accepted by most utilities and manufacturers in North America as an effective screening test for materials to be used for outdoor applications. In this test, cylindrical rod samples placed as spokes of a wheel are subjected to an electric stress of 133 V/mm (20kV_{rms} applied across 150mm of sample length). The wheel rotation subjects the samples to a water spray of conductivity 356 $\mu\text{S/cm}$ once every 90 s. Materials enduring 1000 hours or more on the wheel are considered to be suitable for outdoor applications.

Table 3.3 compares the results of fog chamber tests at 40V/mm and the Tracking Wheel test. It can be seen that the results are in very good agreement. In particular, it must be noted that samples with above 80 pph (44% by weight) of ATH filler passed both tests. It was observed that the mechanism of material failure in both tests was identical. Good agreement between the results of Tracking Wheel and the standard ASTM tests has been reported earlier [32].

Table 3.3: Results From Fog Chamber and Tracking Wheel Test.

MATERIAL	IDENTIFI- CATION	ATH LEVEL (pph)	TIME TO FAILURE (HOURS)	
			Fog CHAMBER	TRACKING WHEEL
EPDM	EO	0	>500	924
	EA	30	310	860
	EB	60	>500	>1000
	EC	80	>500	>1000
	ED	105	>500	>1000
	EE	130	>500	>1000
HTV SILICONE RUBBER	SA	30	240	575
	SB	60	330	475
	SC	80	400	>1000
	SD	105	>500	>1000
	SE	130	>500	>1000

pph: PARTS PER HUNDRED OF POLYMER FORMULATION

3.9 Material Performance as a Function of Water

Conductivity

3.9.1 Need For Such A Study

Good agreement between the results of fog chamber tests at high conductivity and standard accelerated aging tests could be due to the fact that in all these tests, the experimental conditions of electric stress, water conductivity and/or wetting are more severe than those encountered on outdoor insulators. A high leakage current is promoted in a very short time which gives rise to intense dry band activity. This rapidly converts the hydrophobic surface of all polymer materials to a hydrophilic surface and is responsible for

the results to be obtained in a relatively short time (typically in a few minutes to a few hours). Therefore, the outcome of these tests are more dependent on the filler type and concentration than on polymer type and generally materials with greater than 40% by weight of filler show high arc resistance in these tests [32]. It was discussed in Section 1.3.2 that these tests are not entirely representative of service experience. Therefore, such tests have to be used with caution.

Insulator flashover, tracking and erosion are all related to leakage current. Tracking and erosion are initiated by dry band arcing which produces local surface temperatures above 200 °C [21]. Inorganic fillers are added to impart tracking and erosion resistance. However, if a material has the ability of limiting leakage current below that which results in local surface temperature which causes polymer degradation, then for such materials the choice of filler type and concentration becomes less important. For insulators made from such materials, flashover is also reduced due to the low leakage current. Materials which do not have the same capacity to suppress leakage current need substantial (>40% by weight [21]) filler to minimize tracking or erosion.

Fog chamber tests using 200 $\mu\text{S}/\text{cm}$ conductivity water have shown that continuous dry band arcing on silicone rubber material took considerably longer time to be established

when compared to porcelain [33]. This may suggest that the various materials have a different capability of suppressing leakage current. Therefore, a better evaluation of materials may be possible if the materials were subjected to test conditions which produce a gradual increase in leakage current with time, as occurs in service, rather than to test conditions which produce high leakage current right from the start of the test, as is the case in normal laboratory tests. Therefore, a study was initiated to examine the conditions which are believed to contribute to the contradiction between service experience and accelerated aging tests.

3.9.2 Samples

The samples evaluated are shown in Table 3.4. The silicone rubber samples were supplied by a different source and therefore they have been identified in a different manner. The identification of the EPDM samples has been changed accordingly although these samples and those in Table 3.1 were supplied by the same source. Cylindrical rod samples of glazed and unglazed porcelain were also evaluated for comparison of leakage current data. All samples were 25mm diameter rods and 150mm in length.

3.9.3 Experimental Conditions

All samples were subjected to an average electric stress of 60V/mm and evaluated at two levels of water conductivity - 250 $\mu\text{S/cm}$ and 1000 $\mu\text{S/cm}$. An exposure time of 480 hours obtained in 30 cycles was found to be sufficient to bring out the relative performance of the materials studied. In each cycle, the samples were subjected to electric stress and fog continuously for 16 hours for the first part of the cycle. For the next part of the cycle, the voltage and fog were switched off for 8 hours. The 8 hour period was selected on the basis that silicone rubber recovers its surface hydrophobicity which is lost during dry band arcing [34].

For the low conductivity fog test, tap water of conductivity 250 $\mu\text{S/cm}$ was used. The water was changed after every 3 cycles. During the high conductivity (1000 $\mu\text{S/cm}$) test, a fresh solution of salt water was prepared after every 7 cycles. To ensure similar wetting conditions for all the samples, the position of the samples was interchanged after every cycle.

3.9.4 Time to Failure.

Table 3.4 shows the time to failure in 250 and 1000 $\mu\text{S/cm}$ fog from which the following can be noted:

Table 3.4: Time to Failure in Low and High Conductivity Fog.

The silicone rubber samples were supplied by Dow Corning Corporation, Midland, Michigan; The EPDM samples were supplied by National Rubber, Toronto, Ontario.

MATERIAL	IDENTIFICATION	FILLER		TIME TO FAILURE (HOURS) FOR WATER CONDUCTIVITY	
		TYPE	LEVEL (pph)	250 μ S/cm	1000 μ S/cm
EPDM	EO	NONE	0	92	> 480
	E30A	ALUMINA TRIHYDRATE ATH ($Al_2O_3 \cdot 3H_2O$)	30	140	165
	E120A		120	352	> 480
	E200A		200	> 480	> 480
	E250A		250	> 480	> 480
	E105A	ALUMINA (Al_2O_3)	105	300	150
	E30S	SILICA (SiO_2)	30	130	70
	E130S		130	330	160
E250S	250		> 480	> 480	
HTV SILICONE RUBBER	S5S	SILICA	5	> 480	13
	S30S		30	> 480	15
	S120A	ATH	120	> 480	336
	S200A		200	> 480	> 480
PORCELAIN	GLAZED	NONE	0	> 480	> 480
	UNGLAZED	NONE	0	> 480	> 480

pph: PARTS PER HUNDRED OF POLYMER FORMULATION

3.9.4.1 Low (250 μ S/cm) Conductivity Fog

1. There were no failures of silicone rubber samples.
2. EPDM samples with up to 130 pph of ATH or silica filler failed by tracking.

3. At the same filler concentration, ATH, alumina and silica fillers impart similar resistance to tracking in EPDM material as judged by the similar times to failure. This indicates that the water of hydration in ATH filler does not contribute to the tracking resistance in EPDM material in low conductivity fog.
4. A filler level of 200 pph can be considered as the minimum filler level for satisfactory performance of EPDM samples whereas for the silicone rubber samples the filler level required is considerably lower.

3.9.4.2 High (1000 $\mu\text{S}/\text{cm}$) Conductivity Fog

1. Unfilled and filled EPDM samples had longer times to failure than the correspondingly filled silicone rubber samples.
2. ATH filler imparts much better resistance to tracking and erosion to EPDM material than does alumina or silica filler as judged by the longer times to failure. This indicates that the water of hydration of ATH filler contributes significantly to the tracking and erosion resistance of EPDM material in high conductivity fog.
3. An ATH level of 120 pph seems to be the threshold level in EPDM material whereas in silicone rubber, about 200 pph seems to be the ATH threshold level.

3.9.5 Leakage Current and Cumulative Charge

3.9.5.1 Low Conductivity Fog.

Silicone rubber and EPDM samples were hydrophobic and the porcelain samples were hydrophillic before the test. The surface of the EPDM samples was rendered hydrophillic due to dry band arcing in about 1 hour. But it took about 60 to 70 hours for the hydrophobic surface of the silicone rubber samples to be converted to a hydrophillic surface. This transition was indicated by an increase in the average leakage current from about 0.5 to 5 mA. The variation of cumulative charge with time (cycles) is shown in Fig. 3.16 from which the following can be noted:

1. EPDM samples (both filled and unfilled) had substantially higher cumulative charge than porcelain or silicone rubber.
2. The variation of cumulative charge with time was linear both for the samples that passed and failed the test.
3. The silicone rubber samples S30S and S200A with widely varying amount of filler had very similar cumulative charge. This suggests that there is no correlation between the filler level and leakage current in low conductivity fog.

It was observed that there was a scale deposit (Fig. 3.17) formed on the surface of all the samples. This was identified by EDAX (Energy Dispersive X-ray Analysis [39])

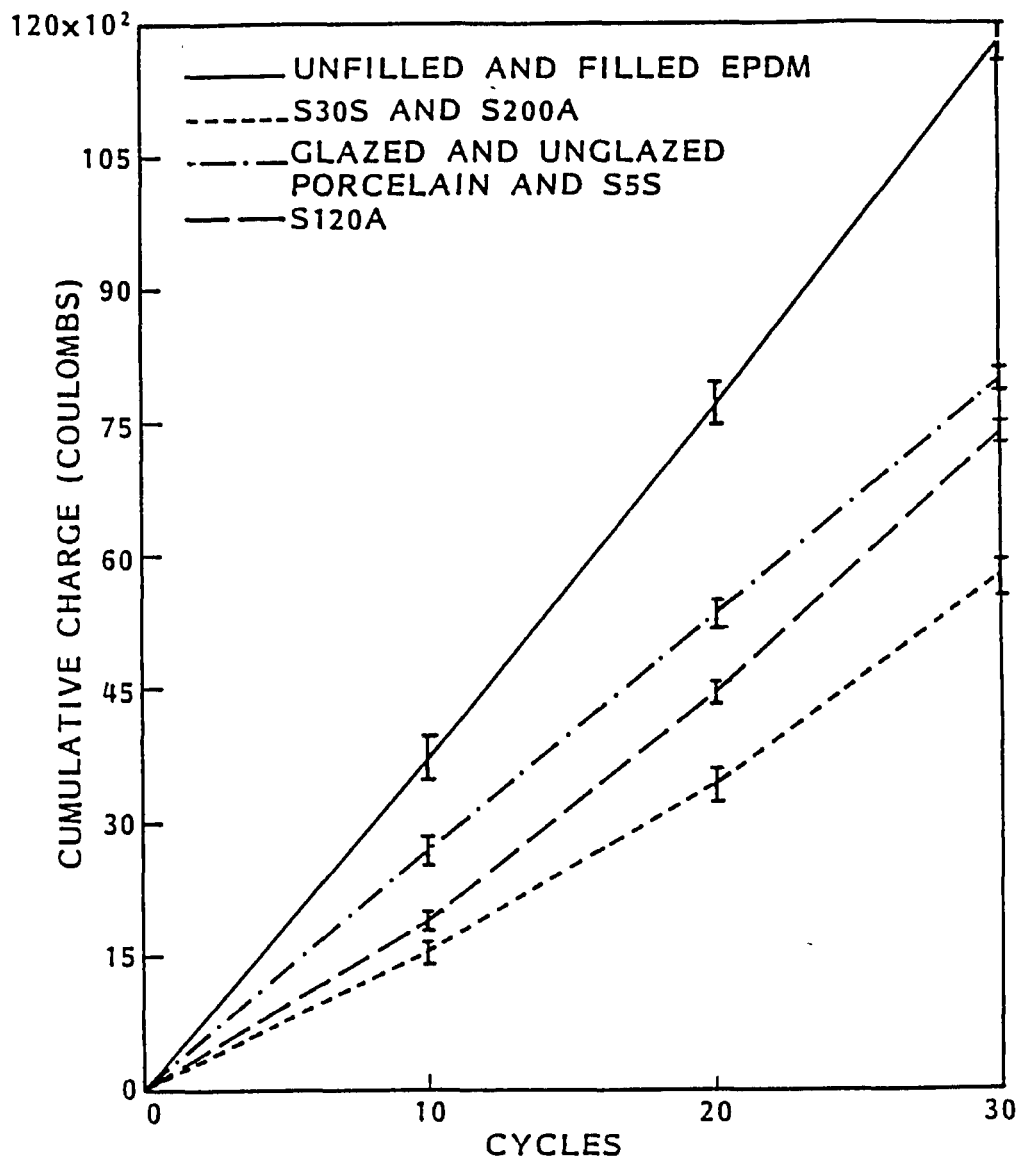


Figure 3.16: Cumulative Charge with Time in Low Conductivity Fog.

and Infra-Red spectroscopic techniques as carbonates of calcium and magnesium which remain on the surface when tap water is boiled off due to dry band heating. The surface area covered by the deposits was visibly less on the silicone rubber samples S30S and S200A and greater on all EPDM samples. On all other samples the extent of the scale deposits was in between these extremes.

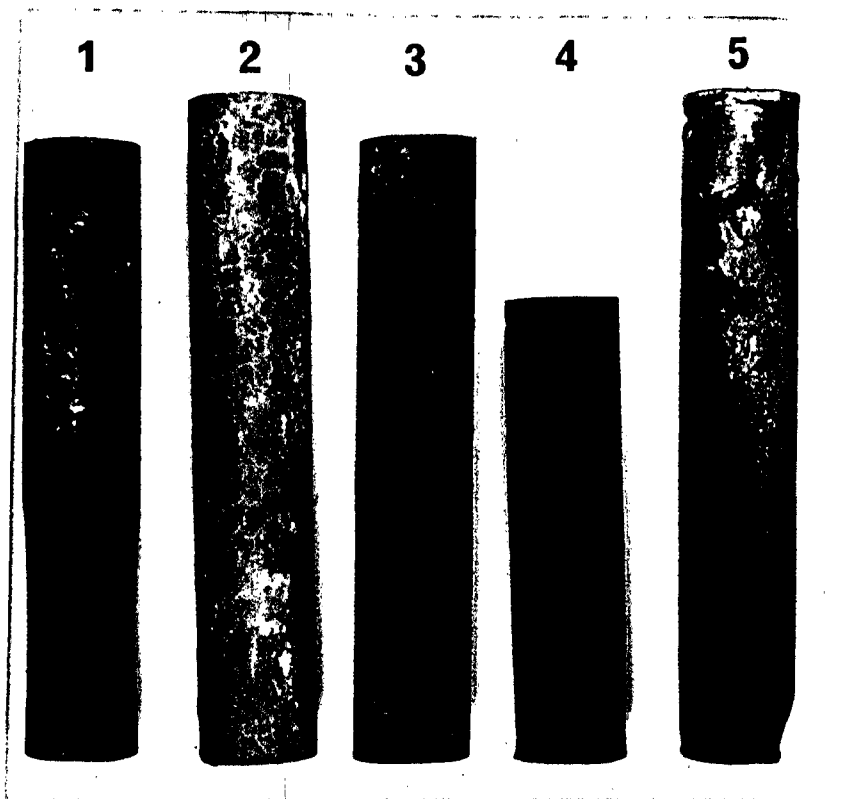


Figure 3.17: EPDM Samples Before and After Low and High Conductivity Test. 1. Tracking of sample EO in low conductivity fog; 2. Heavily deposited sample E250A in low conductivity fog; 3. Tracking failure of sample E120A in low conductivity fog; 4. Clean surface of sample EO in high conductivity fog; 5. Relatively clean surface of sample E250A in high conductivity fog.

The variation in the number of current pulses above a preset threshold is shown in Fig. 3.18. It can be seen that the number of current pulses above 15mA steadily increased with time of exposure and was considerably greater for the EPDM samples than for silicone rubber or porcelain. It was also observed that the highest peak current increased from 20 to 50mA in the last 4 to 5 hours prior to failure of the EPDM samples. It appears that the deposition of scales on

the surface of materials increases the leakage current and the number of current pulses above a preset threshold.

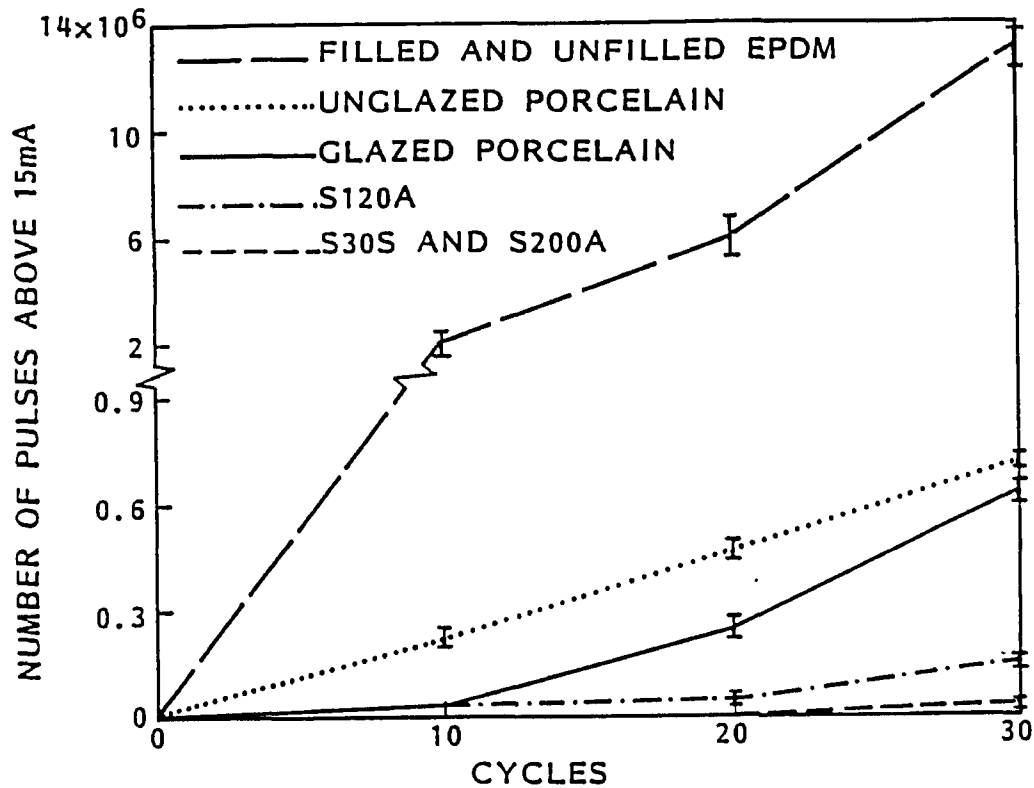


Figure 3.18: Count of Peak Current Pulses above 15mA.

3.9.5.2 High (1000 $\mu\text{S}/\text{cm}$) Conductivity Fog.

It was observed that the hydrophobic surface of the silicone rubber and EPDM samples was converted to a hydrophillic surface in 1 to 2 hours of exposure. The dry band arcing was observed to be extremely energetic and as a result the scale deposition on the samples was very minimal (Fig. 3.17). The variation of cumulative charge with time is shown in Fig. 3.19 from which the following can be noted:

1. Filled silicone rubber and EPDM samples had higher cumulative charge than porcelain.

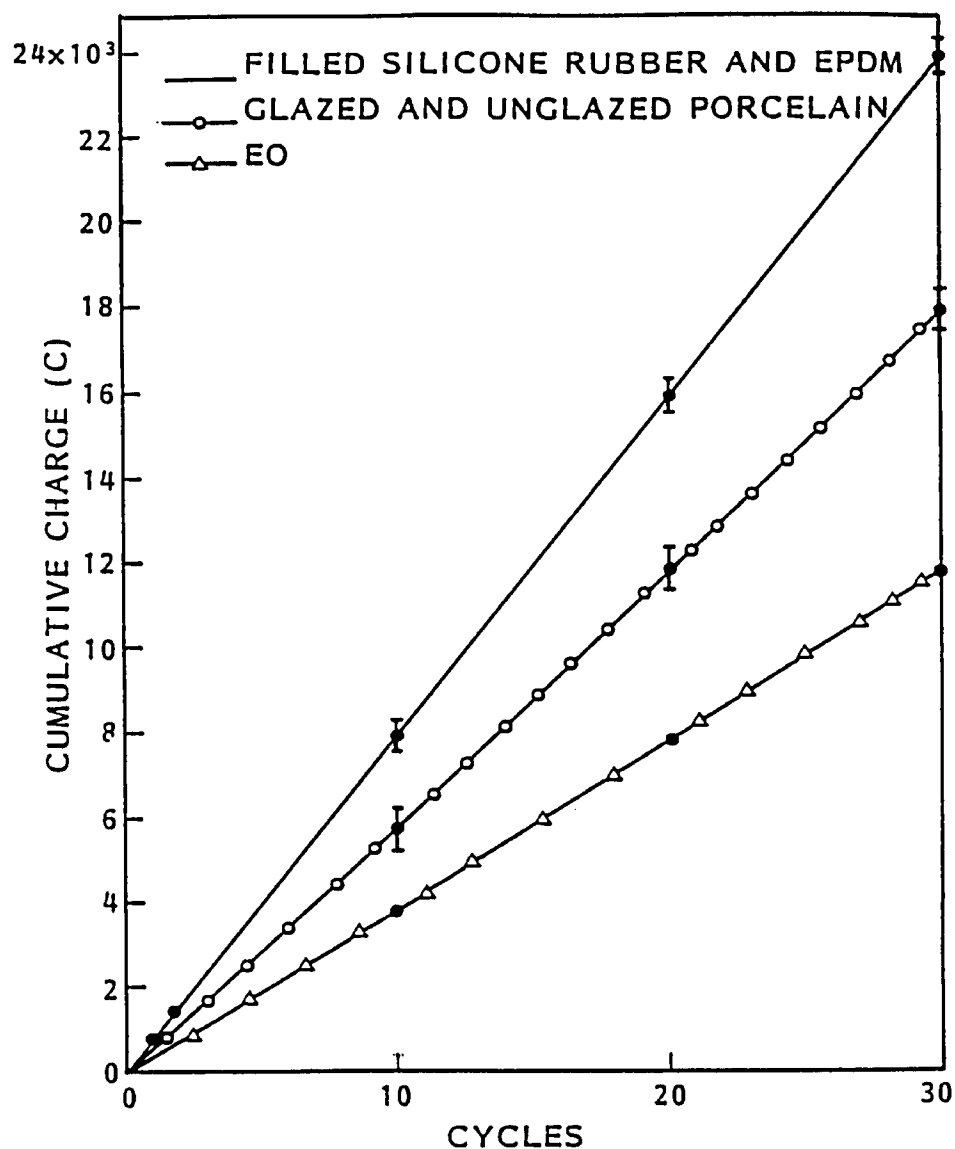


Figure 3.19: Cumulative Charge with Time in High Conductivity Fog.

2. The concentration of filler from 5 to 250 pph did not affect the magnitude of cumulative charge.
3. The variation of cumulative charge with time was linear both for the samples that passed and failed the test.

4. Unfilled EPDM samples had the lowest cumulative charge. This suggests that the presence of inorganic filler or scale deposit contributes to the increased leakage current in EPDM material.

3.9.6 Weight Loss as a Function of Water Conductivity

The weight loss due to dry band arcing was measured after every cycle. At low (250 $\mu\text{S}/\text{cm}$) water conductivity, the samples which passed the test had no weight loss. The samples that failed the test also had no weight loss when measured one cycle prior to failure. However, the ATH filled EPDM samples and the silicone rubber sample S200A which passed the test showed a gradual erosion with time of test. These samples were evaluated at 1600 $\mu\text{S}/\text{cm}$ and all other experimental conditions remained the same.

Fig. 3.20 shows the variation of the final weight loss with water conductivity. It can be seen that the final weight loss increases with increasing water conductivity and decreasing filler concentration.

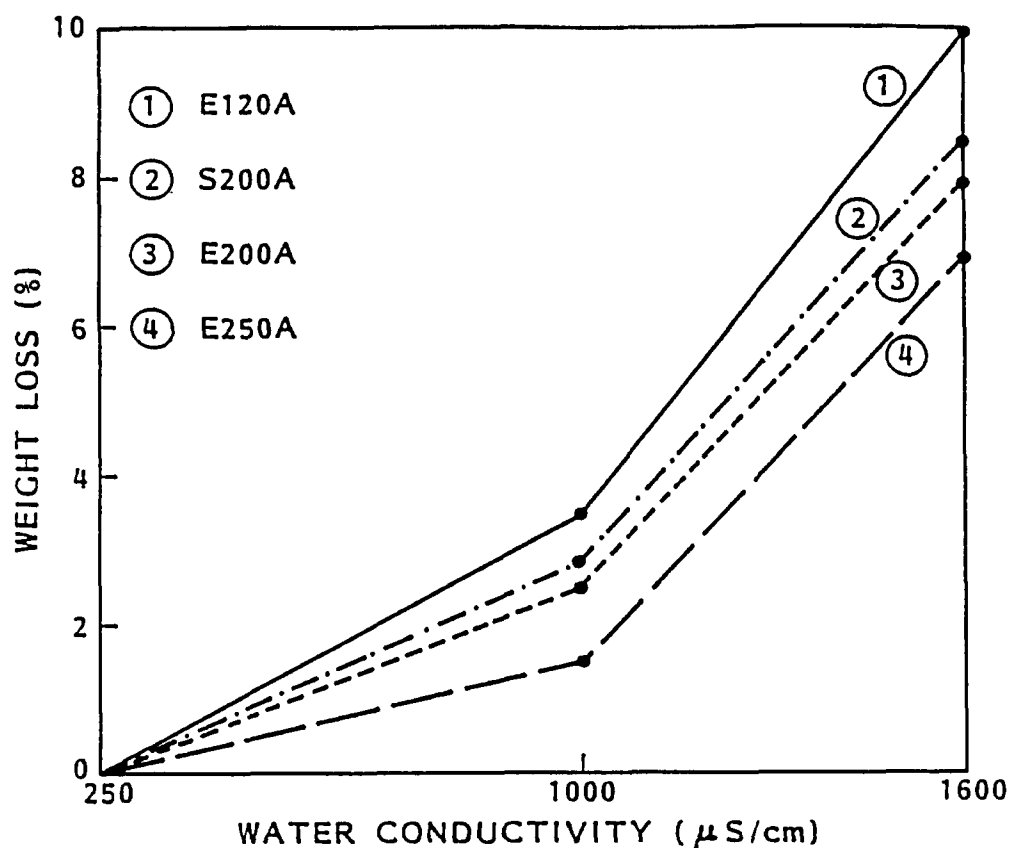


Figure 3.20: Final Weight Loss as a Function of Water Conductivity.

3.10 Correlation of the Results of Low Conductivity Fog Test with Service Experience

Leakage current on outdoor insulators is initially very low. The build up of contaminants, which is inevitable in outdoor environments, is responsible for increasing the thickness of the surface electrolytic film and hence increasing the leakage current. For laboratory tests to be representative of service experience it is necessary that the tests simulate the gradual increase of leakage current. In the low conductivity fog test, the leakage current is initially very low

and similar for silicone rubber and EPDM due to the relatively low electric stress, water conductivity and the hydrophobic surface of the materials. The polymer type is shown to have a considerable effect on the growth of leakage current. The silicone rubber samples maintain their hydrophobic surface for a much longer time than the EPDM samples. The leakage current increases because of the loss of surface hydrophobicity and the subsequent formation of water scales which increases the thickness of the surface electrolytic film.

It can be seen from Table 3.4 that although the filler level in the samples S5S and S30S was low, they passed the low conductivity test. This is due to the good leakage current suppression capability of silicone rubber. The successful performance of such insulators in the field has also been attributed to the same reason [11]. But these samples failed very quickly in the high conductivity test and such materials have also failed quickly in the Tracking Wheel test [3], due to the unrealistic rate at which dry band arcing is promoted.

The ranking of materials obtained from the low conductivity fog test, that silicone rubber performs better than the EPDM material is similar to that obtained from outdoor tests [23] and service experience [11].

The above illustrations indicate that evaluating the materials in low rather than in high conductivity fog yields

results which are in better agreement with service experience.

3.11 Effect on Certain Simulated Environmental Degrading Factors on the Tracking and Erosion Resistance of Materials

3.11.1 Resistance to Moisture Ingress.

Outdoor insulators are exposed to moisture in the form of rain, dew or high humidity. Moisture can attack polymeric insulation in a number of ways [35], but the most serious damage caused by moisture ingress is due to hydrolysis (depolymerization) of polymer chains, thereby causing the material to lose its mechanical and electrical strengths. In fact, it was hydrolysis which was responsible for failure of some of the earlier epoxy insulators [14]. As a part of the minimum requirement for materials to be considered for outdoor insulators, it has been specified [3] that materials when subjected to boiling water at 100 °C for 100 hours should not gain weight in excess of 5%. Based on this work, the samples in Table 3.1 were sealed individually with distilled water in glass tubes and subjected to 100 °C for 100 hours in an oven. After the test it was found that all the samples had a slight weight increase of about 1%. The hydrophobicity of silicone rubber and EPR samples was found to be unaffected by exposure to boiling water.

These samples were subjected for 500 hours in the fog chamber at 40V/mm stress and 1600 $\mu\text{S}/\text{cm}$ water conductivity. It was found that the time to failure, weight loss and the cumulative charge was within $\pm 5\%$ of the corresponding quantities for the virgin samples. This suggests that the tracking and erosion resistance of the materials studied was unaffected by moisture ingress.

3.11.2 Resistance to Alkali Attack

It has been suggested earlier [36] that polymeric insulators encounter more of alkaline than acidic pollutants during service. Electrolysis of the saline pollution results in the formation of NaOH. So the most likely form of alkali to be encountered by polymeric insulators located near the sea coast would be NaOH. As electrolysis is more dominant with dc than ac, polymeric insulators on dc lines near the sea coast are more likely to encounter NaOH. To demonstrate this, samples in Table 3.1 were evaluated for tracking and erosion with +dc voltage at 40V/mm stress and 1600 $\mu\text{S}/\text{cm}$ water conductivity. NaOH was detected near the cathode (grounded bottom electrode) on the samples with dc but not with ac. A volumetric analysis showed that the concentration of NaOH on the samples did not exceed 0.2N during the 500 hours of exposure to salt fog. The leakage current was very similar for both ac and +dc. This resulted in similar (within $\pm 5\%$) times to failure, weight loss and cumulative charge for both ac and +dc voltage. This demonstrated that

the tracking and erosion resistance of the materials studied was unaffected by a weak NaOH solution.

A previous study [36] showed that ATH and silica filled epoxy samples were attacked by a 6N NaOH solution, but the unfilled resin was not affected. Based on this study, a selected number of samples from Table 3.1 were held in a 6N NaOH solution for 30 days. After this exposure, it was found that the ATH filled silicone rubber samples had become brittle. The polymer had visibly degraded exposing the filler to the surface. All samples had a weight loss of about 2%. None of the EPR samples showed any visible signs of degradation. There were no changes in weight. The ATH filled epoxy samples disintegrated in the 6N NaOH solution in about 100 hours.

The silicone rubber and EPR samples were evaluated in the fog chamber at 40V/mm stress and 1600 μ S/cm water conductivity. Table 3.5 shows that the time to failure was drastically reduced for the ATH filled silicone rubber and epoxy samples but was unaffected for the silica filled and unfilled EPDM samples.

All the ATH filled EPR samples failed by tracking and the silicone rubber samples failed by erosion leading to mechanical failure. For the silica filled and unfilled EPDM samples the cumulative charge was very similar (within $\pm 5\%$) to that for the virgin samples.

Table 3.5: Time to Failure for Samples Subjected to 6N NaOH for 30 Days.

SAMPLE	HOURS TO FAILURE	
	VIRGIN	AFTER EXPOSURE TO 6N NaOH
EO	>500	>500
EA	310	<1
EC	>500	<1
EE	>500	<1
EAS	67	60
ECS	113	120
EES	160	145
SA	240	9
SC	400	14
SE	500	16

These observations indicate that although the polymer by itself resists a concentrated NaOH solution, the addition of ATH filler makes the filled material more susceptible to attack by a concentrated NaOH solution.

It should be mentioned that such a high concentration of NaOH is very unlikely to be encountered in outdoor insulator applications and the choice of filler type should not be based on this extreme test.

3.11.3 Resistance to Hydrocarbon Solvent Attack

Polymeric insulators used in urban areas encounter hydrocarbon solvents from exhaust fumes of vehicles. Insulators near railway lines are more likely to encounter hydrocarbon solvents due to their close proximity to the lines. The reaction of the hydrocarbon solvents with the polymer is governed by the solubility parameter δ (the unit of δ is $\text{cal}^{1/2} \text{cm}^{-3/2}$) of both the polymer and the solvent. Similar magnitudes of δ result in mutual interaction causing swelling of the polymer. The magnitude of δ for silicone rubber and EPR is in the range 7 to 8 and about 11 for epoxy [15]. For vehicular fuels like gasoline and diesel, δ is in the range 6.7 to 7.6 [37]. This indicates that the silicone rubber and EPR samples are more prone than epoxy to attack by these hydrocarbon solvents. To demonstrate this, a selected number of samples from Table 3.1 were held for 100 hours in the hydrocarbon solvent naphtha, for which the solubility parameter lies in the same range as for gasoline and diesel fuels [37]. Table 3.6 shows the maximum weight gained and elongation after the 100 hour exposure. It can be seen that the silicone rubber and EPR samples experienced swelling and elongation whereas the epoxy samples were unaffected. It can also be seen that the type of inorganic filler did not influence the swelling and elongation but an increase in the filler concentration decreased the swelling and elongation. By increasing the filler concentration fewer organic mol-

ecules are available for attack by the solvent. The change in the physical structure was temporary and after the samples were removed from the solvent they regained their original shape in about 100 hours.

Table 3.6: Physical Changes and Time to Failure for Samples Held in Naphtha.

SAMPLE	MAXIMUM WEIGHT GAIN (%)	MAXIMUM ELONGATION (%)	HOURS TO FAILURE	
			VIRGIN	AFTER EXPOSURE TO NAPHTHA
EO	155	68	>500	>500
EA	125	55	310	281
EC	80	35	>500	>500
EE	57	30	>500	>500
EAS	120	51	67	61
EOS	78	32	113	115
EES	55	27	160	152
SA	130	57	240	221
SC	80	35	400	388
SE	55	28	>500	>500
XA	<1	<1	115	128
XB	<1	<1	156	170

After the samples had regained their original shape they were evaluated in the fog chamber at 40V/mm stress and 1600 μ S/cm water conductivity. The time to failure shown in Table 3.6 is seen to be unaffected by exposure to naphtha. In addition, the cumulative charge and weight loss for these samples was within $\pm 5\%$ of the corresponding value for the

virgin samples. This suggests that the hydrocarbon solvent did not have any detrimental effect on the tracking and erosion resistance of the materials evaluated.

3.12 Summary

The ac performance of polymeric materials in accelerated aging tests is largely controlled by the experimental conditions employed. Although the results of the high ($\geq 1000 \mu\text{S/cm}$) conductivity test were in good agreement with the standard accelerated aging tests, it was the results of the low conductivity test which were in better agreement with service experience.

Measurement of cumulative charge, weight loss and flash-over voltage yield limited information about surface aging. The number and amplitude of peak current pulses above a preset threshold provides a better indication of surface aging and subsequent failure of all materials under all experimental conditions studied.

Although the ATH filler imparts superior tracking and erosion resistance to materials than does silica filler under high conductivity fog, in low conductivity fog both ATH and silica filler impart similar tracking and erosion resistance.

The tracking and erosion resistance of the materials studied is not affected by moisture ingress, a weak NaOH solution or hydrocarbon solvent naphtha.

Chapter IV

A COMPARATIVE STUDY OF THE AC AND DC PERFORMANCE OF POLYMERIC MATERIALS AND INSULATORS

4.1 Introduction

The effect of polymer type, filler type and concentration, experimental conditions of electric stress and water conductivity on the ac performance of polymeric materials was reported in the previous chapter. Data on the merits of different polymer and filler types, the threshold level of filler to be used for satisfactory performance were obtained. It was also shown that better correlation with service experience was obtained when materials were evaluated in low rather in high conductivity fog. As there is very little information available on the performance of polymeric materials with dc, a detailed study with the objective of acquiring similar information obtained with ac, was therefore undertaken and the results of the comparative study are reported in this chapter.

Outdoor insulators are not in the form of cylindrical rods. In order that the results of material tests using cylindrical rods be applicable to outdoor insulators, it is necessary to establish the correlation between material testing in the form of rods and actual insulator geometries.

This chapter also describes the results of polymeric insulator evaluation with ac and dc.

All the results reported are the average from at least two samples of the same composition for which the variation in the reported quantity was within $\pm 5\%$.

4.2 Experimental

The rod samples were evaluated in low ($250 \mu\text{S}/\text{cm}$) and high ($1000 \mu\text{S}/\text{cm}$) conductivity fog. The supply voltage was kept constant at 9kV and the average electric stress was varied from 28 to 60 V/mm by varying the length of the samples.

Due to the unidirectional current, the electrode which was the anode experienced erosion (about 1% and 5% weight loss in 100 hours with -dc, respectively in low and high conductivity fog). Recycling of water resulted in an increase of conductivity of about 5% in 20 hours. As a result, a fresh water solution was prepared daily.

The carbon electrodes were replaced once every 100 hours during the high conductivity test with -dc. Initially, electrodes made from aluminium, stainless steel, brass and copper were tried, but in all cases, flashover occurred after about 20 hours in high conductivity fog due to erosion deposits from the electrodes settling on the samples. The use of carbon electrodes together with daily changes of the water solution prevented flashover from occurring.

Table 4.1: Material Details and Performance in ac, +dc and -dc.

The silicone rubber samples S30A, S80A and S130A are the same as samples SA, SC and SE of Table 3.1.

MATERIAL	SAMPLE IDENTIFICATION	FILLER		HOURS TO FAILURE AND FAILURE MECHANISM AT WATER CONDUCTIVITY					
		TYPE	LEVEL (pph)	250 $\mu\text{S/cm}$			1000 $\mu\text{S/cm}$		
				ac	+dc	-dc	ac	+dc	-dc
HTV SILICONE RUBBER	S30A	ALUMINA TRIHYDRATE $\text{Al}_2\text{O}_3 \cdot 3\text{H}_2\text{O}$	30	NF	NF	90 ^M	185 ^M	154 ^M	43 ^M
	S80A		80	NF	NF	138 ^M	305 ^M	287 ^M	75 ^M
	S130A		130	NF	NF	185 ^M	NF	NF	141 ^M
	S200A		200	NF	NF	NF	NF	NF	210 ^M
EPDM	E30A	ATH	30	140 ^T	151 ^T	34 ^T	165 ^T	194 ^T	54 ^T
	E80A		80	193 ^T	184 ^T	48 ^T	NF	NF	141 ^M
	E130A		130	368 ^T	328 ^T	69 ^T	NF	NF	221 ^M
	E250A		250	NF	NF	NF	NF	NF	358 ^M
	E30S	SILICA (SiO_2)	30	130 ^T	123 ^T	44 ^T	70 ^T	97 ^T	20 ^T
	E80S		80	184 ^T	192 ^T	57 ^T	120 ^T	112 ^T	42 ^T
	E130S		130	330 ^T	319 ^T	75 ^T	160 ^T	148 ^T	54 ^T
	E250S		250	NF	NF	310 ^T	NF	NF	168 ^T

NOTES:

NF: NO FAILURE

M: MECHANICAL FAILURE

T: TRACKING FAILURE

pph: PARTS PER HUNDRED OF POLYMER FORMULATION

4.3 Time to Failure

Table 4.1 shows the details of samples and time to failure for ac, +dc and -dc. In all cases the bottom electrode was the grounded electrode. It can be seen from the Table that in both low and high conductivity fog, the time to failure for ac and +dc was very similar, whereas for -dc, the time to failure was reduced by a factor of about four. The following can also be noted from the Table:

4.3.1 Low Conductivity Fog

1. Filled silicone rubber samples had substantially longer times to failure than the correspondingly filled EPDM samples.
2. For the same filler concentration ATH and silica filler impart similar resistance to tracking in EPDM material as judged by their similar times to failure. This indicates that the water of hydration does not contribute to the tracking resistance in low conductivity fog.

4.3.2 High Conductivity Fog

1. ATH filled EPDM samples had much longer time to failure than the correspondingly filled silicone rubber samples.
2. For the same filler concentration, ATH filler imparts a superior tracking and erosion resistance to the EPDM material than does silica filler, as seen by the longer times to failure. This indicates that the water of hydration plays a significant role in imparting tracking and erosion resistance in high conductivity fog.

The similarity in performance of materials containing various types of filler with ac and dc indicates that the mechanisms by which fillers impart tracking and erosion resistance to polymers is similar for ac and dc.

4.4 Leakage Current and Cumulative Charge

4.4.1 Low Conductivity Fog

Silicone rubber and EPDM samples were all hydrophobic before the start of the test. With both ac and +dc, the silicone rubber and EPDM samples maintained a hydrophobic surface for about 70 hours and 1 hour respectively. With -dc, the surface of silicone rubber and EPDM samples was converted to a hydrophillic surface in about 40 hours and less than 1 hour respectively. The surface transition was indicated by an increase in the average leakage current from 1 to 10mA. The deposition of scale (CaCO_3 and MgCO_3) which is formed when water is boiled from the surface under dry band heating, was found to be initiated from the bottom of the sample with ac and +dc, and from the top with -dc. The scale deposit with -dc, in terms of apparent area covered on the sample, was at least 2 to 3 times greater than with ac or +dc for the same time duration. This resulted in a higher leakage current with -dc as shown in the variation of cumulative charge with time in Fig. 4.1. The following points can also be noted from the figure:

1. The inability of the cumulative charge to indicate failure which was previously reported for ac is also true for dc. This is indicated by the similar magnitude of the cumulative charge for the samples which passed and failed the test.

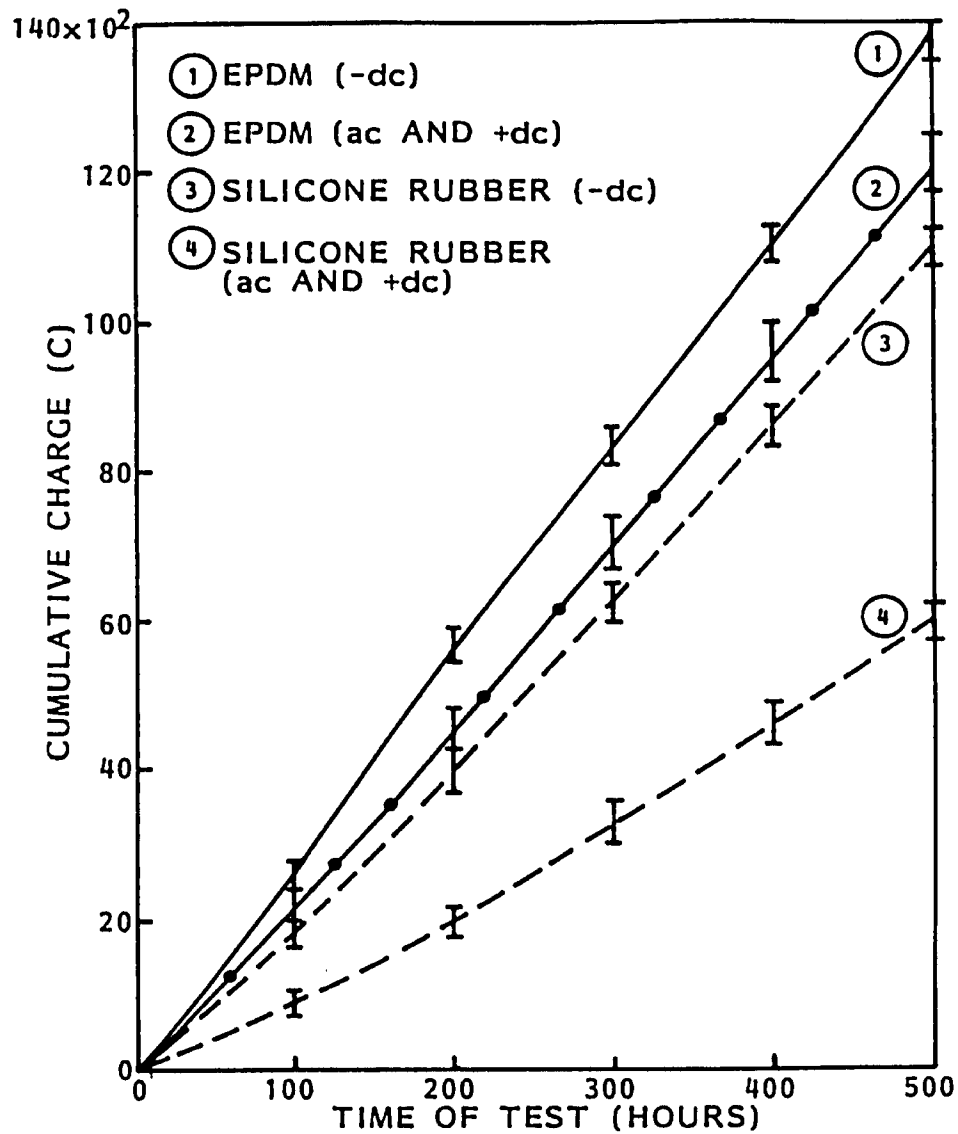


Figure 4.1: Cumulative Charge with Time in Low Conductivity Fog.

2. Initially, silicone rubber had a much lower cumulative charge than the EPDM samples. But this advantage of leakage current suppression of silicone rubber samples was lost when the samples were covered with a thick scale deposit (plots 3 and 4).

4.4.2 High Conductivity Fog

The hydrophobic surface of silicone rubber and EPDM samples was converted to a hydrophillic surface within 1 hour, for both +dc and -dc. However, unlike with ac, where the energetic dry band activity effectively reduced the formation of water scale on the surface, with dc, scale was observed and was much greater for -dc than +dc. As the leakage current is dependent on the thickness of the surface electrolytic film, it is greater for -dc than for ac or +dc as shown by the variation of cumulative charge with time in Fig. 4.2. The cumulative charge in high conductivity fog is independent of polymer type and is only dependent on the experimental conditions as was previously reported for ac.

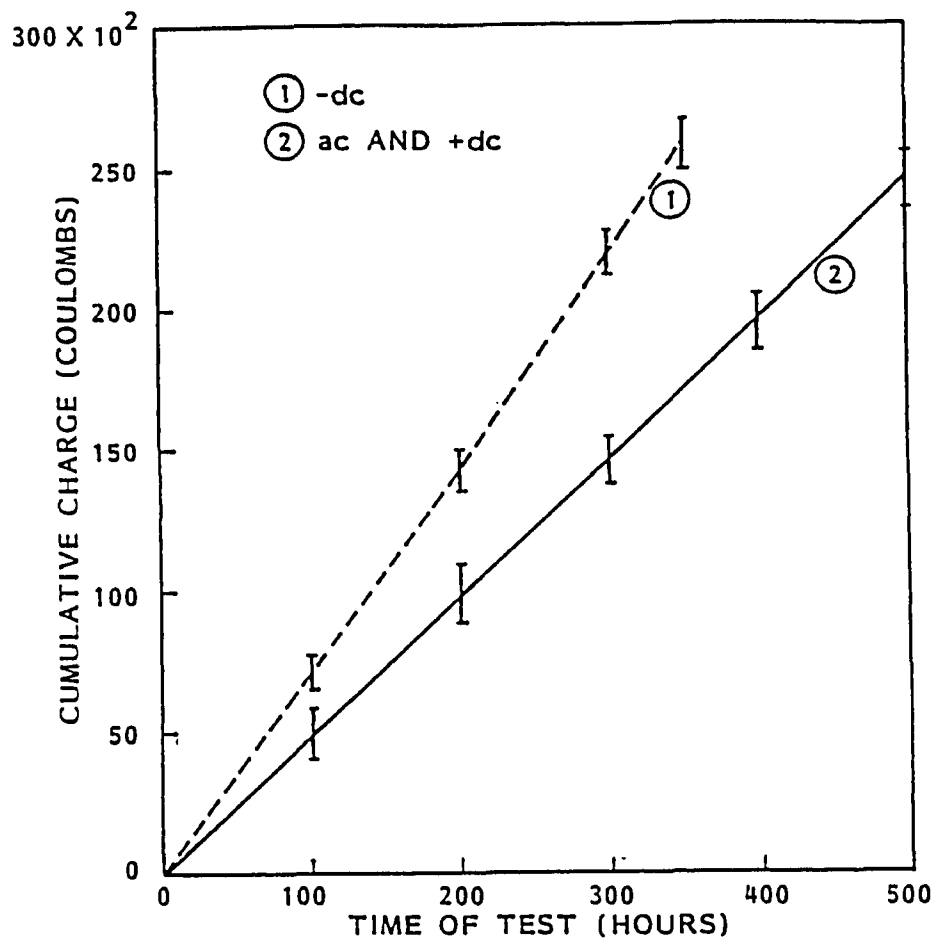


Figure 4.2: Cumulative Charge with Time in High Conductivity Fog.

4.5 Effect of Scale Deposit on Material Performance

On an uncontaminated surface, dry bands once formed will stay in a particular location until the arc roots dry out the surface at which point the arc moves to another favourable location. As the water film on an uncontaminated surface is only a few monolayers thick, the dry bands change their location rapidly. However, once the surface accumulates deposits, the thickness of the water film increases due to

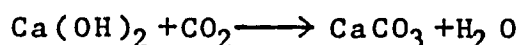
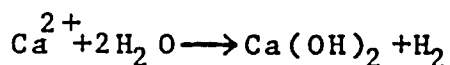
their hygroscopic nature. Therefore, it takes a longer time for the arc roots to dry out the surface and hence dry band arcing occurs for a longer time in one particular location. The scale deposition observed on samples was in the form of patches (Fig. 3.17) and therefore non-uniform. As a result, regions with relatively less deposit which are sandwiched between regions with more deposit are the preferred locations for dry band arcing to occur. Therefore, material degradation on a contaminated surface is more likely to occur at a faster rate than on an uncontaminated surface due to the combination of preferential dry band activity and the longer duration of arcing.

In order to demonstrate that the scale is responsible for initiating degradation, the samples in Table 4.1 which had failed the low conductivity test with ac, were evaluated under the same experimental conditions with distilled-deionized water¹ (5 $\mu\text{S}/\text{cm}$), to which ACS grade NaCl (impurities less than 0.1%) was added to adjust the water conductivity to 250 $\mu\text{S}/\text{cm}$. A fresh solution was prepared every two days. Due to the similar water conductivity, the initial leakage current observed was very similar (typically 5 to 10mA peak) to that obtained when using tap water. But, as the water was devoid of any Ca and Mg impurities there was no scale formed. Therefore, there were no current pulses above 15mA recorded and no failures occurred in 500 hours.

¹ Obtained from the Department of Civil Engineering (Room B 29A).

4.6 Material Degradation as a Function of Supply Polarity

In addition to dry band heating which causes evaporation of water to form a scale, scale formation with dc could also be due to electrolysis of tap water which occurs as follows:



The positively charged Calcium ions migrate towards the oppositely charged electrode (cathode) and combine with water to form Ca(OH)_2 which in turn could combine with CO_2 which is present in air or as a dissolved gas in water, to form CaCO_3 . This explains the initiation of water scales from the cathode observed with both polarities. With time, the scale progresses toward the anode. The hygroscopic nature of the scale causes dry bands to be formed preferentially between the tip of the scale and the anode. For samples oriented vertically, with +dc, dry band activity and erosion occurs more towards the top electrode whereas with -dc, they occur towards the bottom electrode as shown in Fig. 4.3. Due to the relative positions of the fog nozzles and the samples in the fog chamber which favors dry band activity towards the bottom electrode, material degradation is accentuated with -dc when compared with +dc. It can be observed from Fig. 4.3 that the area in the vicinity of the anode is devoid of scale. This observation is consistent with earlier work [55] in which the formation of clean zones has been attributed to the migration of the positively

charged ions from the anode under the influence of an electric field.

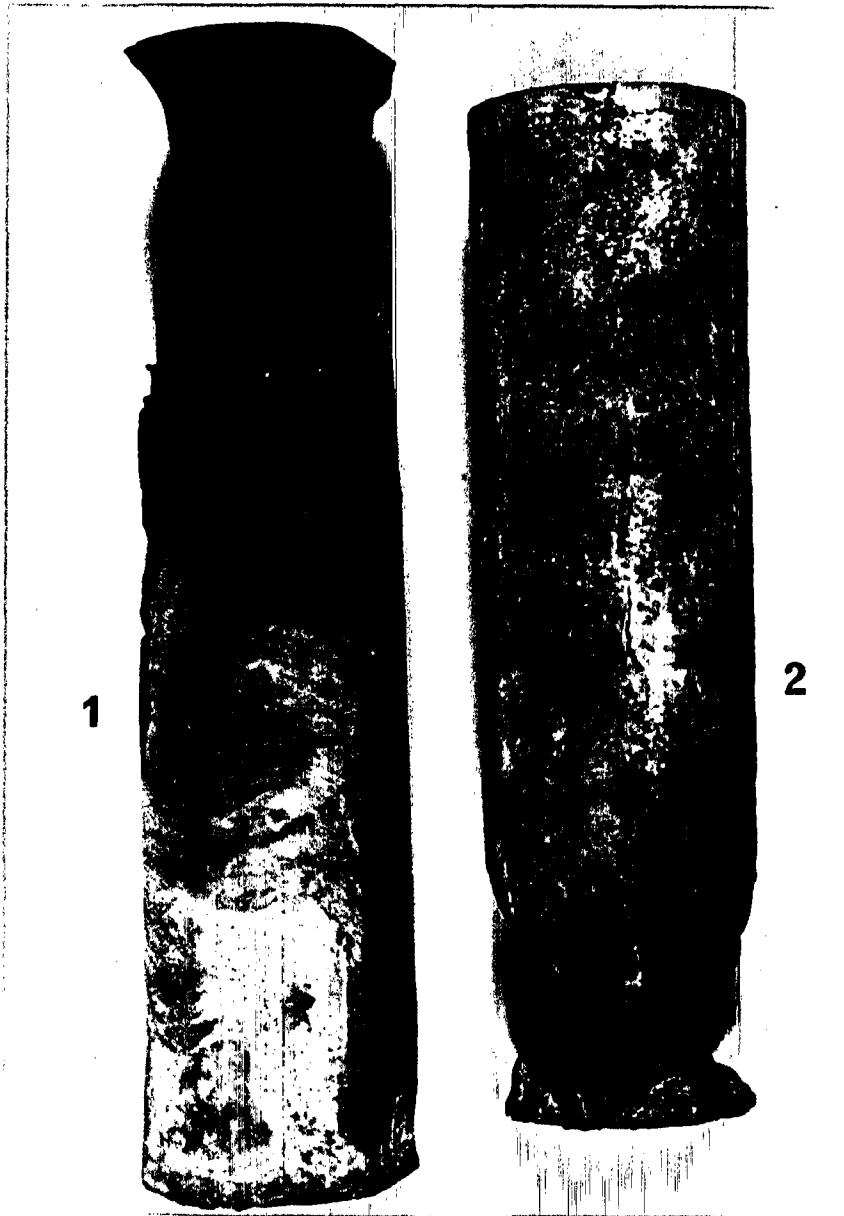


Figure 4.3: Typical Erosion in ATH filled EPDM Samples in High Conductivity Fog with (1) +dc and (2) -dc.

4.7 Weight Loss due to Dry Band Arcing

Fig. 4.4 shows the variation of weight loss with time for the ATH filled EPDM samples in high conductivity fog. It can be seen that the variation of weight loss is very similar for ac and +dc, but for -dc, weight loss occurred at a more rapid rate leading to mechanical separation of the samples and in less time for reasons explained in section 4.6.

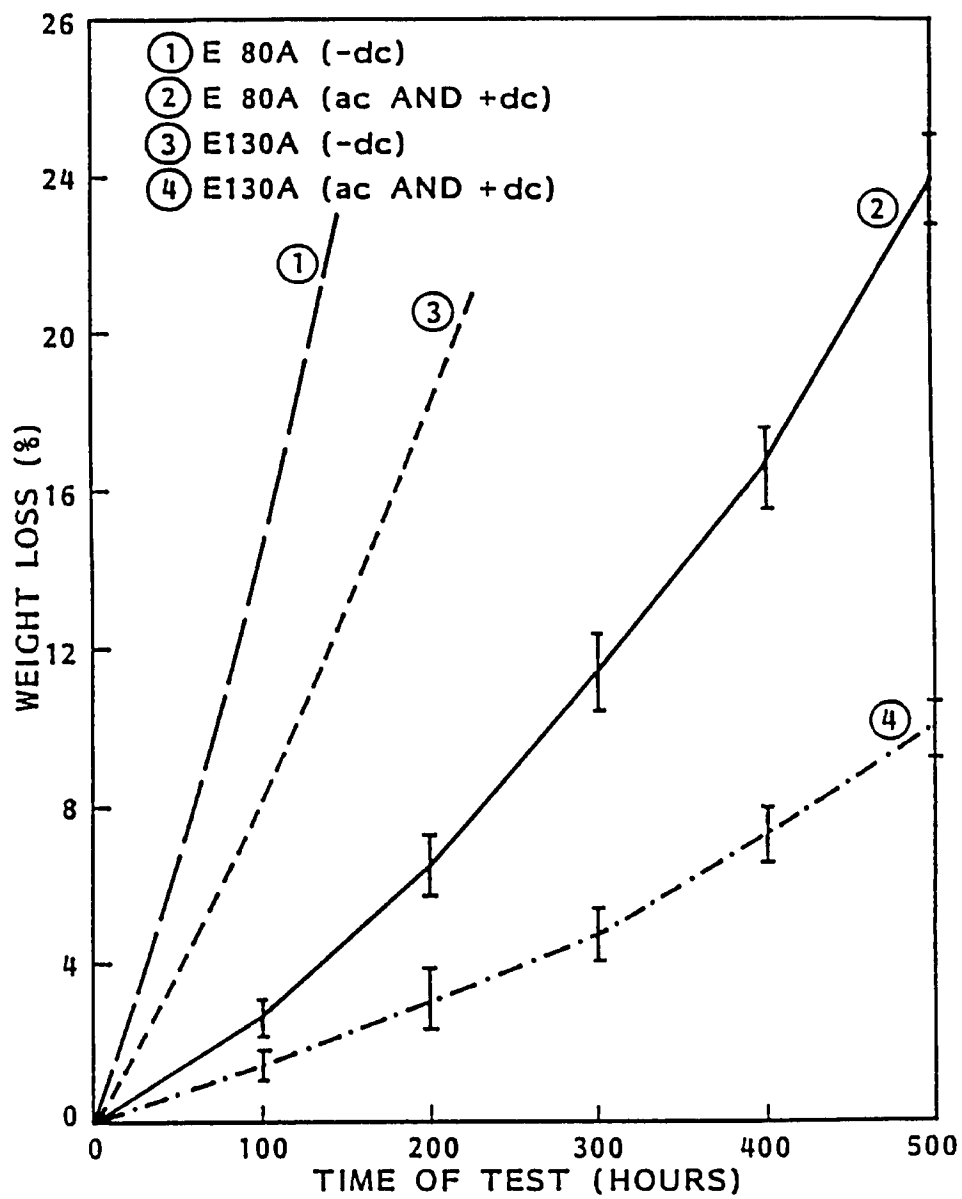


Figure 4.4: Weight Loss with Time in High Conductivity Fog.

4.8 Effect of Sample Orientation on Material Performance

The intense accumulation of scale deposit on the vertically oriented samples is caused by evaporation of water which moves down the sample. In a horizontal orientation, water droplets incident on the sample may not remain on the surface for sufficient time for dry band arcing to raise the water temperature to boiling. Therefore, it can be expected that for the horizontally oriented samples, the deposition of deposits could be considerably reduced and hence the time to failure could increase and the weight loss due to dry band arcing decrease. To confirm this, a selected number of samples were evaluated horizontally in low and high conductivity fog with -dc voltage. The results shown in Table 4.2 indicate that an improved performance was obtained in the horizontal rather than in the vertical orientation.

Table 4.2: Effect of Orientation on Material Performance in High Conductivity Fog with -dc.

SAMPLE	ORIENTATION			
	VERTICAL		HORIZONTAL	
	TIME TO FAILURE (h)	WEIGHT LOSS (%)	TIME TO FAILURE (H)	WEIGHT LOSS (%)
E130A	221	21	NF	10
E250A	358	22	NF	7
S200A	210	21	NF	8.5

NF: NO FAILURE

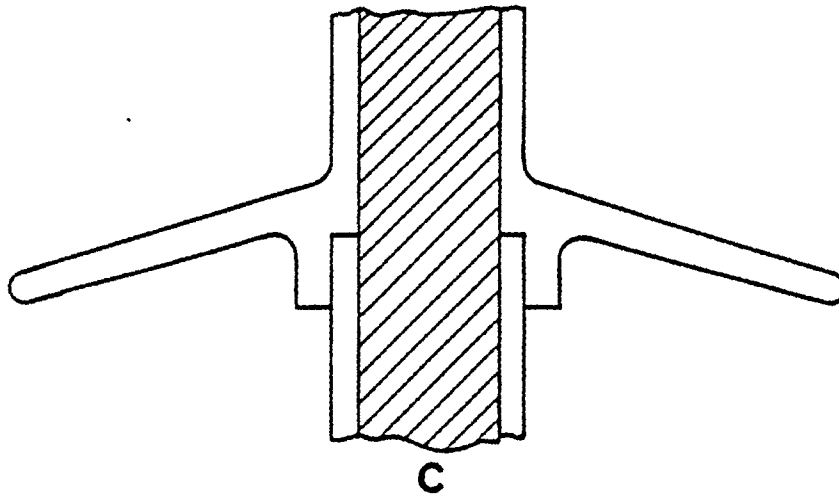
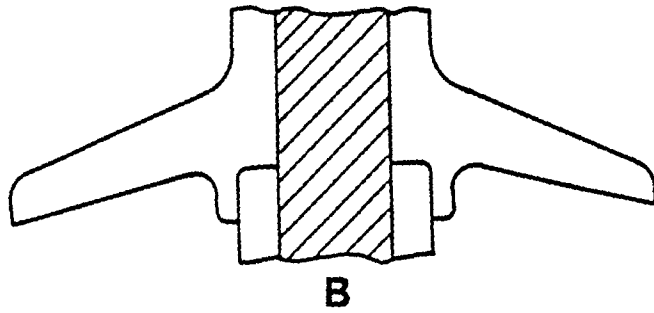
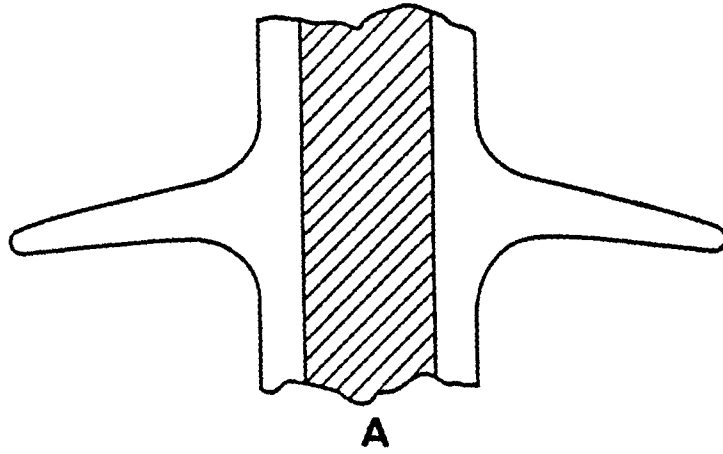
4.9 Performance of Polymeric Insulators

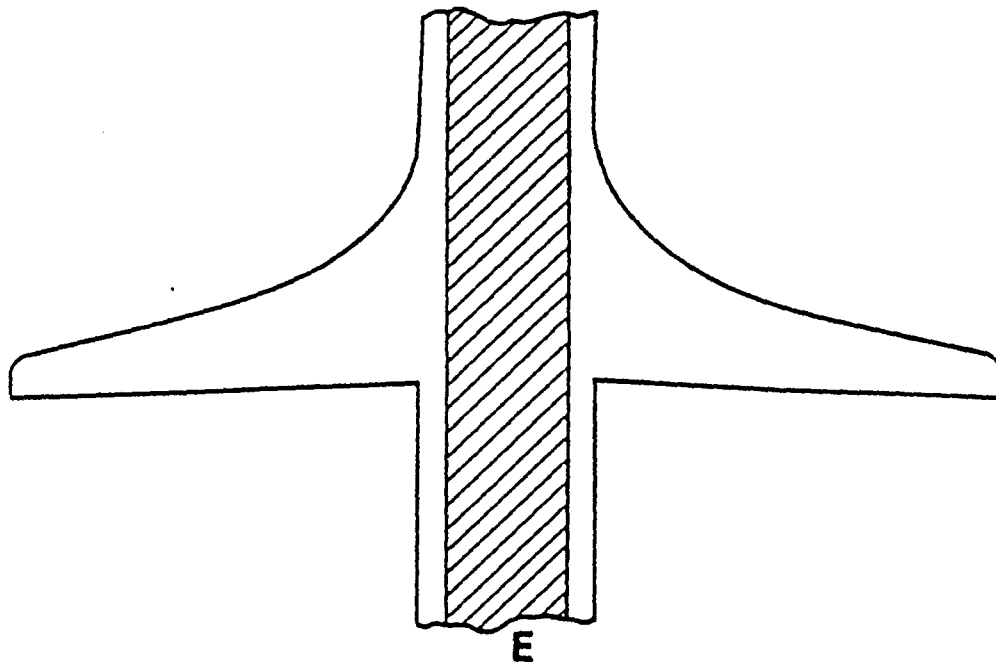
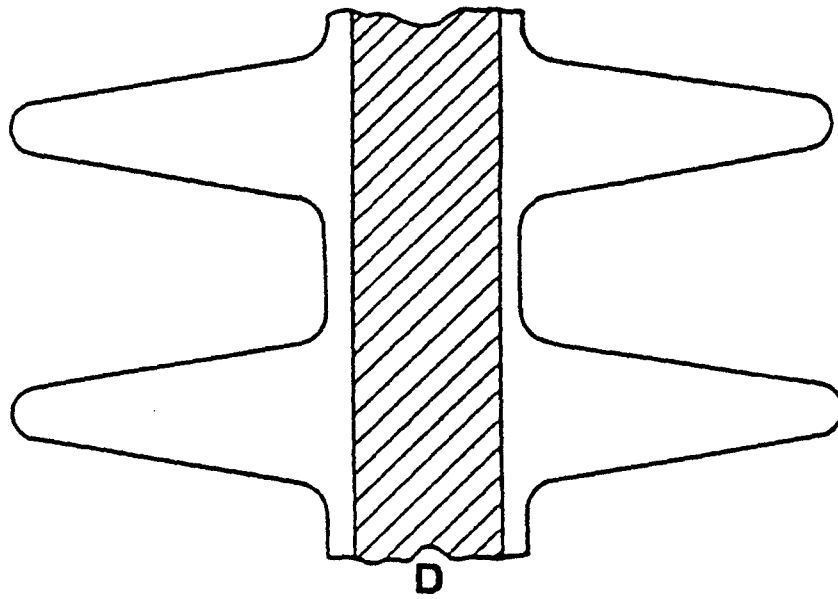
4.9.1 Details of Insulators Evaluated

Sections of commercial polymeric insulators were evaluated with the purpose of establishing correlation with material testing in the form of cylindrical rods. The material details of the insulators are shown in Table 4.3. The cross sectional details are shown in Fig. 4.5. Although the designs evaluated were aerodynamic, that is, the undersurface of the sheds did not contain ribs, for the purpose of describing their performance in the fog chamber, the shed shapes have been classified as follows: (1) protected, where the under surface of the sheds are not easily wetted by fog, (2) open, where the under surface is easily wetted by fog and (3) intermediate, where the shed is partially protected.

From Fig. 4.5, it can be seen that insulators A, B, and C are of a protected design, insulator D of an open design and insulators E and F of an intermediate design. In addition, it can also be noted from Fig. 4.5 that insulators A, D, E and F are constructed from a one piece weathershed, whereas insulators B and C are of a modular design. The weathersheds in insulators C are epoxy bonded. A silicone gel seals the interface between the fiberglass rod and the sheds in insulator B.

The end fittings were removed and carbon electrodes 5 mm thick and of diameter equal to the shank of the insulators were used. As the shape of the end fitting of each insulator





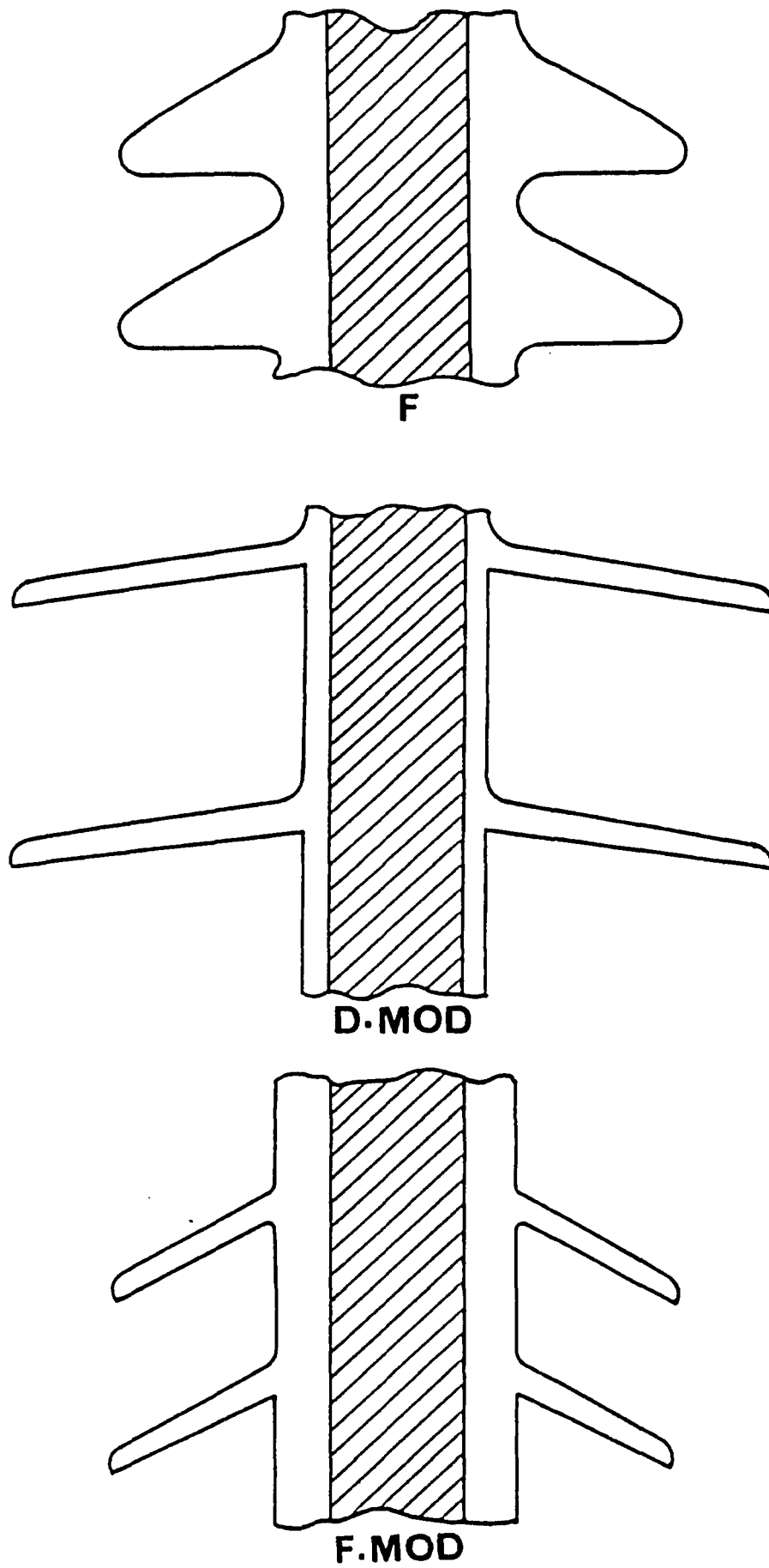


Figure 4.5: Insulator Profiles Evaluated.

was different, using carbon electrodes ensured that insulator performance was independent of end fitting geometry.

4.9.2 Insulator Performance

It was shown [26] that the leakage current on insulators with protected sheds is a function of the ratio l/A , where l is the leakage distance and A is the surface area. It was reported that the leakage current decreased with increasing l/A and hence such insulators perform better in contaminated areas. This parameter has been investigated further in the present work for insulators with various shed profiles.

Tables 4.3 and 4.4 show the time to failure and cumulative charge respectively, under various experimental conditions. Only those insulators that passed the low conductivity test were evaluated at high conductivity. The following can be noted from the Tables:

1. Epoxy insulator F with substantial ATH filler and subjected to a lower stress failed in a much shorter time than silicone rubber and EPDM insulators. Thus the ranking of materials obtained by evaluating insulators is similar to that obtained by evaluating rod samples.
2. As in the case with rod samples, evaluating insulators in -dc results in a shorter time to failure and increased cumulative charge.
3. Although the l/A ratio was similar, insulators with protected design have a much lower leakage current than those with an open or intermediate design. In

Table 4.3: Insulator Details and Performance with ac, +dc and -dc.

INSULATOR IDENTIFICATION	WEATHER-SHED MATERIAL	APPROX. ATH LEVEL (PPH)	$\frac{l}{A} \times 10^{-3}$ (mm ⁻¹)	AVERAGE ELECTRIC STRESS V/mm	HOURS TO FAILURE AT WATER CONDUCTIVITY			
					250 μ S/cm		1000 μ S/cm	
					ac	-dc	ac	-dc
A	EPDM	140	5.8	60	NF	NF	NF	NF
B	EPDM	45	6.07	58	NF	NF	NF	NF
C	EPDM	120	5.07	57	NF	NF	NF	NF
D	EPDM	200	5.25	55	NF	300	NF	126
E	HTV SILICONE RUBBER	30	5.6	62	NF	324	NF	-
F	EPOXY	220	6.2	40	206	80	-	-
DMOD	EPDM	200	5.25	55	NF	NF	NF	NF
FMOD	EPOXY	220	6.2	40	NF	NF	-	-
E130A (ROD SAMPLE)	EPDM	130	-	60	368	69	NF	221

NOTES:

NF = NO FAILURE

PPH = PARTS PER HUNDRED OF POLYMER FORMULATION

order to demonstrate this further, insulators D and F were machined to impart a protected shape to the sheds (Fig. 4.5, D Mod and F Mod). The performance, as judged by the data in Table 4.3, of the modified insulators under identical conditions is seen to be far superior than that obtained with the existing designs.

4. A comparison of the typical cumulative charge for rod samples and insulators reveals that these quantities are much higher for rod samples. Therefore, evaluating materials in the form of cylindrical rods yields results in a much shorter time.

Table 4.4: Cumulative Charge For Insulators With ac, +dc and -dc.

INSULATOR	CUMULATIVE CHARGE (C) AT WATER CONDUCTIVITY			
	250 μ S/cm		1000 μ S/cm	
	ac	-dc	ac	-dc
A	980	1360	1310	1610
B	960	1820	2130	2630
C	880	1580	1180	1700
D	4140	6970	6100	2020
E	990	1650	2080	2560
F	4800	3560	-	-
D MOD	1600	2100	2450	2600
F MOD	1580	2000	-	-
E130A (ROD SAMPLE)	12000	≈14000	24000	30000

5. Insulators with modular and a one piece weathershed construction performed alike.

Insulators in Table 4.3 which failed at the high electric stress were evaluated in low conductivity fog with -dc at reduced values of electric stress. The results in Table 4.5 show that the time to failure increased with decreasing stress as was reported earlier with rod samples (Fig. 3.1). The results also suggest that there is a threshold current of about 15mA below which little material degradation can occur under the experimental conditions used.

The insulator D which failed the high conductivity test with -dc, eroded in a similar manner as the rod samples

Table 4.5: Time to Failure of Insulators at Various Electric Stress in Low Conductivity Fog with -dc.

INSULATOR	ELECTRIC STRESS (V/mm)	TYPICAL PEAK CURRENT (mA)	HOURS TO FAILURE
D	65	30 - 50	300
	30	<15	>500
	25	<15	>500
F	60	30 - 50	80
	40	25 - 40	206
	30	<15	>500
	20	<15	>500
E	62	20 - 30	324
	40	<15	>500
	30	<15	>500

before exposing the fibre glass rod (Fig. 4.6). The silicone rubber insulator E failed by erosion (Fig. 4.7) as was the case with the rod samples (Fig. 3.12). The epoxy insulator D (Fig. 4.8) tracked as was the case with rod samples (Fig. 3.14).



Figure 4.6: Erosion Leading to Tracking Failure of Insulator D in High Conductivity Fog in High Conductivity Fog with -dc.



Figure 4.7: Erosion Failure of Insulator E in High Conductivity Fog with -dc.

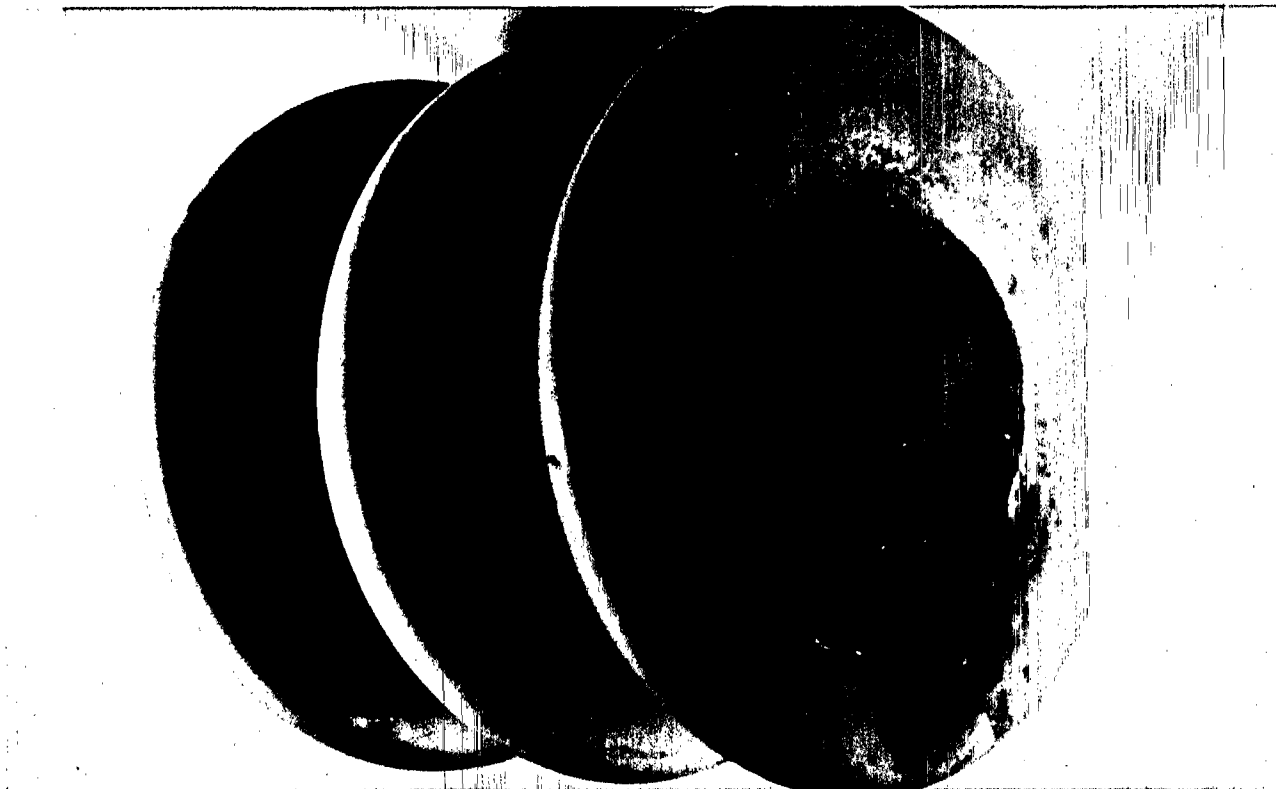


Figure 4.8: Tracking in Insulator F in Low Conductivity Fog with -dc.

4.10 Summary

The performance of polymeric materials under accelerated aging is dependent on whether the electric stress is ac or dc. For ac and +dc, similar performance was obtained whereas for -dc, a marked reduction in the tracking and erosion resistance was observed.

In order to differentiate between the leakage current suppression capability of various materials for dc, the evaluation must be done in low conductivity fog but at a much lower electric stress than for ac.

Although similar ranking of material performance was obtained on cylindrical rods and practical insulator geometries of materials, the time of evaluation required is considerably lower when cylindrical rods of materials are used. The shape of the shed has a significant effect on the insulator performance.

Chapter V

EXPERIMENTAL TECHNIQUES USED TO INVESTIGATE MATERIAL PERFORMANCE UNDER ACCELERATED AGING

5.1 Introduction

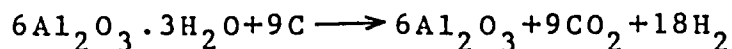
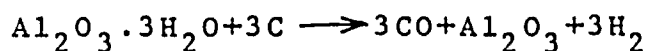
This chapter reports the results from different experimental techniques used to investigate material performance under accelerated aging. The dominant mechanisms by which fillers impart tracking and erosion resistance to various materials under different experimental conditions is discussed through measurements of released gases, temperature due to dry band arcing and Thermo Gravimetric Analysis (TGA) of materials. The role of filler dispersion in initiating tracking or erosion failure in high conductivity fog has been investigated by Energy Dispersive X-ray Analysis (EDAX). Material surface study by Electron Spectroscopy for Chemical Analysis (ESCA) helped in determining the mechanisms responsible for:

1. The hydrophobic surface of materials to be converted to a hydrophillic surface during dry band arcing.
2. The mechanisms responsible for hydrophobicity exhibited by the silicone rubber material despite the accumulation of surface contamination.

5.2 Mechanisms by which Fillers Impart Tracking and Erosion to Polymeric Materials

5.2.1 Measurement of Released Gases During Dry Band Arcing

A chemical mechanism has been suggested by which hydrated fillers impart tracking and erosion resistance to materials. Although not demonstrated experimentally on filled elastomers, it has been postulated that when the temperature of filler particles exceeds 900°K during dry band arcing, the water of hydration of the filler combines with free carbon produced from breakdown of the polymer chains forming CO₂ or CO gases as indicated by the following reactions [20]:



To test the validity of the chemical mechanism, an experiment to monitor the emission of gases was conducted. A small salt fog box (150X150X150mm) was constructed to test 50mm long samples at 60V/mm electric stress with 3200 μS/cm water conductivity while connected to a Varian Mat Model CH5DF Mass Spectrometer. The higher water conductivity was chosen to promote increased dry band activity leading to increased production of carbonaceous products.

The dimensions of the box was chosen to allow easy insertion and removal of the sample and also that there would be a better chance of detecting the gases from dry band arcing if the volume of the box was comparable to that of the ionizing chamber of the mass spectrometer which was 1.5 l.

The materials evaluated were EPDM samples EO and EF in an atmosphere of nitrogen. If CO and/or CO₂ were detected it would validate the chemical mechanism.

The box was first flushed with nitrogen. With the high voltage off, the sample was subjected to a continuous water spray and the mass spectrometer sampled the box to provide a reference spectrum. Two methods were tried in order to detect the generation of CO and CO₂. In the first method, the mass spectrometer continuously monitored the salt fog box, while the sample was subjected to dry band arcing. During the test which lasted for about 20 minutes, no peaks in the spectrum corresponding to CO and CO₂ was observed. In the second method, arcing on the samples continued for about 20 minutes in an attempt to increase the concentration of gases before allowing the mass spectrometer to sample the salt fog box. The magnitude of CO₂ detected was similar for EO (1.12%) and EF (1.1%). Although there was a weight loss of about 1% in the sample EF, the similar magnitude of CO₂ detected indicated that the water of hydration has not reacted with carbon from the polymer to form CO₂.

5.2.2 Measurements of Surface Temperature During Dry Band Arcing

To further disprove the chemical mechanism, temperature indicating paints (Omega Engineering Inc.) which change their color irreversibly at a specific temperature were used to record the local surface temperature during dry band arc-

ing. The response time of these paints is specified in the order of milliseconds. At the bottom electrode where the greatest dry band activity was found, a temperature above 260 and below 400°C was established in the high (1000 and 1600 $\mu\text{S}/\text{cm}$) conductivity tests. On other parts of the sample, the local surface temperature was found to be below 260°C.

In the low conductivity fog test with ac, on the EPDM samples which had accumulated greater amount of scale, the local surface temperature measured was in the range 200 to 300°C. On other samples which had relatively less scale deposit, the local surface temperature recorded was below 200°C.

When the filler particles reach temperatures above 200°C, a physical cleaning mechanism has been suggested by which hydrated fillers impart tracking and erosion resistance to materials. At this temperature, the water of hydration is released as vapor. The resulting sputtering action physically cleans the surface of degradation products and therefore prevents the formation of a continuous track [20].

The physical cleaning action of hydrated fillers can readily be demonstrated additionally on EPDM and epoxy samples by subjecting them to a flame at a temperature of about 300°C.

The physical mechanism was not observed in the ATH filled silicone rubber samples (except in S200A) when subjected to

a flame. One possible reason could be that the bonding between the ATH filler and the silicone backbone is much stronger than in EPDM or epoxy material. Thus the water of hydration of the ATH filler cannot be easily liberated from the silicone rubber material as it is from EPDM and epoxy. The surface temperature due to dry band arcing in the high conductivity fog test (above 260 °C) could be sufficient to cause scissions in the polymer chains. This could explain the sudden failure of silicone rubber samples after a certain period of exposure to high conductivity fog.

5.2.3 Thermo Gravimetric Analysis (TGA) of Polymeric Materials

A TGA of polymeric materials gives information about their thermal stability. In this technique [38], a sample (about 0.1g) of the material is heated at a constant rise of temperature (10.°C/min) in an atmosphere of nitrogen, while the sample weight is continuously monitored. The TGA plots of the unfilled, ATH and silica filled EPDM samples, shown in Fig. 5.1 indicates that the polymer is stable up to 175 °C. A similar weight loss is registered between 175 and 250 °C for all the samples which indicates that the polymer begins to degrade at temperatures above 175 °C. Between 250 and 400 °C, the ATH filled samples register a greater weight loss than the others indicating that the water of hydration from the filler is liberated at temperatures above 250 °C. The final weight loss is related to the inorganic filler concentration.

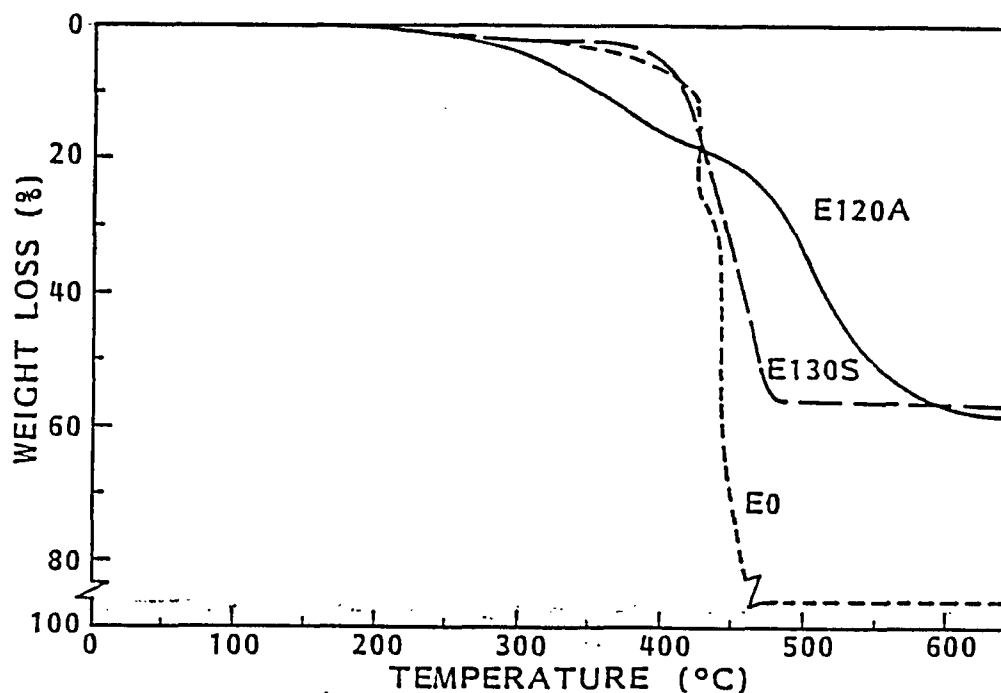


Figure 5.1: TGA Plots of EPDM Samples.

The TGA plots of the filled silicone rubber samples from the two sources, used in this work are shown in Figs. 5.2 and 5.3. It can be seen that there is a significant difference in the temperature at which degradation is initiated. The samples of Table 3.1 are stable up to 250°C (Fig. 5.3) whereas the samples of Table 3.4 are stable up to about 175°C (Fig. 5.2). This is likely the reason for the different times to failure observed at 1000 and 1600 $\mu\text{S}/\text{cm}$ (Table 3.4 and Fig. 3.1) for samples with similar filler concentration.

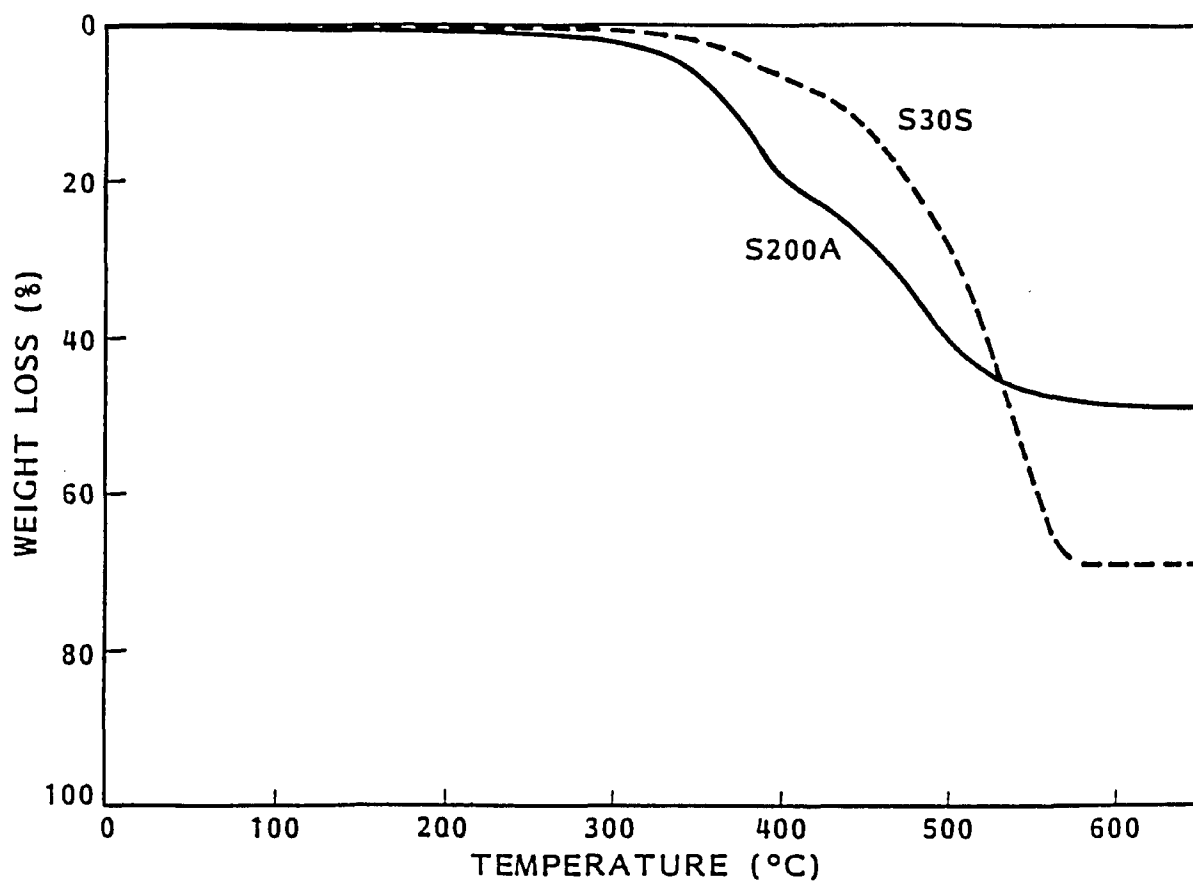


Figure 5.2: Typical TGA plots of Silicone Rubber Samples of Table 3.4.

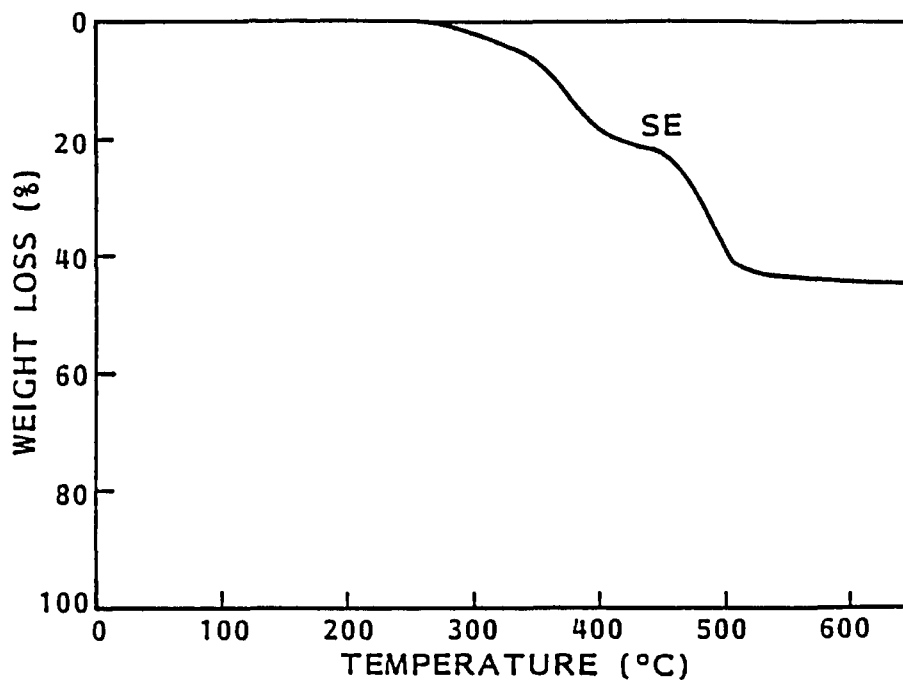


Figure 5.3: Typical TGA plot of Silicone Rubber Samples of Table 3.1.

5.2.4 Dominant Filler Mechanisms in Low and High Conductivity Fog

As the chemical mechanism is not operative during dry band arcing, the mechanisms by which fillers impart tracking and erosion resistance to the polymer are: (1) the physical cleaning action and (2) volume effects. A weight loss with time is associated with the first but not with the second mechanism.

From Tables 3.4 and 4.1 and Fig. 3.1, it can be seen that all materials had an increase in the time to failure with an increase in filler concentration. This was true for all experimental conditions which suggests that volume effects impart increased tracking and erosion resistance under all conditions. For materials with unhydrated fillers (SiO_2 and

Al_2O_3), volume effects is the only mechanism by which the filler imparts tracking or erosion resistance to the polymer. From Fig. 3.20 it can be seen that the ATH filled EPDM samples showed an appreciable weight loss at higher (1000 and 1600 $\mu\text{S}/\text{cm}$) water conductivities but not at low conductivity. This indicates that the physical cleaning action of the filler is operative only at higher water conductivities. Furthermore, ATH filled EPDM samples had much higher times to failure than all other materials evaluated. This suggests that the physical cleaning action of the filler is more effective than volume effects in imparting tracking or erosion resistance to the EPDM material in high conductivity fog.

The measured surface temperature and the TGA plots suggest that the dry band arcing associated with the larger leakage current (typically 75 to 100 mA peak) during the high conductivity test is capable of raising the local surface temperature above 250°C which is sufficient for the ATH filler to liberate the water of hydration and hence remove the degradation products from the surface. Therefore, the EPDM materials with ATH filler show substantial erosion. During the low conductivity test, it is possible that the dry band arcing associated with the lower leakage current (typically 20 to 30 mA peak) raises the surface temperature sufficiently to cause the EPDM polymer to carbonize but not enough for the ATH filler to liberate the water of hydra-

tion. Therefore, the carbonaceous products are not removed from the surface thereby leading to tracking failure.

For comparison to EPDM samples containing ATH filler, EPDM samples with hydrated silica filler ($\text{SiO}_2 \cdot \text{H}_2\text{O}$) were also evaluated in low and high conductivity fog. For samples having the same filler concentration, the time to failure, failure mechanism and the weight loss of the hydrated silica filled samples was very similar to the corresponding ATH filled EPDM samples. In addition, the observations made on the ATH filled samples on the mechanisms by which the filler imparts tracking and erosion resistance to the material in low and high conductivity fog were found to be valid for the hydrated silica filled EPDM samples also. This clearly indicates the dominant role played by the water of hydration of the filler in imparting tracking and erosion resistance to the EPDM material.

The superior performance of the silicone rubber samples in the low conductivity test is due to the very low leakage current (Figs. 3.16 and 3.18) which ensures that the local surface temperature is below that which initiates polymer degradation.

5.3 Surface Studies by Energy Dispersive X-ray Analysis (EDAX)

The concentration and dispersion of filler (volume effects) are thought to play a significant role in the tracking and erosion resistance of materials [21]. At high filler concentration, fewer organic molecules are exposed at the surface to the heat of arcing. Also high concentration of filler improves the thermal conductivity of materials which in turn improves the heat dissipation and helps prevent local hot spots from developing.

To study filler volume effects, the surface of samples before and after salt fog tests were studied in a SEMCO Model Nanolab 7 Scanning Electron Microscope (SEM) equipped with an energy dispersive X-ray attachment (EDAX)¹.

5.3.1 Principle of EDAX

When a beam of high energy electrons is incident on a material, characteristic X-ray radiation is produced by the interaction of the incident electrons of the atoms in the sample. Occasionally the beam may dislodge K, L or M inner shell electrons and leave the atom in an excited or ionized state. The atom returns to its ground state by the transition of an outer electron into the vacancy in the inner shell. When the relaxation of the atom back to its original state occurs, the atom loses energy in the process by the emission of a photon of X-ray radiation. The electrons of

¹ EDAX work carried out at the Department of Engineering Materials, University of Windsor.

the atom are in discrete energy levels described by the quantum numbers of the atom. Since the electrons are in discrete energy levels, the emitted X-ray photon will also have a discrete energy equal to the energy difference between the initial and final states of the atom. Therefore, the wavelengths and energy of the characteristic radiation are specific for atoms of an atomic number. Detection of the presence of a characteristic X-ray line indicates that the element is present in the sample. These characteristic energies are used to obtain the composition of a sample of interest [39]. The spectrum obtained is a plot of the count rate of X-rays as a function of energy. The count rate gives an indication of the quantity of a particular element present in a material.

This technique is useful for the detection of elements with atomic number above 10 [40] and therefore it is useful for detecting Al in ATH and Si in SiO₂. In silicone rubber samples, X-rays are emitted from Al in the ATH filler and from Si in the polymer chain. A deficiency of filler is indicated by a decrease in the Al count rate and an increase in the Si count rate. In EPDM and epoxy samples the X-rays are of course emitted from the filler particles alone.

The specimens for the SEM studies were prepared by cutting 10X10X5 mm thick sections from the samples which were coated with 200 to 300 Å⁰ of spectroscopic grade carbon. At the accelerating voltage of 30 kV used in the study, the

depth of electron penetration is typically less than 2 μm [40]. X-rays were counted for one minute at 15 locations on the surface of the specimens for an indication of the filler distribution.

5.3.2 Distribution of Filler in Samples

From each sample of material and filler concentration, three to four specimens were prepared from the surface and from the bulk of the samples for SEM studies of the filler distribution. Fig. 5.4 shows the uniformity of ATH filler particles in silicone rubber samples SE and SA. Similar results have been obtained for EPDM samples. In general, improved uniformity of filler was obtained with increased concentration of filler. In samples having a low concentration of filler (SA in Fig. 5.4), the dispersion was as high as 100%. Despite the high ATH levels in the epoxy samples, a non-uniform filler dispersion as shown in Fig. 5.5 was observed.

In molds where the material flows together to form a joint, non-uniform dispersion of filler has been found. An example of this is shown for silicone rubber sample SD in Fig. 5.6.

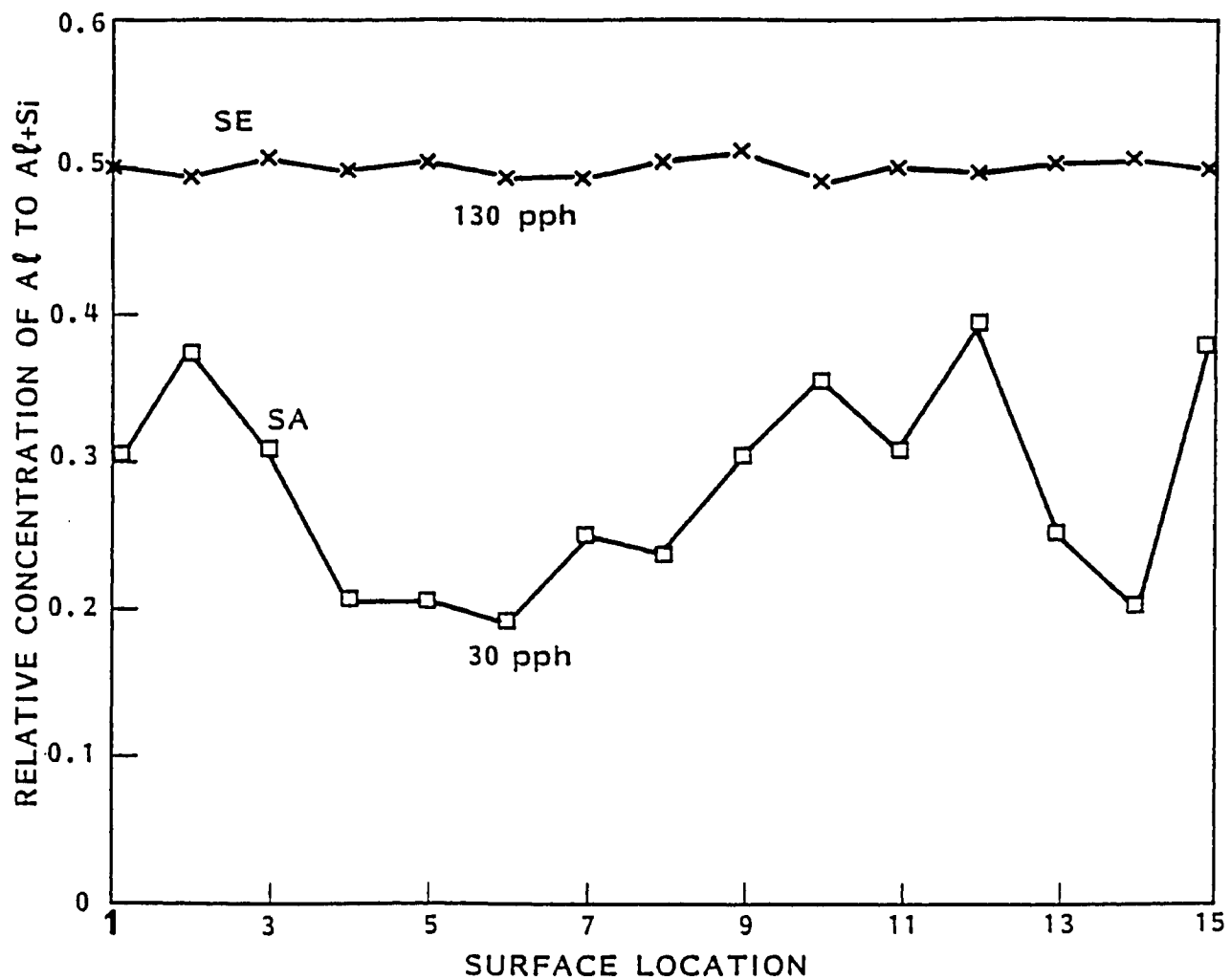


Figure 5.4: Distribution of Filler Particles in Silicone Rubber Samples SE and SA.

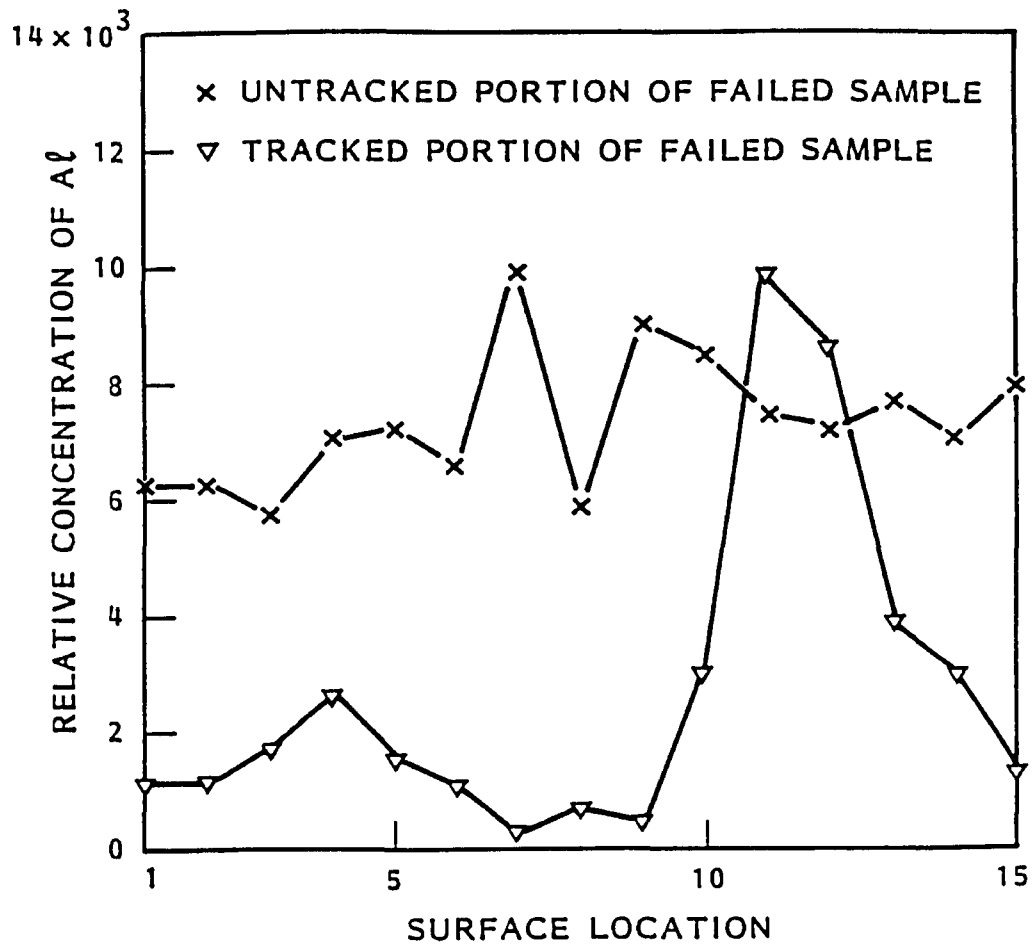


Figure 5.5: Distribution of Filler Particles in Epoxy Sample XA.

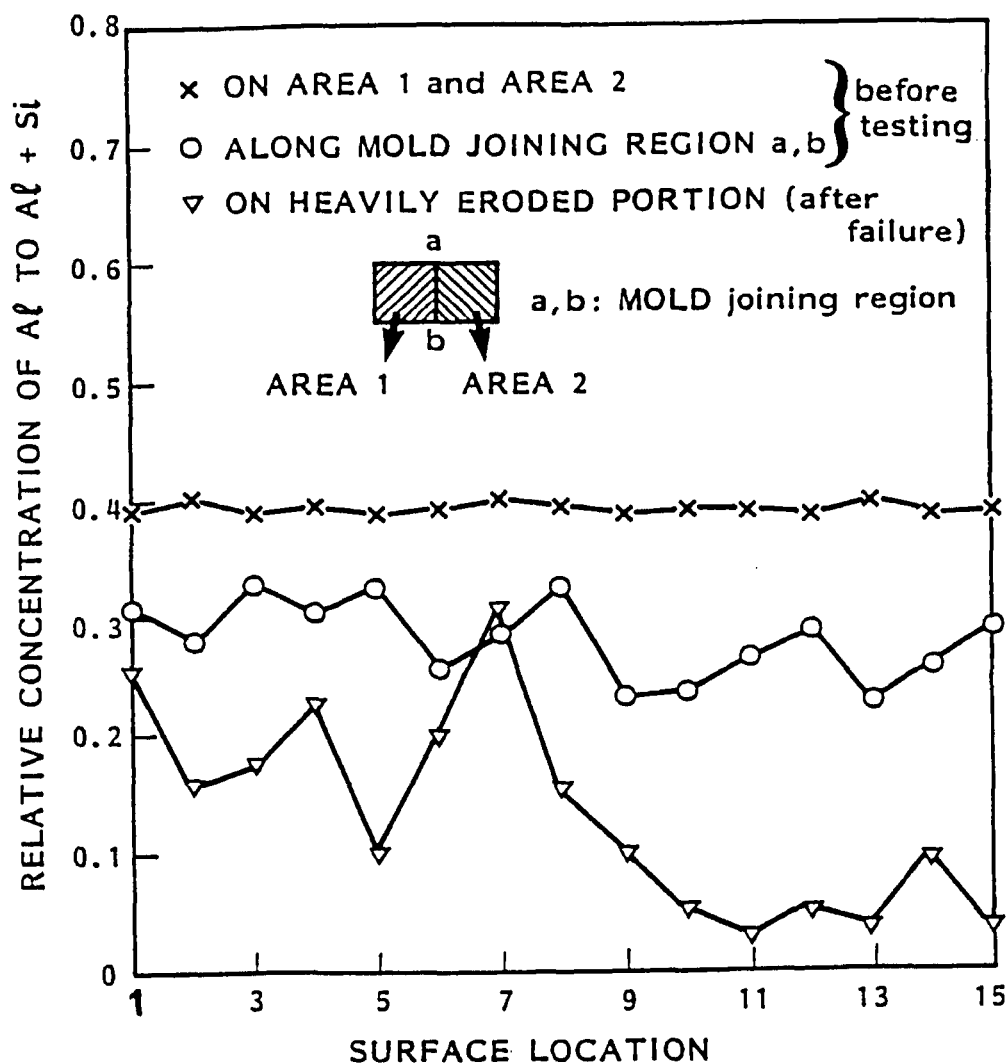


Figure 5.6: Distribution of Filler Particles in Silicone Rubber Sample SD.

5.3.3 Distribution of Filler in Failed Samples

Specimens were prepared from samples which failed by either tracking or erosion in the high (1600 $\mu\text{S}/\text{cm}$) conductivity test. Examples of the non-uniform distribution of filler along eroded and tracked sections of the samples are shown for epoxy, silicone rubber and EPDM in Figs. 5.5, 5.6 and 5.7 respectively. It is evident that in these specimens the filler distribution is highly non-uniform.

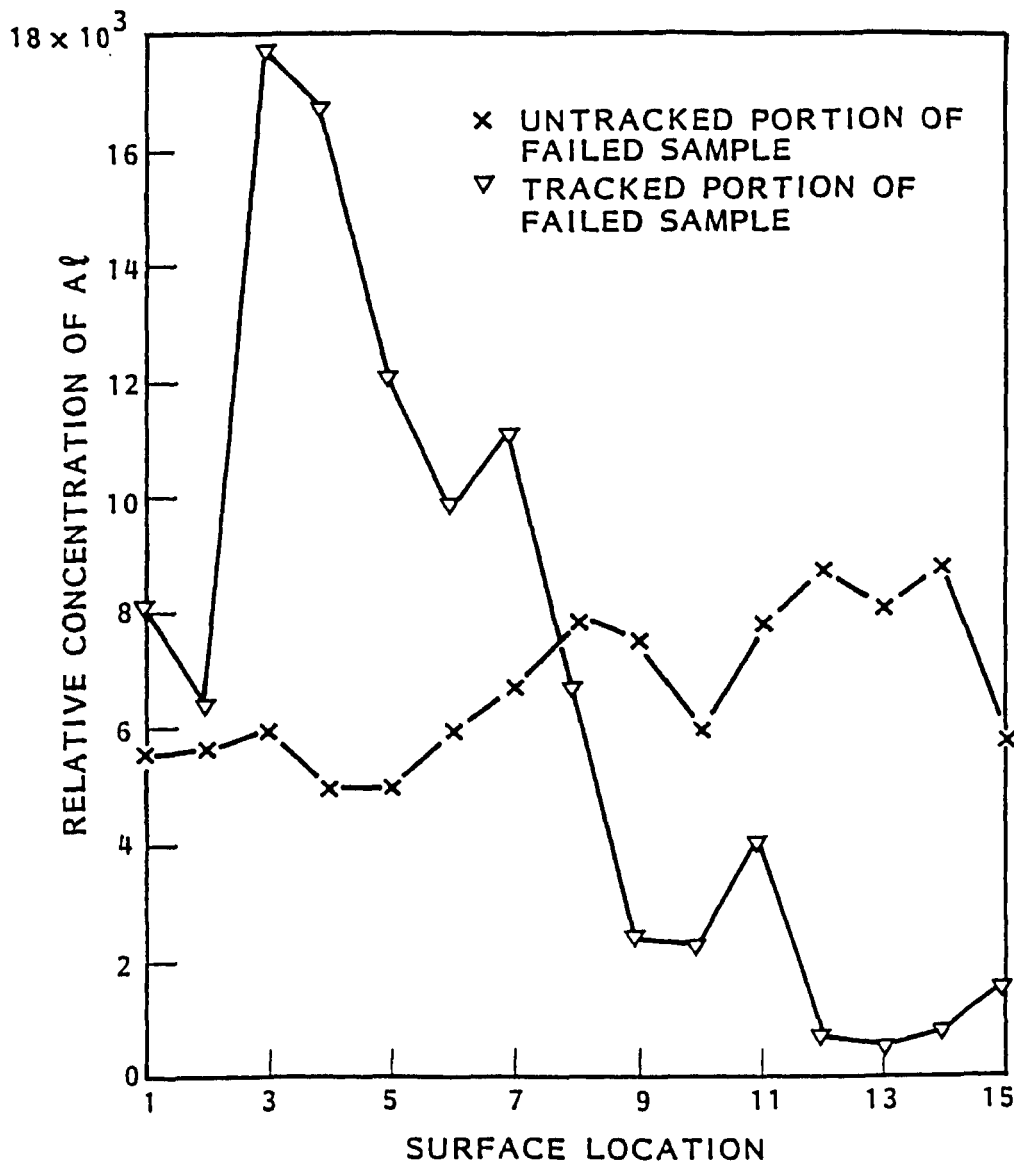


Figure 5.7: Distribution of Filler Particles in EPDM Sample EB.

It is postulated that a non-uniform distribution of filler particles in materials leads to the formation of dry bands across areas devoid of filler. The reason for this can be attributed to the hygroscopic nature of the fillers. As a result, dry band arcing initiates tracking and erosion in these regions which are rendered less resistant to arcing

due to a deficiency of filler. The superior performance of sample EO with no ATH or silica filler in high conductivity fog (1000 and 1600 $\mu\text{S}/\text{cm}$) can be explained by the fact that no inhomogeneities are created on the surface. Therefore, there are no preferential locations on the surface for dry band arcing to occur. The reduced magnitudes of the cumulative charge and the amplitude of the leakage current pulses suggest that the dry bands are wider and also that the temperature of the surface due to arcing is lower when compared to the filled samples.

In samples which failed the low conductivity test, it was observed that the filler dispersion where tracking had initiated was very similar to areas not affected by tracking and there were no indications of a highly non-uniform filler dispersion. This indicated that the tracking failure of these materials in low conductivity fog could not be attributed to filler dispersion. The mechanism of failure in low conductivity fog has been outlined in Section 5.2.4.

5.4 Material Surface Study

5.4.1 Introduction

Polymeric materials, being low surface energy materials, do not allow a continuous water film to be formed on a virgin surface. This is because the advancing contact angle of water droplets on such surfaces is greater than 90° which causes them to bead up [41]. The transition to a hydrophil-

lic surface, which occurs during dry band arcing, could be due to increased exposure of hygroscopic filler particles at the surface and/or surface changes favorable for wetting. The former was discounted based on the fact that the unfilled EPDM sample EO was also found to wet readily after exposure to electric stress and fog. To understand the transition from a hydrophobic to a hydrophillic surface, it is therefore necessary to follow the changes in surface composition before and after being subjected to corona which causes the transition.

It has been postulated that the hydrophobicity exhibited in silicone rubber insulation in the field despite the accumulation of surface contamination, could be due to the diffusion of silicone oil (which is used in manufacture) to the surface [42]. In addition, there may be a number of low molecular weight polymer chains in the material which are highly mobile due to their relatively low surface tension [41]. These mobile species could also diffuse to form a thin silicone layer on the surface thereby causing water to bead up.

In order to study the diffusion process and the surface transition from a hydrophobic to a hydrophillic surface during dry band arcing, the material surface was analyzed by Electron Spectroscopy for Chemical Analysis (ESCA) [43]. The reasons for choosing this technique were:

1. Only the top few monolayers (10 to 50 Å⁰ [43]) of the surface is analyzed. Thus, there is a greater chance of detecting changes in the surface composition caused by the diffusion of mobile species from the bulk to the surface.
2. An X-ray beam is used for analysis instead of an electron beam which is used in several other methods [40]. Therefore, insulating materials can be analyzed as is, without a conducting coating which is required to dissipate charges which are generated on the surface of a sample when subjected to an electron beam. This is an advantage when the surface has to be analyzed after treatment with corona with the least elapsed time.
3. The time of analysis is fairly fast (about 30 minutes required for a broad elemental scan).

5.4.2 Principle of ESCA

Surface analysis by ESCA or X-ray Photoelectron Spectroscopy (XPS) is accomplished by irradiating a sample with monoenergetic soft X-rays and analyzing the emitted electrons on the basis of their energy. Mg K α (1253.6 eV) or Al K α (1486.6 eV) X-rays are normally used. These photons have limited penetrating power in a solid, of the order of 1-10 μ m. They interact with atoms in this region by photoelectric effect, causing electrons to be emitted. The emitted electrons have kinetic energies given by: $KE = hv - BE - \phi$; where hv is the energy of the photon, BE is the binding energy of the atomic

orbital from which the electron originates, and ϕ is the spectrometer work function.

The probability of electrons interacting with the sample is far greater than that for photons. Therefore, the path length of the photons is of the order of micrometers and that of the electrons is of the order of tens of Angstroms. Thus, while ionization occurs to a depth of a few micrometers, only those electrons that originate within tens of Angstroms below the solid surface can leave the surface without energy loss. It is these electrons which produce the peak in the spectra and are most useful.

The electrons leaving the sample are detected by an analyzer according to their kinetic energy. The analyzer normally is operated as an energy "window", accepting only those electrons having an energy within the range of this fixed window, referred to as pass energy. The spectrum obtained is a plot of the number of emitted electrons per energy interval versus their kinetic energy. Each element has a unique elemental spectrum and the spectral peaks from a mixture are approximately the sum of the individual constituents [43]. In this technique, the surface composition of all elements, except hydrogen and helium, can be obtained. A typical ESCA spectrum of a silicone rubber material is shown in Fig. 5.8.

The ESCA instrument used in the present study was a Surface Science Laboratory SSX-100 instrument equipped with a

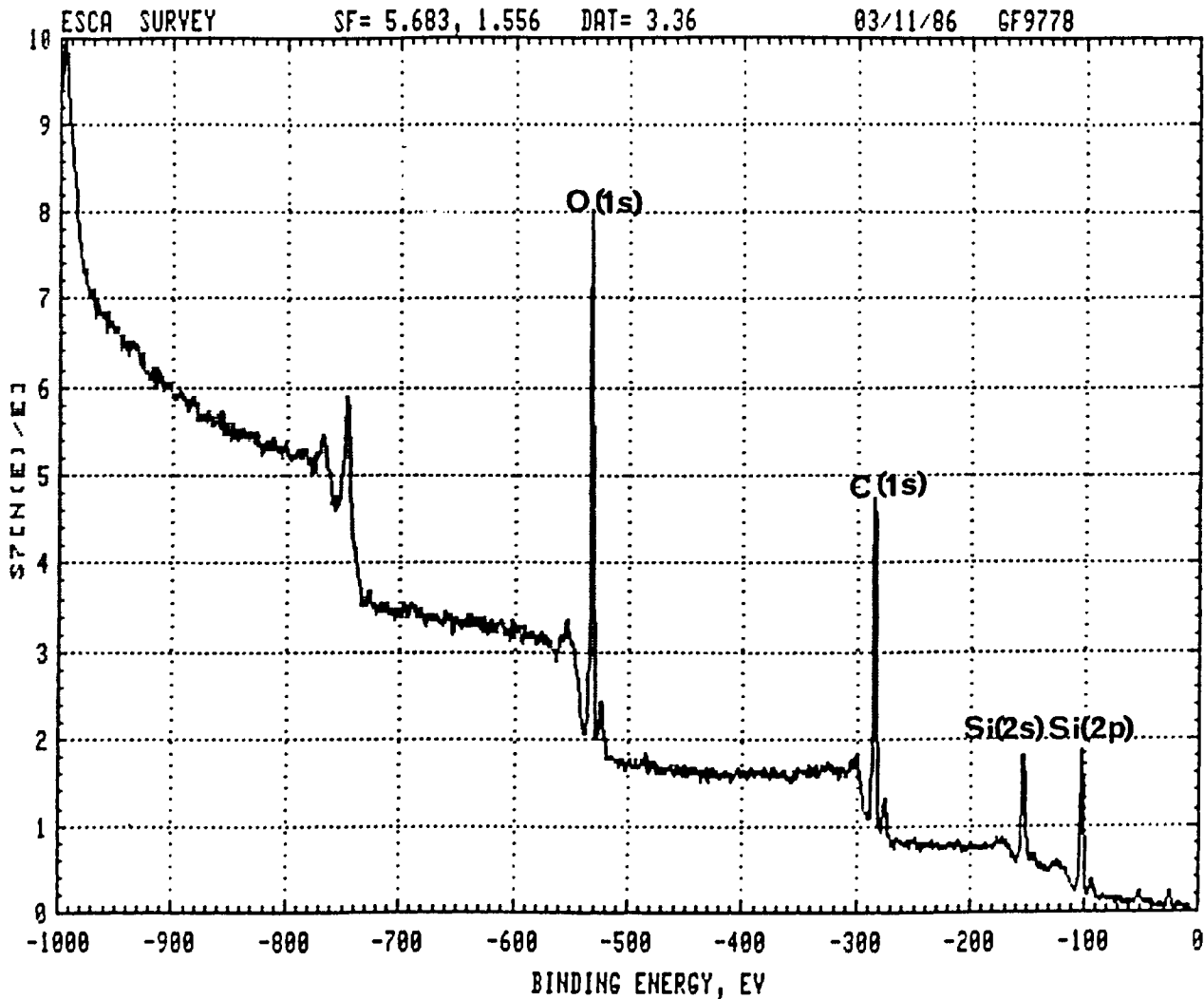


Figure 5.8: Typical ESCA Spectrum of Silicone Rubber Material.

hemispherical analyzer and monochromatized Al K α X-ray source. The specimens for this study were typically 3X3X2 mm thick and were cleaned with methanol to remove any mold release agent.

5.4.3 Results Using ESCA¹

In order to demonstrate the diffusion process, the virgin surfaces of the silicone rubber samples were analyzed and then coated (by evaporation) with a layer of carbon (about 1 μm thick). The coated samples were then analyzed after some elapsed time.

The samples evaluated were vinyl-dimethyl silicone rubber with the vinyl content less than 1%. Therefore, in a predominantly dimethyl silicone rubber material, the expected surface composition would be O = 25%, Si = 25% and C = 50%. The results of the surface analysis are in Table 5.1. It can be seen that the composition of the virgin specimen closely corresponds to that expected. The absence of Al on the virgin surface indicates that the ATH filler does not occupy the top 50 \AA of the surface. With time, the composition of the coated surface approaches that of the virgin surface which is a clear demonstration of diffusion.

As oils are used in the processing of EPDM samples, diffusion is to be expected in these materials also. But the rate of diffusion could be different from that in silicone rubber due to the difference in the mobilities of the polymer chains in the two materials [41]. To demonstrate this, the silicone rubber and EPDM samples which had accumulated scale deposits during the low conductivity test were ana-

¹ ESCA work carried out at Surface Science Western, University of Western Ontario, London, Ontario.

Table 5.1: Surface Analysis of Silicone Rubber and EPDM Samples.

MATERIAL	COATING MATERIAL AND THICKNESS	SURFACE COMPOSITION (%)					TIME LAPSED AFTER COATING (HOURS)
		O	Si	C	Ca	Mg	
SILICONE RUBBER (S120A)	NONE (VIRGIN)	26.60	21.10	52.30	0	0	--
	CARBON $\approx 1 \mu\text{m}$	12.63	10.26	77.11	0	0	1
		13.24	13.34	73.42	0	0	12
		14.76	13.94	71.30	0	0	18
		16.29	16.90	66.81	0	0	24
25.00		20.49	54.51	0	0	50	
	WATER SCALES $\approx 0.335 \text{mm}$	30.90	13.52	40.10	2.32	13.16	200
EPDM (E120A)	WATER SCALES $\approx 0.26 \text{mm}$	41.52	2.11	30.22	4.53	21.61	200

lyzed after about 200 hours on removal from the fog chamber. The EPDM sample was tested for a much shorter time than the silicone rubber sample and so the thickness of the scale on the silicone rubber sample was greater. The results of the analysis shown in Table 5.1 indicates a higher concentration of Ca and Mg on the EPDM sample when compared to the silicone rubber sample. These results clearly demonstrate that the silicone oil diffuses through the scale deposit as well.

In order to understand the surface transition during dry band arcing, specimens whose virgin surface were analyzed, were then subjected to corona discharges in air for about 30

minutes from a portable high frequency generator. After corona treatment, the surface was found to promote a continuous water film. The surface was analyzed immediately and after about 24 hours at which stage the surface had recovered its hydrophobicity. The results of the analysis shown in Table 5.2 indicate that the corona treatment is responsible for a large increase in oxygen concentration and a corresponding decrease in carbon concentration. This could be due to the deposition of hydroxyl (OH) groups from the atmosphere which favours the wetting of the surface.

Table 5.2: Effect of Corona and Recovery on Surface Composition of Silicone Rubber.

MATERIAL	SURFACE CONDITION	SURFACE COMPOSITION (%)		
		O	Si	C
SILICONE RUBBER S120A	VIRGIN	26.6	21.1	52.3
	CORONA TREATED	45.3	24.0	30.7
	24 HOURS AFTER CORONA	30.97	21.14	47.89

The recovery of hydrophobicity in uncontaminated silicone rubber materials after exposure to corona has been attributed to the reorientation of hydrophilic groups away from the surface and/or migration of low molecular weight polymer chains to the surface [44]. The data obtained in the present study demonstrates that the migration of low molecular

weight chains to the surface is the more dominant mechanism responsible for the recovery of hydrophobicity.

5.5 Summary

The dominant mechanisms by which the filler imparts tracking and erosion resistance to the polymer is governed by experimental conditions. While the volume effects of the filler is effective in imparting tracking and erosion resistance under all conditions, the physical cleaning action of the hydrated filler is effective only in high conductivity fog tests. The chemical mechanism of the hydrated filler cannot be substantiated under dry band arcing conditions.

Studies of filler dispersion by EDAX demonstrate that a highly non-uniform filler distribution is responsible for initiating tracking or erosion in high conductivity fog.

Surface study by ESCA demonstrate that the migration of silicone oil and/or low molecular weight polymer chains through the contamination to the surface is responsible for the prolonged hydrophobicity in silicone rubber material.

Chapter VI

THEORETICAL MODEL TO PREDICT THE PERFORMANCE OF POLYMERIC MATERIALS DURING DRY BAND ARCING

6.1 Introduction

When a rod specimen of an insulating material is subjected to dry band arcing, the subsequent heating of the material is due to heat transfer by conduction. If a circular area of radius R on the surface ($R = \sqrt{x^2 + y^2}$) is heated uniformly by a heat flux Q (due to dry band arcing), the transient heat conduction equation in the cartesian coordinates x , y , z system is given by [45]:

$$\alpha \left[\frac{\partial^2 T}{\partial x^2} + \frac{\partial^2 T}{\partial y^2} \right] = \frac{\partial T}{\partial t} \quad (1)$$

where T = temperature of the material above ambient, $^{\circ}\text{C}$

t = time duration of dry band arcing in a particular location, s

α = thermal diffusivity of the material, cm^2/s .

Initially, $T=0$ at $t=0$ and one boundary condition is $T \rightarrow 0$ as $z \rightarrow \infty$.

If the heat flux (Q) is incident (i.e., $z=0$) on the circular area and zero elsewhere (this assumption is valid because the temperature drops rapidly outside the region of interest [46]), the second boundary condition is:

$$HT - \frac{K\partial T}{\partial z} = \begin{cases} Q & \text{for } r \leq R \text{ and } t > 0 \\ 0 & \text{for } r > R \text{ and } t > 0 \end{cases}$$

where H =surface heat transfer coefficient, $W/cm^2 \text{ } ^\circ C$

and K =thermal conductivity of the material, $W/cm \text{ } ^\circ C$.

The parameter H in the present problem accounts for the surface cooling by convection due to the presence of water and pressurized air in the fog chamber.

Equation (1) with the above boundary conditions has been solved [45] to yield the transient temperature of the circular area. In its final form:

$$T = T_{nc} - \frac{2Q}{H} \int_0^w \left[1 - e^{-h^2 R^2 / 4w^2} \right] w e^{w^2} \operatorname{erfc}(w) dw \quad (2)$$

and T_{nc} = temperature without surface cooling

$$= \frac{QR}{K} \left[\frac{2}{\sqrt{\pi}} \left(\frac{\alpha t}{R^2} \right)^{1/2} \left(1 - e^{-h^2 R^2 / 4\alpha t} \right) + \operatorname{erfc} \frac{R}{2\sqrt{\alpha t}} \right]$$

where $w = h \sqrt{\alpha t}$, $h = H/K$, $\operatorname{erfc}(\beta) = 1 - \operatorname{erf}(\beta)$ = complimentary error function and $\operatorname{erf}(\beta) = \frac{2}{\sqrt{\pi}} \int_0^\beta e^{-\beta^2} d\beta$ = Gaussian error function.

Both $\operatorname{erf}(\beta)$ and $\operatorname{erfc}(\beta)$ are tabulated function and their numerical equivalents are available [46].

6.2 Effect of ATH or Silica Fillers on the Thermal Conductivity and Diffusivity of Materials

Table 6.1 shows the various physical constants for ATH and silica fillers, silicone and EPDM rubbers. The filled rubber samples are composite materials in which a volume

fraction x_1 is composed of rubber and the remaining ($1-x_1 = x_2$) is composed of filler. Assuming a uniform filler dispersion (which has been validated by EDAX for concentrations above 50% by weight, K , the effective thermal conductivity is calculated analogous to calculating electrical resistances in series [47] and is given by:

$$K = \frac{K_1 K_2}{K_1 x_2 + K_2 x_1}$$

Table 6.1: Physical Constants of Materials Evaluated.

MATERIAL	THERMAL CONDUCTIVITY ¹ W/cm °C	THERMAL DIFFUSIVITY ¹ cm ² /s	DENSITY g/cm ³
SILICONE RUBBER	19 X 10 ⁻⁴	15 X 10 ⁻⁴	1.074 ²
EPDM	19 X 10 ⁻⁴	15 X 10 ⁻⁴	0.99 ²
ATH	2135 X 10 ⁻⁴	675 X 10 ⁻⁴	2.42 ³
SILICA	150 X 10 ⁻⁴	80 X 10 ⁻⁴	2.65 ³

1. FROM REFERENCE [47]
2. FROM VOLUME AND WEIGHT MEASUREMENTS
3. FROM SUPPLIERS

where K_1 and K_2 are the thermal conductivities of rubber and filler respectively. Since the exact quantity by weight of filler is known, x_1 and x_2 can be calculated for rubber samples for different filler concentrations.

The effective thermal diffusivity, α , of the filled rubber samples is calculated on the basis that the energy required to raise a mass of composite material by ΔT is

equal to the sum of the energies required to raise the individual components of the composite mass through the same temperature difference [49].

If ρ_1 and ρ_2 are the densities of polymer and filler, respectively, C_{p1} and C_{p2} are the specific heat capacities of polymer and filler respectively, it can be shown that the effective thermal diffusivity,

$$\alpha = \frac{K}{\rho_1 x_1 C_{p1} + \rho_2 x_2 C_{p2}}$$

Fig. 6.1 shows the variation of K and α of the rubber samples as a function of filler concentration.

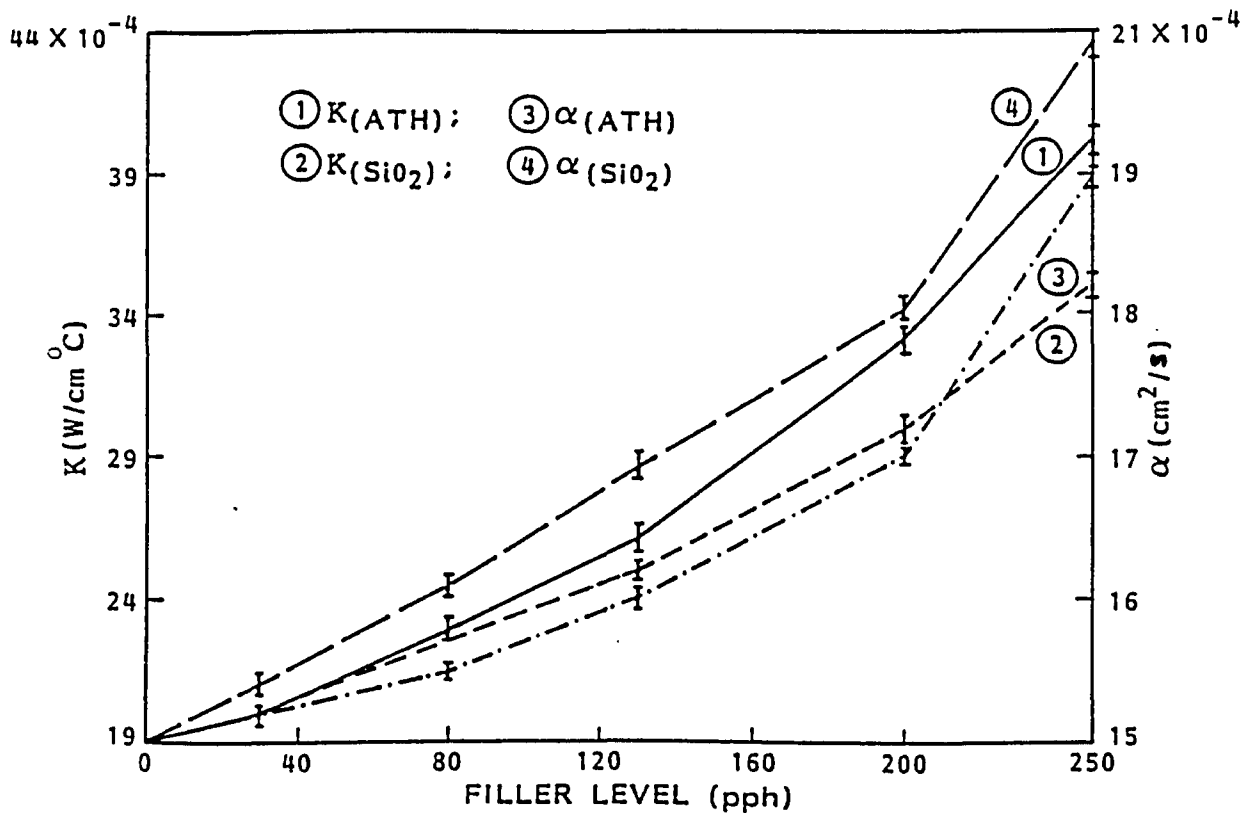


Figure 6.1: Effective Thermal Conductivity and Diffusivity of ATH and Silica Filled Rubber Samples.

6.3 Heat Flux Q due to Dry Band Arcing

In order to determine the surface temperature during dry band arcing, the heat flux Q needs to be known accurately. The method used by Wilkins [28] to calculate Q is as follows:

The thermal decomposition temperature and the time to cause thermal breakdown was determined experimentally for various polymeric materials. Knowledge of the thermal conductivity and diffusivity and the time to thermal breakdown enables the calculation of surface temperature using equation (2). According to this approach, for a 6.4mm spacing between electrodes on a material, the calculated heat flux does not exceed 10 W/cm^2 . For the limiting case without cooling, the surface temperature can be shown to be less than 200°C , which is insufficient to cause degradation of materials like silicone rubber and EPDM. In the present study, tracking and erosion of these materials have occurred on samples subjected to cooling from fog, under experimental conditions which gives the same order of leakage current as that used by Wilkins for calculation of heat flux. This implies that the surface temperature is much higher than that predicted by Wilkins' model. Therefore, this necessitates a different approach for the calculation of heat flux.

The heat flux, in the present study, is calculated from the electric stress-current characteristics of the dry band discharge. The electric stress E is related to the current i as follows [50]:

$$E = 530i^{-0.24} \text{ V/cm for } i \leq 15 \text{ mA}$$

$$= 63i^{-0.76} \text{ V/cm for } i > 15 \text{ mA}$$

If d is the diameter of the arc root (cm), the power input per unit area P is given by the product of the electric stress and surface current density (i/d). Thus,

$$P = \frac{Ei}{d} \text{ W/cm}^2.$$

Oscillographic monitoring of samples during ac tests of dry band arcing showed that the conduction period varied in the range from 2 to 6ms in each half cycle of the 60 Hz wave. A separate experiment utilizing a timing circuit (details in Appendix), was carried out to determine the distribution of the conduction period of dry band scintillations. The results in Table 6.2 show that 90% or more of the dry band scintillations had a conduction period between 2 to 3ms on each half cycle. Therefore for a typical average duration of 2.5ms, the heat flux Q or the average power dissipated per unit area is given by:

$$Q = \frac{1}{F} \int_0^F P df = \frac{P}{3.6d} \quad (3)$$

where F =time period of the 60 Hz wave and f =2.5ms.

An examination of the samples which had failed by tracking or erosion showed that the minimum width of the tracked or eroded portion was about 3mm. High speed photographs of the arc root on aqueous electrodes [51] has yielded an arc diameter in the range 2 to 7mm. Visual observations of dry

band arcing indicated that the arcs were definitely not in the forms of filamentary streaks but were rather diffused [52]. An average value of $d=4.5\text{mm}$ was taken for the calculation of Q .

Table 6.2: Distribution of the Conduction Period of Dry Band Discharges.

SAMPLE	WATER CONDUCTIVITY ($\mu\text{S/cm}$)	LEAKAGE CURRENT PULSES	
		CONDUCTION PERIOD (ms)	PERCENT OF TOTAL PER HOUR (%)
S200A	1000	> 6	0
		> 4	2.4
		> 3	5.4
		> 2	91
E120A (WITH SCALE)	250	> 6	0.3
		> 4	4
		> 3	10
		> 2	92

6.4 Surface Heat Transfer Coefficient

The resulting surface temperature of the sample during dry band arcing is dependent on the value of the surface heat transfer coefficient H , which takes into account the cooling provided by the presence of water and pressurized air in the fog chamber. Literature [48] provides the range of H for different modes of cooling, but as the magnitude of H varies over a wide range, the calculated temperature also varies over a wide range. Hence, it is desirable to determine the appropriate value of H for the experimental set-up in use.

The rate of heat transfer q by convection between a surface and a fluid is given by [48]:

$$q = HA(T_2 - T_1)$$

$$\text{Thus } H = q/A(T_2 - T_1)$$

where $T_2 - T_1$ is the difference between the surface temperature and the surrounding fluid, $^{\circ}\text{C}$, and A is the heat transfer area, cm^2 .

To determine the heat transfer coefficient for the fog chamber, a 2.54cm diameter steel rod, 28cm in length, with an electric heater (1cm diameter) in the center of the rod was placed in the same location as the rubber samples. Four thermocouples (copper constantan) were soldered on to the rod at different locations. The water and air supply were turned on and after 30 minutes, the steady state temperature was measured with a thermometer. The power input q to the heater was measured with a wattmeter. The heater supply was then switched on and after one hour the steady state temperature difference ($T_2 - T_1$) was measured. The value of H was found to vary in the range 0.02 to 0.03 $\text{W}/\text{cm}^2\text{ }^{\circ}\text{C}$ for different locations of the rod corresponding to the various positions of the samples. An average value for H of 0.025 $\text{W}/\text{cm}^2\text{ }^{\circ}\text{C}$ was used for the model.

6.5 Duration of Dry Band Arcing

On a sample subjected to electric stress and fog, the mass rate of water which remains on the sample dm/dt (g/s) is the difference of the mass rate being sprayed m_s (g/s) and the mass rate evaporated m_e (g/s) due to dry band arcing.

$$\text{i.e., } dm/dt = m_s - m_e \quad (4)$$

The mass rate of water evaporated can be calculated from $mh = Vit$; where h is the latent heat of vaporization of water (J/g).

$$\text{Therefore } m/t = vi/h = m_e$$

Integrating equation (4),

$$(m_s - vi/h)t = m_f - m_i \quad (5)$$

where m_f = final mass of water before the dry band changes location and m_i is the initial mass of water.

For a dry band to move to another location on the surface, the arc roots must dry up, i.e., $m_f = 0$.

Therefore equation (5) can be written as

$$(vi/h - m_s)t = \tau A \rho \quad (6)$$

where τ = initial thickness of the water film (cm), A = surface area of the sample (cm²) and ρ = density of water (g/cm³).

Dividing equation (6) by A

$$(vi/Ah - m_s/A)t = \tau \rho \quad (7)$$

$vi/A = Q$; m_s/A is the rate of water spray per unit area of the sample and is dependent on the type of fog generated. Based on earlier work [53], values of m_s/A ranging from 0.8

to $3 \text{ mg/cm}^2 \cdot \text{min}$ were used and found to have little effect on the value of t .

The thickness of the water film τ was calculated by the difference in the weight of dry and wet samples which had accumulated different amounts of scale during ac and dc study.

The duration of dry band arcing, t , was calculated using equation (7) for various values of leakage current obtained during the low and high conductivity tests and for water films of varying thickness. The results are shown in Fig. 6.2.

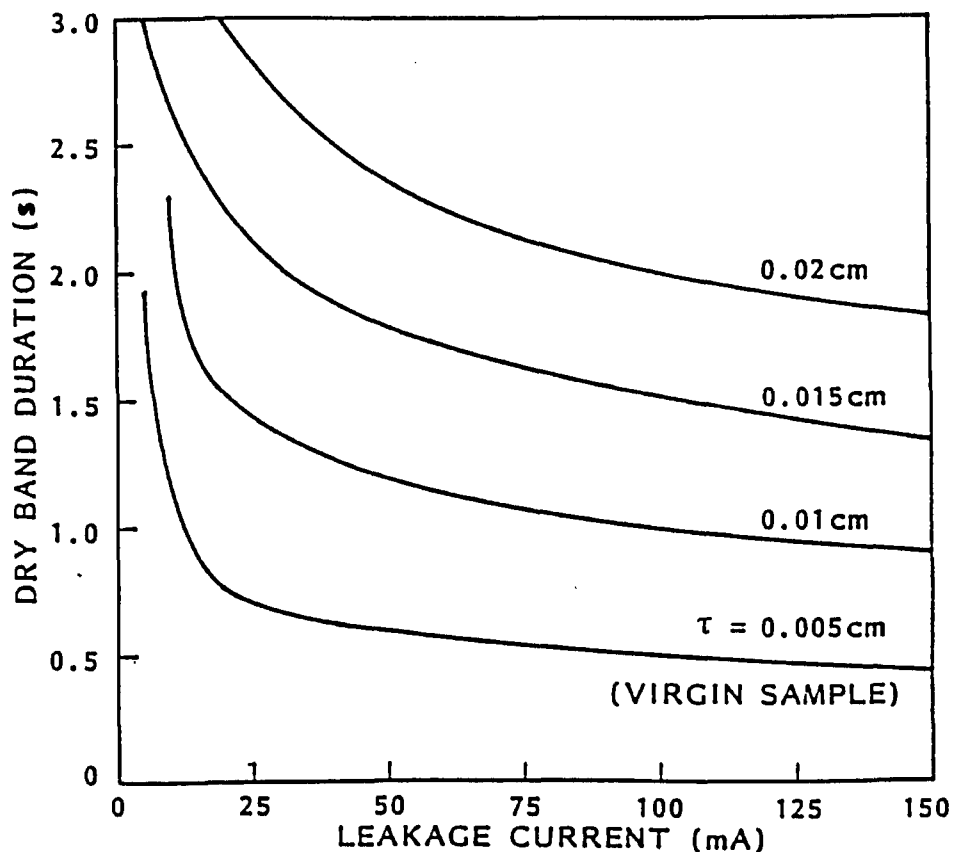


Figure 6.2: Time of Arcing as a Function of Water Film Thickness.

6.6 Surface Temperature During Dry Band Arcing

The hot spot temperature T given by equation 2 was evaluated by Simpson's rule [54] for various values of Q (as determined from equation 3) and t (obtained from Fig. 6.2) corresponding to the time of arcing in a particular spot on surfaces having different thickness of water film. Fig. 6.3 shows the typical variation of the hot spot temperature T with time t for various values of leakage current obtained during the low and high conductivity tests with ac. The values of the effective thermal conductivity K and diffusivity for the calculation was obtained from Fig. 6.1.

In order to correlate the model predictions with the experimental observations, Fig. 6.3 has been divided into zones: (1) 0 to 175 °C, (2) 175 to 250 °C and (3) above 250 °C. These divisions are based on TGA results of EPDM and silicone rubber samples (Figs. 5.1 and 5.2).

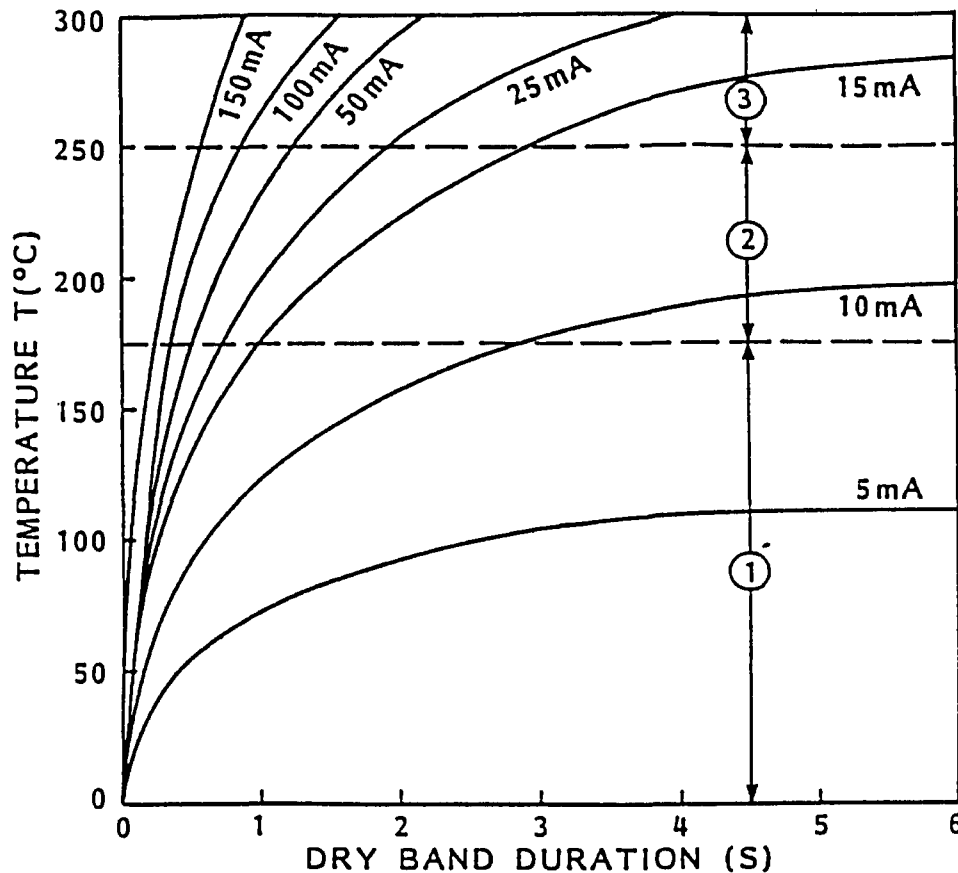


Figure 6.3: Hot Spot Temperature as a Function of Time and Leakage Current for Rubber Samples With 120 pph of Inorganic Filler.

6.7 Correlation of Model Predictions With Experimental Findings

The following points show the correlation between experimental findings and model predictions:

1. The model predicts that under conditions where the peak leakage current is less than 15mA, degradation of samples with little ($\tau < 0.01\text{cm}$) or no scale will be slow as the surface hot spot temperature is below 175 °C, the thermal stability limit of silicone rubber and

EPDM materials. Table 6.3 shows the results of material evaluation at various electric stress in low conductivity fog. It can be seen that at low electric stress when the peak leakage current was less than 15mA, no failure occurred in 500 hours. Failures occurred at higher electric stress when the typical peak leakage current exceeded 15 to 20mA.

Table 6.3: Time to Failure and Leakage Current as a Function of Electric Stress in Low Conductivity Fog.

SAMPLE	AVERAGE STRESS V/mm	ac		-dc	
		HOURS TO FAILURE	PEAK CURRENT (mA)	HOURS TO FAILURE	PEAK CURRENT (mA)
E130A	28	NF	8 - 10	NF	12 - 15
	40	NF	10 - 15	142	25 - 35
	60	368	20 - 30	69	40 - 50
E130S	28	NF	5 - 8	NF	10 - 15
	40	NF	5 - 10	126	25 - 35
	60	330	10 - 15	75	40 - 50
S130A	28	NF	3 - 5	NF	8 - 15
	40	NF	5 - 8	NF	10 - 20
	60	NF	10 - 15	185	20 - 40

NF: NO FAILURE

The practical significance of this data is that as long as the leakage current is suppressed below the threshold value, satisfactory performance can be expected. Therefore a material with good leakage current suppression capability can be operated at a relatively higher electric stress, whereas materials with

poor leakage current suppression capability has to be operated at a much lower electric stress. This has also been discussed in Chapter 4 with regard to insulators (Table 4.5).

2. In high conductivity fog where the peak leakage current is typically 75 to 125mA, local surface hot spots exceed 250°C even if dry bands persist in one location for a relatively short duration (less than 1s) as shown in Fig. 6.3. Therefore ATH filled EPDM samples can be expected to erode and have much longer times to failure than silica filled EPDM samples. The results shown in Fig. 3.1 and Tables 3.4 and 4.1 indicate that this is indeed the case.
3. As the effective thermal conductivity and diffusivity of ATH and silica filled samples are very similar (Fig. 6.1), in low conductivity fog where the local surface temperature due to the low leakage current (20 to 30 mA peak) is insufficient to liberate the water of hydration from the ATH filler, similar times to failure can be expected for samples with the same filler concentration. This is indeed true as illustrated by the results in Tables 3.4, 4.1 and 6.2.
4. As the accumulation of surface deposits is more rapid with -dc, the critical thickness of surface deposit required to cause dry band arcs to stay rooted to a particular spot to cause material degradation, is

built up in a much shorter time than with ac or +dc. Therefore, the time to failure can be expected to be much lower in -dc which is in agreement with the results shown in Tables 4.1 and 6.3.

5. Local surface temperature measurements during dry band arcing in low and high conductivity tests using temperature sensitive paints are in good agreement with that predicted by the model.

Chapter VII

CONCLUSIONS

1. The experimental conditions used in the fog chamber tests have a significant effect on the performance of silicone and EPDM rubbers. In low ($250 \mu\text{S}/\text{cm}$) conductivity fog, silicone rubber performed better than the EPDM material whereas in high ($\geq 1000 \mu\text{S}/\text{cm}$) conductivity fog, the order of performance was reversed. The epoxy resin exhibited an inferior performance when compared to the elastomers.

The ranking of materials obtained in low conductivity fog is consistent with that obtained in service. The superior performance of silicone rubber is due to the higher resistance offered by the material to the development of surface leakage current leading to rapid dry band activity. The development of leakage current is dependent on the type of polymer which is also consistent with service experience.

The ranking of materials in high conductivity fog is due to the difference by which the ATH filler imparts increased tracking and erosion resistance to silicone and EPDM rubber. The leakage current is independent of the polymer type which is in contradiction to what is observed in service.

As a much better correlation with service experience was obtained by evaluating materials in low rather than in high conductivity fog, this work raises serious concerns about the ability of existing test methods to evaluate materials in accordance with service experience.

2. The dominant mechanisms by which fillers impart tracking and erosion resistance to the materials is also governed by the experimental conditions.

In low conductivity fog, the widely used fillers, ATH and silica, impart similar resistance to tracking to the EPDM material through the mechanism of volume effects, which refers to the improvement in the heat dissipating properties of the material obtained with increasing filler concentration. In high conductivity fog, ATH filler imparts a superior resistance to tracking and erosion to the EPDM material than does silica filler by virtue of the physical cleaning mechanism. This mechanism refers to the liberation of water as steam and the resulting sputtering physically removes the carbonaceous deposits formed on the surface as a result of polymer degradation.

The chemical mechanism of the hydrated filler which refers to the removal of carbonaceous products as gases is shown not to be operative under dry band arcing conditions.

3. The filler level required for satisfactory performance is dependent on the leakage current suppression capability of the polymer. Based on the low conductivity test, a high filler level of 200 pph is necessary for the EPDM material, whereas for the silicone rubber material, the filler level required is considerably lower.
4. A study of filler dispersion in materials with the EDAX demonstrates that tracking and erosion could be initiated from areas with highly non-uniform filler dispersions.
5. The tracking and erosion resistance of the materials studied was similar for ac and +dc but was significantly reduced for -dc for samples oriented vertically. The reduction was due to the way in which scale was formed with -dc, which prolongs dry band activity at the bottom of the sample. For samples oriented horizontally, there was no discernable difference in the performance with ac, +dc and -dc.

In order to differentiate between the leakage current suppression capability of materials for dc, evaluation has to be done in low conductivity fog, but at a much lower electric stress than for ac. This is due to the thicker scale formed with dc, which increases the leakage current which in turn promotes rapid dry band activity in a shorter time interval when compared to ac.

6. Continuous measurement of cumulative charge, periodic measurement of weight loss due to dry band arcing and flashover voltage yield limited information about surface aging and failure of polymeric materials. On the other hand, the number and amplitude of peak current pulses above a preset threshold is a better indicator of surface aging and subsequent failure.
7. Similar ranking of materials is obtained by evaluating materials in the form of cylindrical rods and actual insulators. However, the use of cylindrical rods yields results in a much shorter time.

The shape of the sheds has a significant effect on insulator performance. Insulators with a protected leakage path perform better than those with an open or partially protected leakage paths.

8. ESCA studies demonstrate that the migration of silicone oil and/or low molecular weight polymer chains to the surface through the contamination is responsible for the prolonged hydrophobicity exhibited by the silicone rubber material.
9. The tracking and erosion resistance of the materials studied is unaffected by moisture ingress, a weak NaOH solution and the hydrocarbon solvent naphtha.
10. The model developed is shown to be in good agreement with the experimental findings. The most significant conclusion drawn from the model is that material deg-

radation is a function of leakage current magnitude and the time duration for which dry bands are rooted in a particular spot. As the latter is dependent on the accumulation of surface contamination, which is inevitable in outdoor environment, it is very important that the material and insulator design chosen are capable of suppressing leakage current to very low values.

Chapter VIII

RECOMMENDATIONS FOR FURTHER WORK

1. From the point of view of understanding polymer-filler interaction, the factors responsible for the absence of the physical cleaning by sputtering of the ATH filler in most silicone rubber samples is an aspect which needs further investigation. As sputtering was observed only in the sample S200A, it appears that it is dependent on the entire material composition. Knowledge of the type of base polymer, vulcanizing agent and additives used during processing could enable better understanding of the sputtering mechanism.
2. The diffusion of mobile species in silicone rubber material is related to the surface tension of the side groups in the polymer chain. It has been shown earlier, in connection with thin films, that by varying the composition of the side groups the leakage current suppression capability and the rate of recovery of hydrophobicity can be enhanced [34]. It is important to determine whether a similar improvement can be obtained in filled elastomers as it will enable the development of more suitable material compositions for outdoor insulation applications.

A theoretical model to predict the time dependent diffusion process in polymeric materials could also be developed.

Although it has been shown that in low conductivity fog, silicone rubber maintains a hydrophobic surface for a significantly longer time than the EPDM material, the reasons for this have not been determined. Intuitively, it can be expected that under mild dry band activity associated with low leakage current, the rate of formation of the hydroxyl groups which is responsible for the surface transition, is much slower in silicone rubber than in EPDM. An ESCA study of materials which have been subjected to controlled partial discharges, could enable in determining the rates of surface transition of different materials.

3. It has been observed from service experience that the type of contamination found on polymeric insulators is dependent on the type of polymer. For example, it has been reported [56] that low surface energy materials like silicone rubber and Teflon tend to accumulate low surface energy or hydrophobic type of contaminants, whereas high surface energy materials like porcelain and glass tend to accumulate hydrophillic type of contaminants. It has also been reported [57] that for insulators located in the same site, near a sea coast, the concentration of NaCl deposited on EPDM insulators

is significantly greater than on on silicone rubber insulators. The leakage current, which is determined by the surface conductivity, which is inturn dependent on the nature of the contaminants, is therefore different on different materials. As a result, insulator performance in the field is also dependent on the nature of surface contamination. For successful application of polymeric insulators, it is necessary to determine the mechanisms responsible for the preferential accumulation of contamination exhibited by different insulating materials.

4. A test method to evaluate polymeric materials and insulators has to be developed. Although this work has shown that materials have to be evaluated in low conductivity fog, work still needs to be done before a suitable test procedure can be outlined. For example, the effect of surface treatment, parameters like water flow rate, air pressure and type of fog generation, all of which influence the wetting, on material performance has to be determined in order to determine the optimum test conditions.
5. Work still needs to be done in order to fully understand the dc performance of polymeric materials. Electrolysis explains the initiation of scale from the cathode but does not account for the rapid accumulation of scale observed with -dc. To ensure that the

difference in material performance under the two polarities is not related to the experimental set-up, it is necessary to determine the dc performance from different set-ups. If similar results are obtained, then it means that for satisfactory operation, the leakage distance of insulators for the two polarities has to be different.

Appendix A

DATA ACQUISITION SYSTEM

The hardware used for data acquisition consists of an 8 bit, 16 channel A/D converter (Mountain Computer Inc.) located in slot#4 of an APPLE Clone computer (64K memory), two Quantin disk drives (for 5.25 inch floppy disks), an Electrohome video monitor and a Gemini 10-X printer.

The software, developed by McAvoy [58], is designed to continuously monitor the voltage signals proportional to the leakage current of the samples, and give the following information:

1. the positive and negative peak current in a given period.
2. the number of current pulses between specified current limits.
3. the positive and negative cumulative charge in a given time interval which is the integral of the leakage current over the time interval.
4. the average positive and negative leakage current in a given time interval which is the ratio of the cumulative charge to the time interval.

A major portion of the software description given below is reproduced from Reference [58].

A.1 Algorithm for Numerical Integration

Based on the speed of computation, amount of memory used and the ease of programming, the trapezoidal method of numerical integration was used to evaluate the cumulative charge. The trapezoidal rule was implemented as follows:

Let the voltage signal applied to the A/D converter be v , which is related to the leakage current, i , of the sample by $v=ixK$. K is the value of the resistance used to convert the current signal to the voltage signal. The cumulative charge for a given period of time, from t_1 to t_2 is

$$Q = \int_{t_1}^{t_2} i dt = 1/K \int_{t_1}^{t_2} v dt$$

Let N be the number of samples taken in a period $t_2 - t_1$ seconds. The time between samples is $T = (t_2 - t_1) / N$.

The 8 bit A/D converter converts voltages in the range of -5 to +5 volts to digital values ranging from 0 to $2^8 = 256$, denoted by $x(n)$. The relationship between the number $x(n)$ and the corresponding voltages is

$$x(n) = 25.6v(nT) + 128$$

The numbers are adjusted to eliminate the 128 offset.

$$x(n) = x(n) - 128$$

$$x(n) = 25.6v(nT)$$

Since positive and negative currents are integrated separately, they must be added separately. In this derivation,

only the the calculation of the positive charge is shown as the negative charge can be calculated in a similar manner.

For the calculation of the positive charge, $x(n)$ is defined as

$$x(n) = 25.6v(nT), \text{ for } v(nT) > 0 \\ = 0, \text{ for } v(nT) < 0$$

According to the trapezoidal rule,

$$Q = 1/K \int v dt = T/K [v(0)/2 + v(T) + v(2T) + \dots + v(nT)/2]$$

$$\text{i.e., } Q = (T/25.6K) [x(0)/2 + x(1) + x(2) + \dots + x(n-1) + x(n)/2]$$

$$\text{Define } \text{SUM}(n) = x(0)/2 + x(1) + x(2) + \dots + x(n-1) + x(n)$$

$$\text{Thus } Q = (T/25.6K) (\text{SUM}(n) - x(n)/2)$$

$$\text{If } \text{SUM}(n-1) = x(0)/2 + x(1) + x(2) + \dots + x(n-1)$$

$$\text{then } \text{SUM}(n) - \text{SUM}(n-1) = x(n)$$

$$\text{or } \text{SUM}(n) = \text{SUM}(n-1) + x(n)$$

Hence $\text{SUM}(n)$ is obtained by successively adding to it the present value of $x(n)$. The average current $i = Q/(t_2 - t_1)$. A

The time interval $t_2 - t_1$ corresponds to the time between the data printouts and it may be adjusted by the user to a value no less than 1 minute. The number of samples obtained in the time interval $t_2 - t_1$ depends on the sampling frequency.

A.2 Program Design

The software package used in this work consists of three programs. A brief description of these are outlined in this section.

A.2.1 HELLO

HELLO is a program which is automatically booted when the computer is switched on. This program, written in Applesoft BASIC, provides screens to the user on the various capabilities of the software.

A.2.2 SAMPLE

SAMPLE, a program also written in Applesoft BASIC, initializes the variables to be used in the signal processing program, SAMPLE.CODE. Before running the signal processing program, SAMPLE prompts the user to enter the pertinent information. First, the user must enter the date and time of the experiment. SAMPLE then creates a file using the date and time of the experiment entered for identification.

SAMPLE then prompts the user to enter the number of insulating samples used in the experiment and to identify the samples. It is also required to enter the time between data printouts, the desired sampling frequency, the value of the resistor used and the current limits in which the count of pulses is required.

SAMPLE then prompts the user to prepare the printer before calling SAMPLE.CODE. Once the system begins to monitor the signals, the user can stop the signal processing by pressing CTRL-S. The user can switch to a different resistor and continue the sampling or terminate the program. The flow chart of SAMPLE is shown in Fig. A.1.

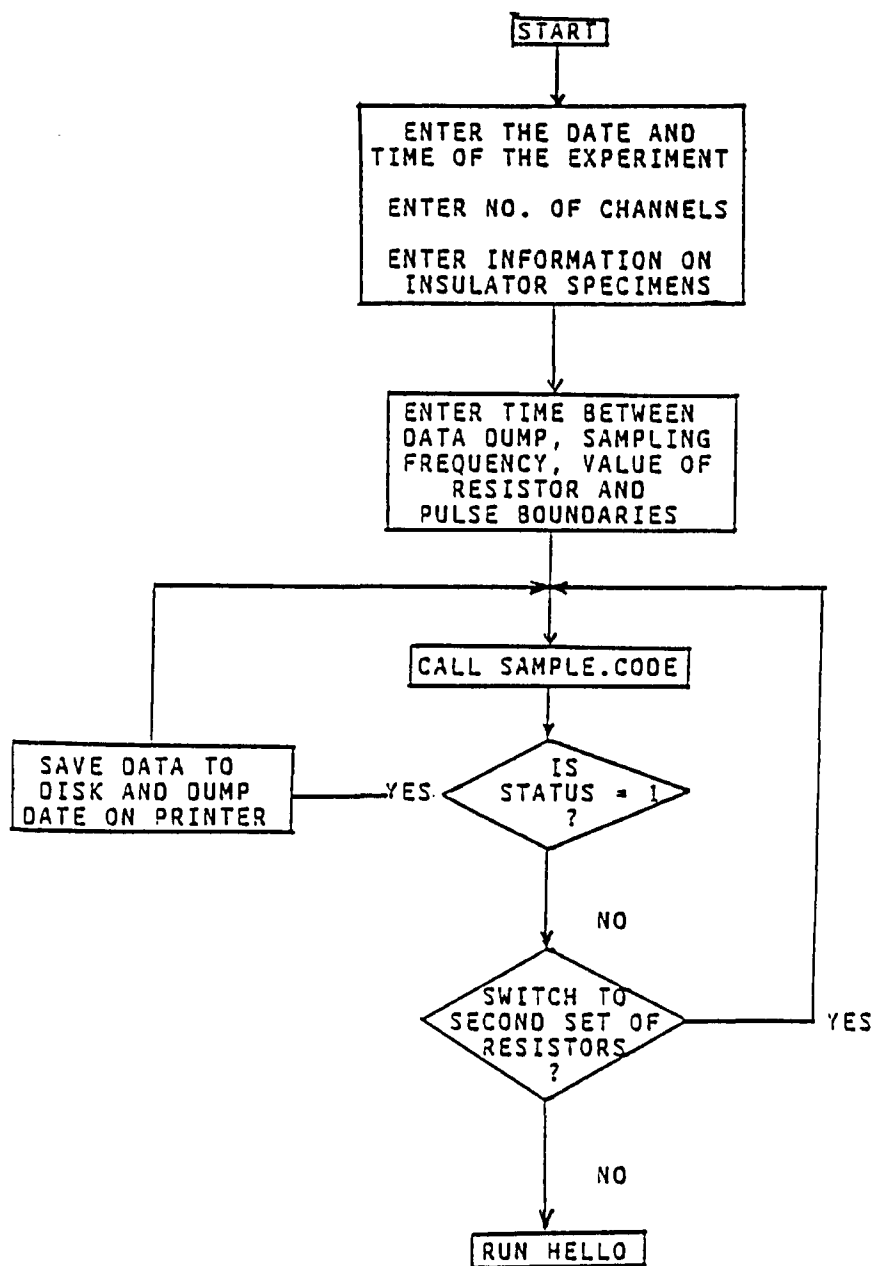


Figure A.1: Flow Chart of Program SAMPLE.

A.2.3 SAMPLE.CODE

This program performs the actual real time signal processing and is written in 6502 machine language. The program determines the peak and average leakage current, the cumulative

charge and the number of current pulses between preset current limits within a specified time interval. At the end of each interval, SAMPLE.CODE returns control to SAMPLE so that the data can be stored on disk and also printed out. SAMPLE then reinitializes the variables and calls SAMPLE.CODE to continue sampling. The flow chart of SAMPLE.CODE is shown in Fig. A.2.

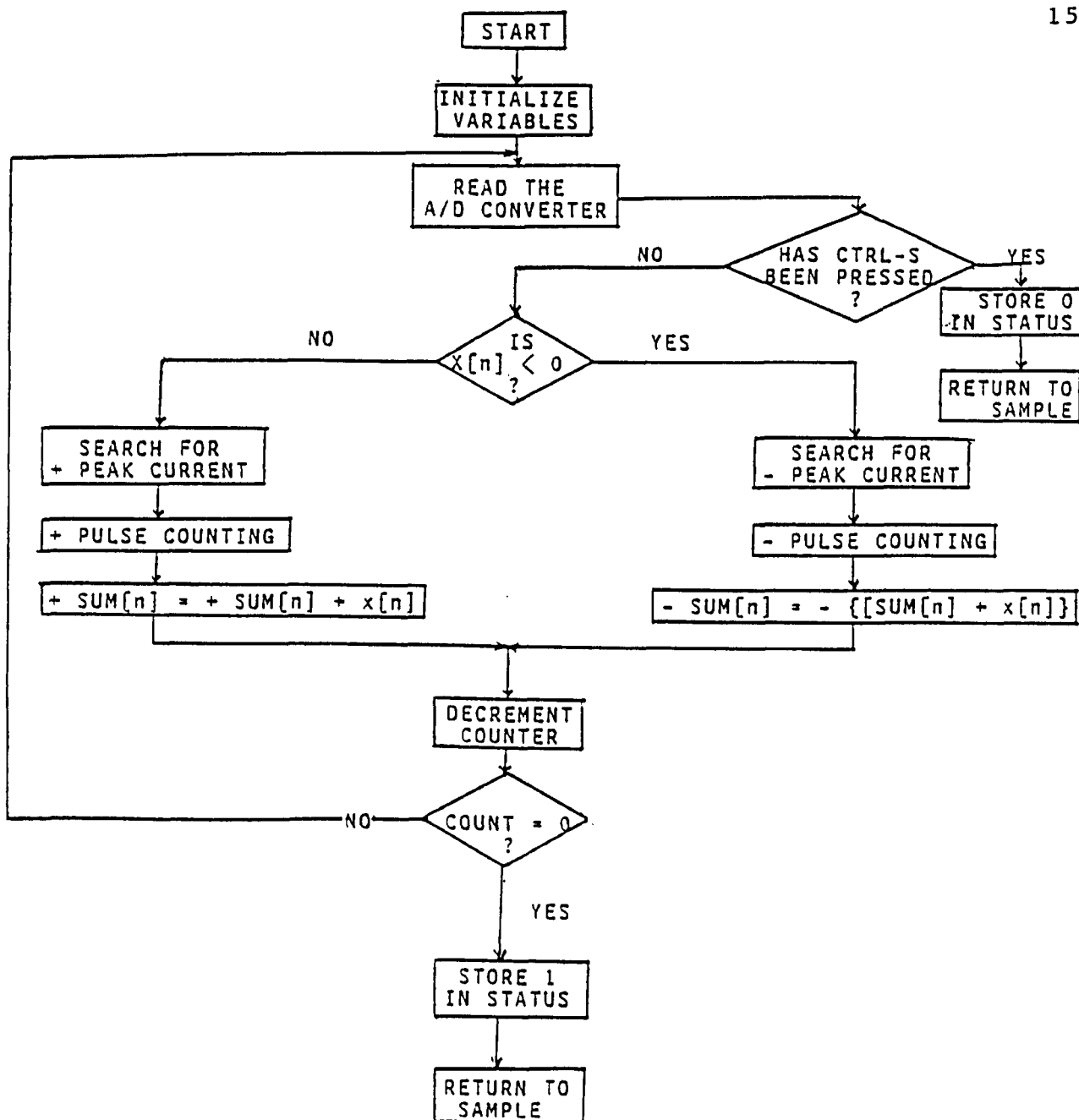


Figure A.2: Flow Chart of Program SAMPLE.CODE.

Appendix B

TIMING CIRCUIT

Fig. B.1 shows the schematic of the timing circuit used to determine the distribution of the conduction period of dry band discharges which functions as follows:

A voltage signal proportional to the input ac supply is fed to a zero crossing detector (ZCD). The falling edges of the output of the ZCD triggers a monostable multivibrator M. Another voltage signal proportional to the leakage current of the sample is fed to a comparator C. The output of C and M are in phase opposition. By varying the timing elements of M, its output waveform can be extended so that a part of it is in phase with the output of C. These two outputs are AND gated. Since the amount of pulse extension is known, the counter N_1 gives the number of current pulses having a width greater than a particular value. Another counter N_2 gives the total number of current pulses in a particular time interval. The ratio N_1/N_2 for different settings of the timing elements of M gives the distribution of the conduction period of the dry band discharges.

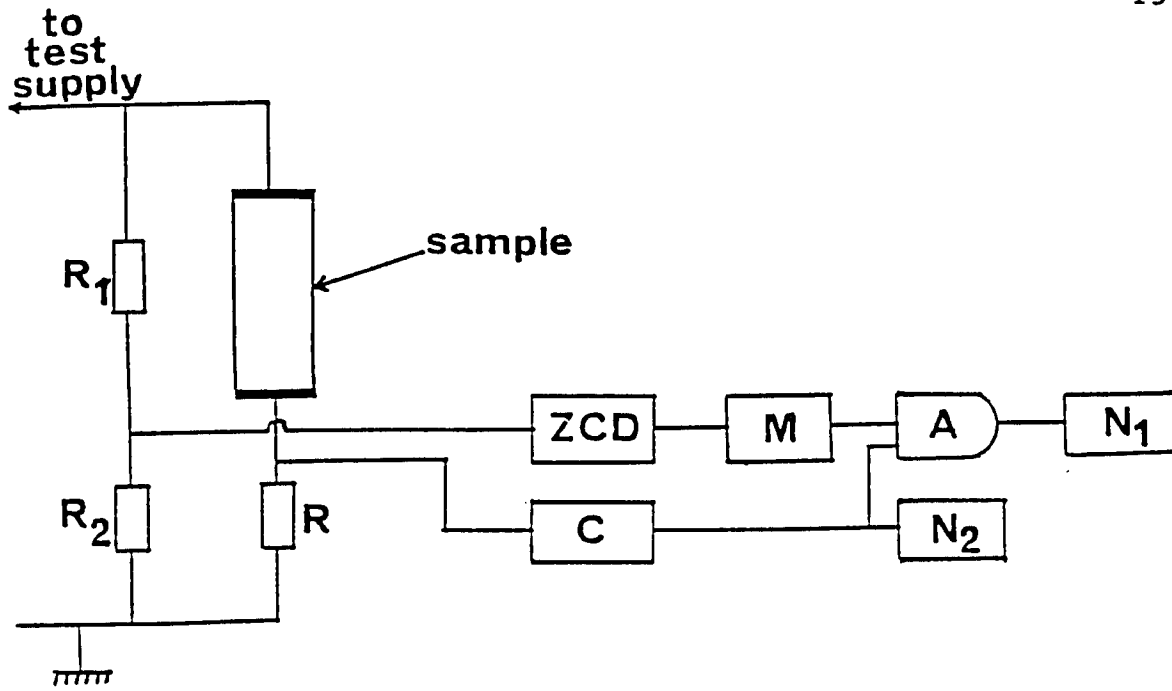


Figure B.1: Schematic of the Timing Circuit.. ZCD. LM311 comparator configured as a zero crossing detector; C. LM311 comparator; M. 555 timer configured as a monostable multivibrator; A. 7408 AND gate; N₁ and N₂. Hewlett- Packard 5326-B counters.

BIBLIOGRAPHY

1. Clark, F.M. Insulating Materials For Design And Engineering Practice. John Wiley and Sons, 1962.
2. Hampton, B. F. Flashover Measurements of Polluted Insulation. Proc IEE, pp 985-990, 1964.
3. Cherney, E. A. et al. Minimum Test Requirements For Non-Ceramic Insulators. Trans IEEE, Vol PAS-100, pp 882-890, 1981.
4. Rodriguez, G. D. An Overview of Non-Ceramic Insulation. Presented at the Pacific Coast Electrical Insulation, Engineering and Operating Section, Mar- 1980.
5. Bauer, E., Karner, H., Muller, K. H. and Verma, P. Service Experience with the German Long Rod Insulator with Silicone Rubber Weathersheds Since 1967. Paper 22-11, CIGRE, 1980.
6. Cherney, E. A. State-of-the-Art Review on Composite Insulators Above 69kV. Paper ST-118, Prepared for the Canadian Electrical Association, Apr-1982.
7. Cherney, E. A. Polymer Horizontal Line Post Insulators for Distribution. Paper ST-118, Prepared for the Canadian Electrical Association, Mar 1984.
8. Niemi, R. G. and Orbeck, T. High Surface Resistance Protective Coatings for High Voltage Insulators. Paper C72 557-7, Presented at the IEEE PES Summer Meeting, 1972.
9. Jolly, D. C. Contamination Flashover Theory and Insulator Design. Journal of Franklin Institute, Vol-294, Dec 1972, pp 483-500.
10. Lambeth, P. J. Effect of Pollution on High Voltage Outdoor Insulators. Proc IEE, IEE Reviews, Vol-118, pp 1107-1130, 1971.
11. Dietz, H. et al. Latest Developments and Experience with Composite Long Rod Insulators. Paper 15-09, CIGRE, 1986.

12. Weedy, B. M. Electric Power Systems. Third Edition, John Wiley and Sons, 1979.
13. Cherney, E. A. Cement Growth Failure of Porcelain Suspension Insulators. Trans IEEE, Vol PAS-102, pp 2765-2774, 1983.
14. Cherney, E. A. State-of-the-Art Review on Composite Insulators for Distribution. Paper SD-4, Prepared for the Canadian Electrical Association, Mar 1985.
15. Hall, C. Polymer Materials. The MacMillan Press Ltd, 1981.
16. Mitchell, G. R. Present Status of ASTM Tracking Test Methods. Journal of Testing and Evaluation, Vol-2, No. 1, pp 23-31, 1974.
17. Cherney, E. A., Reichman, J., Stonkus, D. J. and Gill, B. E. Evaluation and Application of Dead-End Type Polymeric Insulators to Distribution. Trans IEEE, Vol PAS-102, pp 121-132, 1984.
18. Cherney, E. A. State-of-the-Art Review of Dead-End Type Composite Insulators Below 69kV. Prepared for the Canadian Electrical Association, Jan 1982.
19. Cherney, E. A. Power Arc on Dead-End Type Composite Insulators for Distribution. Prepared for the Canadian Electrical Association, Mar 1982.
20. Norman, R. S. and Kessel, A. A. Internal Tracking Mechanism for Non-Tracking Organic Insulators. Trans AIEE, 77, pp 532-536, 1958.
21. Parr, D. J. and Scarisbrick, R. M. Performance of Synthetic Insulating Materials Under Polluted Conditions. Trans IEE, Vol-112, pp 1625-1632, 1965.
22. Cojan, M. et al. Polymeric Transmission Insulators: Their Application in France, Italy and the U. K. Paper 22-10, CIGRE, 1980.
23. Houlgate, R. G. et al. Field Experience and Laboratory Research on Composite Insulators for Overhead Lines. Paper 15-12, CIGRE, 1986.
24. Artificial Pollution Tests on High Voltage Insulators to be used on AC Systems. IEC Report 507, 1975.
25. Jolly, D. C. A Quantitative Method for Determining the Resistance of Polymers to Surface Discharges. Trans IEEE, Vol EI-17, pp 293-299, 1982.

26. Cherney, E. A. and Stonkus, D. J. Non-Ceramic Insulators for Contaminated Environments. Trans IEEE, Vol PAS-100, pp 131-142, 1981.
27. Sheriff, E. M. and Vlastos, A. E. Long Term HVDC and HVAC Performance of Composite Insulators. Paper Presented at NORD-IS, Helsinki, Finland.
28. Wilkins, R. W. and Billings, M. J. Effect of Discharges Between Electrodes on the Surface of Organic Insulation. Trans IEE, Vol-116, pp 1777-1784, 1969.
29. Billings, M. J., Warren, L. and Wilkins, R. Thermal Erosion of Electrical Insulating Materials. Trans IEEE, Vol EI-6, pp 82-90, 1971.
30. Neta, T., Nagai, K., Naito, K. and Hasegawa, Y. Studies on Performance of Contaminated Insulators Energized With DC Voltage. Trans IEEE, Vol PAS-100, pp 518-527, 1981.
31. Reynaert, E. A., Orbeck, T., and Seifferly, J. A. Evaluation of Polymer Systems for Outdoor HV Insulators Application by Salt-Fog testing. IEEE Int Symps on Electrical Insulation, Conference Record CH 1780 4182-000-0242, 1982.
32. Kurtz, M. Comparison of Tracking Test Methods. Trans IEEE Vol EI-6, pp 76-81, 1971.
33. Orbeck, T. and Hall, J. RTV Protective Coating for Porcelain Insulators. Trans IEEE, Vol PAS-101, pp 4689-4696, 1982.
34. Lee, C. L. and Homan, G. R. Silicone Elastomer Protective Coating for High Voltage Insulators. IEEE Conference on Electrical Insulation and Dielectric Phenomena, pp 435-443, 1981.
35. Clabburn, R. J. T., Penneck, R. J. and Swinmurn, C. J. The Outdoor Performance of Plastic Materials Used as Cable Accessories. Trans IEEE, Vol PAS-92, pp 1833-1842, 1973.
36. Scarisbrick, R. M. Electromechanical Erosion of Epoxy Resin Outdoor Insulators. Trans IEE, Vol-21, pp 779-783, 1974.
37. Barry, A. J. and Beck, H. N. Inorganic Polymers. Academic Press, pp 189-320, 1962, Ed Graham, W. A. G. and Stone, F. G A.

38. Billings, M. J., Smith, A. and Wilkins, R. Tracking in Polymeric Materials. Trans IEEE, Vol EI-21, pp 175-182, 1972.
39. Goldstein, J. I. and Yakowitz, H. Practical Scanning Electron Microscopy Electron and Ion Microprobe Analysis. Plenum Press, 1975.
40. Allen, A. W. and Wild, R. K. Probing the Secrets of Solid Surface. CEGB Research, No. 11, pp 11-30, 1981.
41. Adamson, A. W. Physical Chemistry of Surfaces. Third Edition, John Wiley and Sons, 1976.
42. Agee, J. E. and Kise, J. A. Artificial Versus Natural Contamination on Silicone Rubber Weathershed - The DC Case. Presented at the HVDC Insulator Symposium, University of Southern California, Nov, 1985.
43. Muilenberg, G. E. (Editor). Handbook of X-Ray Photoelectron Spectroscopy. Perkin Elmer Corporation, 1978.
44. Owen, M. J., Gentle, T. M., Orbeck, T. and Williams, D. E. Dynamic Wettability of Hydrophobic Polymers. Presented at the Eighth Rocky Mountain Regional ACS Meeting, June 1986, Denver, Colorado.
45. Thomas, P. H. Some Conduction Problems in the Heating of Small Areas on Large Solids. Quarterly Journal, Mech and Applied Math, Vol-10, pt 4, 1957 pp 483-493.
46. Carslaw, H. S. and Jaegar, J. C. Conduction of Heat in Solids. Oxford Press, 1959.
47. Touloukian, E. (ed). Thermo Physical Properties of Matter. Vol 2 and 4, Plenum Press.
48. Kreith, F. Principles of Heat Transfer. Harper and Row Publishers, 1972.
49. Thermodynamics. 4th Edition, McGraw Hill, 1983.
50. Mason, J. H. In Discussion Proc IEE, Vol-130, pt 8, p285, 1983.
51. Mercure, H. P. and Drouet, M. G. Dynamic Measurements of the Current Distribution in the Foot of an Arc Propagating Along the Surface of an Electrolyte. Trans IEEE, PAS, pp 725-736, 1981.
52. Nasser, E. Flashover of Contaminated Surfaces. ETZ-A, Bd-93, H-6, pp 321-325, 1972.

53. Karady, G. The Effect of Fog Parameters on the Testing of Contaminated Insulators. Trans IEEE, Vol PAS 75 PP 378-387, 1975.
54. Davis, P. J. and Rabinowitz, P. Methods of Numerical Integration. Academic Press, 1975.
55. Wu, C. T. and Cheng, T. C. Formation Mechanisms of Clean Zones During the Surface Flashover of Contaminated Insulators. Trans IEEE, Vol EI-13, No 3, pp 149-155, 1978.
56. Niemi, R. G. and Orbeck, T. Test Methods Useful in Determining the Wet Voltage Capability of Polymeric Insulator Systems after Time Related Outdoor Exposures. Trans IEEE, Vol EI-9, No 3, pp 102-108, 1974.
57. Sheriff, E. and Vlastos, A. E. Performance of Long-Rod Composite Insulators Under Various Environmental Conditions. Presented at the HVDC Insulator Symposium, University of Southern California, Nov-1985.
58. McAvoy, D. Signal Processing of Data Obtained From the testing of High Voltage Insulators. Third Year Project Report, Department of Electrical Engineering, University of Windsor, March 1986.

PUBLICATIONS FOR THESIS

1. R. S. Gorur, E. A. Cherney and R. Hackam, "A Comparative Study of Polymer Insulating Materials Under Salt-Fog Conditions", Trans IEEE, Vol EI-21, No. 2, pp 175-182, 1986.
2. R. S. Gorur, E. A. Cherney and R. Hackam, "Performance of Polymeric Insulating Materials in Salt-Fog", Trans IEEE PAS-86 SM 424-6.
3. R. S. Gorur, E. A. Cherney, R. Hackam and T. Orbeck, "The Electrical Performance of Polymeric Insulating Materials Under Accelerated Aging in a Fog Chamber", To be presented at the 1987 Winter PES meeting.
4. R. S. Gorur, E. A. Cherney and R. Hackam, "The AC and DC Performance of Polymeric Insulating Materials Under Accelerated Aging in a Fog Chamber", Submitted to IEEE Trans PES Summer meeting, 1987.
5. R. S. Gorur, E. A. Cherney and R. Hackam, "A Comparative Study of Polymeric Insulating Materials Under Contaminated Conditions", Canadian Electrical Association, Engineering and Operating Division Transactions, Vol-25, 1985-86.
6. R. S. Gorur, E. A. Cherney and R. Hackam, "Electrical Performance of Polymer Insulating Materials: Effect of Material and Filler Type", IEEE 1985 Annual Report, Conference on Electrical Insulation and Dielectric Phenomena, pp 350-355.
7. R. S. Gorur, E. A. Cherney and R. Hackam, "Electrical Performance of Organic Insulating Materials as Affected by Environmental Degrading Factors", Conference Record of the IEEE International Symposium on Electrical Insulation, pp 294-297.
8. R. S. Gorur, E. A. Cherney and R. Hackam, "Factors Affecting the Performance of Polymeric Insulating Materials in Contaminated Environments", IEEE 1986 Annual Report, Conference on Electrical Insulation and Dielectric Phenomena, pp 339-344.

9. R. S. Gorur, E. A. Cherney and R. Hackam, "A Study of Ceramic and Non-Ceramic Insulating Materials Under Contaminated Conditions", Report IRI 18-30, University of Windsor, Prepared for Dow Corning Corporation, Midland, Michigan, May 1986.

VITA AUCTORIS

31 July 1958 - Born in Bangalore, India

April 1974 - Completed High School from the National English High School, Rajajinagar, Bangalore, India.

April 1976 - Completed the Pre-University Course from St. Joseph's College, Bangalore, India.

July 1981 - Received the Bachelor of Engineering Degree in Electrical Engineering from the University Visveswaraya College of Engineering, Bangalore University, India.

July 1983 - Received the Master of Engineering Degree in Electrical Engineering from the Indian Institute of Science, Bangalore, India.

October 1986 - Candidate for the Degree of Doctor of Philosophy in Electrical Engineering from the University of Windsor, Windsor, Ontario, Canada.